TRANSLATION SERIES

AEC-tr-4516
PHYSICS

GAMMA-RADIATION OF AN ATOMIC EXPLOSION

By
O. I. Leĭpunskiĭ

Translated from a publication of the State Committee of the Council of Ministers of the U.S.S.R. on the Utilization of Atomic Energy, Moscow, 1959.

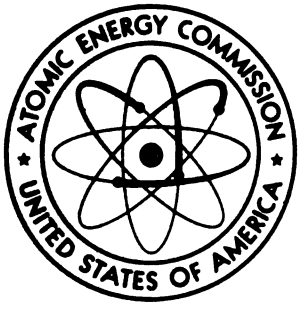

UNITED STATES ATOMIC ENERGY COMMISSION
Division of Technical Information

A translation of: Gamma-Izluchenie Atomnogo Vzryva. O. I. Leĭpunskiĭ. Izdatel'stvo Glavnogo Upravleniya po Ispol'zovaniyu Atomnoĭ Energii pri Sovete Ministrov S.S.S.R., Moskva, 1959.

Translated by the U. S. Joint Publications Research Service, New York, a federal government organization established to service the translation and research needs of the various government departments.

In the interest of expeditious dissemination this publication has been reproduced directly from copy prepared by the translating agency.

Printed in USA. Price $2.75. Available from the Office of Technical Services, Department of Commerce, Washington 25, D. C.

Issuance date: September 1961.

USAEC Division of Technical Information Extension, Oak Ridge, Tennessee

O. I. Leipunskii

GAMMA-RADIATION OF AN ATOMIC EXPLOSION

PUBLICATION OF THE MAIN ADMINISTRATION
ON THE USE OF ATOMIC ENERGY OF THE
COUNCIL OF MINISTER USSR

Moscow 1959

TABLE OF CONTENTS

TABLE OF CONTENTS (continued)

NOTATION

r - roentgen;
E_{TT} - explosion energy in kilotons of TNT (1 kiloton = 1 thousand tons of TNT = 10^{12} megacalories = $= 4.18 \times 10^{19}$ ergs);
E - explosion energy in arbitrary units;
R - distance from the source of gamma radiation;
" " " center of explosion;
R_f - radius of front of shock wave;
R_l - lethal radius;
$R_{1,2}$, $R_{2,3}$ - distances that mark the regions of application of interpolation formulas for the calculation of doses;
r - radius of active surface on the earth;
H - height of detector above the earth;
x - thickness of active absorber; thickness of flat layer of absorber;
l_0 - minimum distance from detector to the earth;
$l = \frac{x}{\cos\varphi}$ - oblique thickness of flat layer of absorber;
φ - angle of incidence of quanta on the surface;
θ - angle between specified direction and the direction of motion of the quantum prior to scattering;
Θ - angle between the directions from the detector to the source and to the considered volume element of the scattering medium;
α - energy of quantum in m_0c^2 units;
α - coefficient in the empirical expression for the attenuation coefficient;
σ_{ph} - cross section of the photoeffect per atom;
σ_p - cross section of pair production per atom;
σ_C - cross section of Compton scattering per electron;
σ_e - cross section of transfer of energy to electron;
σ_γ - cross section of transfer of energy to quantum;
$a\sigma_C$, $a\sigma_e$, $a\sigma_\gamma$ - corresponding cross section per atom;
σ_t - total interaction cross section per atom;
σ_{te} - total cross section for the absorption of energy per atom;
σ_{act}, σ_{capt} - cross sections of activation and capture of neutrons by isotopes;
σ - density of activation
n_e - number of electrons per cm^2;
N_e - number of electrons in a column of absorber with a cross section of 1 cm^2;
n - number of atoms in 1 cm^2;

n - exponent in the formula for the variation of air density (12.8);

N - quantum flux density, quantum/cm^2;

ρ - density of medium;

ρ_0 - " " undisturbed medium;

ρ_f - " on the front of the shock wave;

μ - linear coefficient of absorption, cm^{-1}; $\mu = n\sigma_t$;

μ/ρ - mass coefficient of absorption, cm^2/g;

$\lambda = 1/\mu$ - mean free path;

$\mu_e = n\sigma_{te}$ - linear coefficient of absorption of energy, cm^{-1};

$\lambda_e = 1/\mu_e$; μ_e/ρ - range and mass coefficient of absorption corresponding to μ_e;

μ_{ph}, μ_p - linear coefficients of absorption of the photoeffect and of pair production;

μ_{eff} - effective linear coefficient of absorption in the empirical expresion (7.14) for the dose power;

λ_{eff} - effective range;

ε - quantum energy;

E - quantum energy flux density, equal to $N\varepsilon$;

ε_0 - initial energy of quanta in continuous spectrum due to scattering of quanta with energy ε_0;

λ_0, μ_0 - range and absorption coefficient corresponding to ε_0;

$\bar{\varepsilon}_1$ - arbitrary average energy of quantum in non-monoenergetic radiation;

ε_γ - quantum energy after scattering;

ε_e - energy of recoil electron;

G - activity of source, Mev/sec;

G_c - activity of source of capture radiation, Mev/sec;

g - specific activity of source, Mev/sec-cm^3;

$u(t)$ - activity of fission fragments per fission event;

$u_e(t)$ - induced activity of earth per fission event;

ν - exponent in formula (2.1) for the decrease of activity with time;

A - coefficient in formula (2.1) for the decrease of fragment activity with time;

A - coefficient in the empirical formula for calculation of doses, (14.3);

A_h - coefficient in the empirical formula in the case the dose of hard component;

A - atomic weight;

Q - number of neutrons formed during the explosion;

W_{t_1, t_2} - energy radiated by the fragment per fission event within the time interval $t_1 - t_2$.

W - energy radiated by the fragments during the entire decay time;

$\bar{W}$ - energy radiated by the fragment over the effective time of radiation during the explosion, t_{eff};

J - intensity of radiation, Mev/cm^{2}sec;

J_0 - intensity of radiation of the direct ray;

J_v - intensity of radiation in vacuum;
B_r - dose accumulation factor;
B_J - intensity accumulation factor;
B_N - factor of accumulation of the number of quanta;
K_r - dose attenuation factor;
K_J - intensity attenuation factor;
K_N - attenuation factor of number of quanta;
P - dose power, r/sec;
P_0 - dose power of direct ray;
P_c - dose power of captured radiation;
K_D - dose cavity factor;
K_P - dose power cavity factor;
L - radius of cavity surrounding the source;
L_{eff} - effective radius of cavity in shock wave;
$\bar{L}_{eff}$ - average value of effective radius of cavity after time t_{eff} of radiation of gamma quanta;
L_{fb} - radius of fireball;
Δ - optical thickness;
D - dose of gamma radiation;
D_h - dose of hard component of gamma radiation;
D_0 - dose ahead of shielding layer;
$D(\omega)$ - dose produced by radiation contained in a unit solid angle, in space;
$\delta(\theta)$ - dose produced by radiation contained in a unit solid angle, expressed in units of total dose, at the place considered;
δ_b - dose produced by radiation traveling from the "backward" half-space, expressed in units of the total dose;
$a(\varphi, \epsilon, K)$ - coefficient of reduction in attenuation in a layer of absorber due to oblique incidence of quanta of energy ϵ at an angle φ.
t - time
t_{eff} - effective time of accumulation of dose due to fission fragments in the explosion;
T - period of decay;
T_{eff} - effective period of reduction of gamma activity of fragments;
$T_{1/2}$ - half life;
$\lambda_i = 1/T_i$ - decay constant of the i-th isotope;
τ - lifetime of neutrons in air;
Π - neutron flux density, neutron/cm^2;
z - atomic number;
q - fraction of neutrons absorbed in air;
$f(H, \epsilon, r)$ - coefficient expressing the dependence of the dose above the active surface on ϵ;
$F(H, \epsilon, r, x)$ - coefficient expressing the dependence of the dose above the active layer on H, ϵ, r, and x;
NTP - normal temperature and pressure.

FOREWORD

If we examine an atomic explosion as a physical phenomenon, many problems arise in the analysis of the physical picture of the explosion. The present book is devoted to the physics of the action of gamma radiation in atomic explosions. It is known that the damaging action of an atomic explosion includes, to a considerable extent, the radiation sickness due to the action of gamma rays and neutrons. We shall confine ourselves only to consideration of gamma rays, since they are the main factors that determine the damaging action. The action of the gamma radiation is determined by the magnitude of the so-called dose, i.e., the absorption of gamma-radiation energy.

The purpose of this book is to estimate the dose of gamma radiation and to analyze the physical factors that influence its magnitude.

The analysis is based on the results of the theory of multiple scattering (diffusion) of gamma quanta. A new factor in the theory is the influence of the shock wave on the propogation of gamma radiation, as noted by Ya. B. Zel'dovich and the author.

The calculations of the doses are referred to explosion energies of 20 megatons. This figure has no relation whatever to the present state of the art, and is chosen arbitrarily.

The problems that arise in the analysis of the physical picture of the action of the gamma radiation due to atomic explosion are closely related to problems involving protection against gamma radiation, encountered in the atomic industry. Therefore the book can be useful for a wide circle of scientific workers and engineers interested in problems of shielding and the dosimetry. The author has benefited from the interest and from much advice by Ya. B. Zel'dovich, and expresses him great gratitude.

The author is also grateful to V. N. Sakharov, P. A. Yampol'skii, N. Ya. Gen, N. Ya. Buben and B. V. Novozhilov for discussing individual sections of the book.

In preparing the book, great help was rendered the author by B. V. Novozhilov and V. N. Sakharov, V. I. Kolesnikov-Svinarev and V. I. Tereshchenko who undertook the preparation of most of the tables and diagrams, as well as B. P. Bulatov and A. S. Strelkov. The author takes this opportunity to thank them for their help.

--The Author

INTRODUCTION

The overall picture of the action of γ rays produced by atomic explosion is as follows. Starting with the instant of the explosion, contained within the volume about the center of the explosion, inside the region of the incadescent air, contains a few seconds a powerful source of γ rays. This source consists essentially of fission products. A smaller, but still significant role is played by sources from a different origin, for example, γ rays due to capture of neutrons by the nitrogen of the air. After a few seconds following the explosion, the incadescent air rises upward, carrying with it the explosion product in the form of a radioactive cloud.

In spite of the fact that the radioactive products remain near the center of the explosion for a short time, they succeed in producing a considerable radiation in the explosion region, i.e., in a space of radius of several kilometers from the center of the explosion. For example, when a 20-megaton bomb explodes, the radius of the lethal damage by γ rays in an open locality is 1.2 kilometers.

In the region of the epicenter of the explosion, after the departure of the radioactive cloud, there may remain a source of γ rays which acts for a long time. It is formed by the fission fragments which settle on the earth, and also by the neutrons due to atomic explosion, which reach the earth and activate the soil, which then emits γ rays for a long time. The fission fragments carried away upward by the air currents propagate over the earth in the form of a radioactive cloud and gradually settle on the earth, producing an extensive region of radioactive contamination -- the trail.

The greatest damage is produced in the trail in the case of explosions on the surface of the earth, when the dust rays by the explosion is mixed with the fragments and accelerates their precipitation. In this case there is formed near the center of the explosion a section of strong contamination, whereas in the case of explosions in the air the precipitation of fragments in the region of explosion is negligible.

The trail may extend over hundreds of kilometers from the upper center of the explosion in length, and tens and hundredths of kilometers in width. Some of the fragments enter the stratosphere and settle over the entire earth's sphere, with an approximate settling time of 10 years.

Thus, the γ radiation produced as a consequence of an atomic explosion is observed not only simultaneously with the explosion, but appears also as remote aftereffects of the explosion, resulting from the radioactivity of the long-lived fragments.

The region of action in the γ rays is not confined to the region of the explosion, and includes large areas on the earth and

in the air. On the trail, the damaging factor of the atomic explosion is only the γ radiation from the long-lived fragments (β particles play an important role only when the fragments enter inside the organism). In the region of explosion, on the other hand, i.e., within a radius of several kilometers from the center of explosion, all the damaging factors of the atomic explosion are effective, namely, γ radiation, the shock wave, neutrons, and light.

In the explosion region, the main part of the γ-ray energy is emitted by the fragment and in the form of capture radiation, within several seconds after the explosion, and the long-lived gamma radiation of the activated soil and of the fragments that fall out from the cloud produce an appreciable smaller fraction of the total amount of the energy of gamma radiation (although in absolute magnitude this fraction may be large).

In the present book we deal only with gamma radiation in the region of the explosion. We do not consider the trail and the radioactive cloud.

The damaging action of gamma radiation is characterized by the magnitude of the energy of the gamma rays absorbed in the air. The dose is determined by the intensity and by the spectrum of the gamma rays passing through the place under consideration, i.e., it is determined in the final analysis by the properties of the gamma-radiation sources produced during the explosion and by the properties of the absorbing media which are located on the path of propagation on the gamma rays from their sources towards the place of action.

Thus, in order to obtain the physical characteristics of the action of the gamma rays due to atomic explosion, it is necessary to evaluate the sources of gamma radiation during the explosion and to consider the formation and the magnitudes of the doses from the point of view of the theory of propagation of gamma rays in absorbing layers.

Let us give the most typical examples of the action of gamma rays in the region of explosion and the corresponding problems involved in the propagation of gamma rays.

1. Action in an open locality produced by gamma rays emerging from the radioactive cloud during the first few seconds after the explosion, i.e., before the rise of the cloud (Figure 1a). This form of action produces in the region of the explosion the main part of the gamma-ray dose.

Within a few seconds after the explosion, the fission fragments are still located close to the center of the explosion, and at distances of several hundred meters from the center of the explosion their totality can be considered as a point source of gamma rays. As a result of the passage of the shock wave, the front of which is followed by a region of rarefied air, the air density along the path of propagation of the gamma rays is not constant.

This action of the gamma rays gives rise to the following computation problem: a point source of gamma rays is located in an infinite air medium. The air medium can be inhomogeneous, and the air density varies with the distance from the source in accordance with a definite law, so that there exists a region of rarefied air around the source.

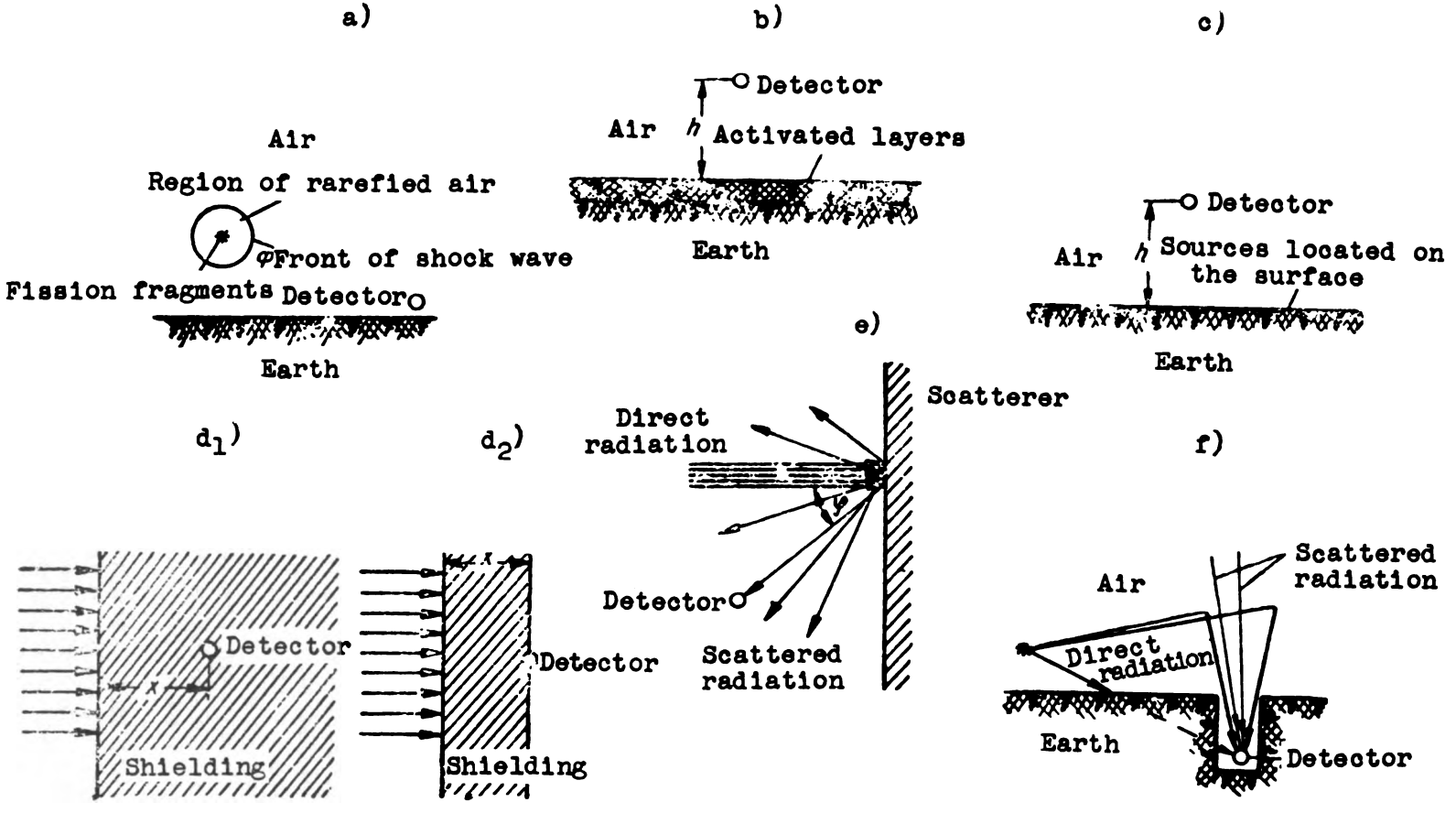

Figure 1. Cases of action of gamma radiation which are typical for an aerial explosion; arrangements of the sources of gamma radiation of the absorbing and scattering media, and of the detector;
a) Radiation due to an atomic explosion in an open location; b) radiation from a plane active layer, (for example, activated soil);
c) radiation due to activity distributed over a surface, for example, deposited fission fragments); d) attenuation of radiation in shielding layers; e) radiation scattered from walls (the albedo problem);
f) radiation scattered from the air.

In the case of a surface explosion, the air medium in which the source of gamma rays is located should be regarded as semi-infinite and bounding on a semi-infinite denser medium, namely the earth.

2. The action of the gamma rays from the elements in the earth and the activating neutrons which are liberated during the explosion. These gamma rays emerge from the upper layer of the earth (Figure 1b).

The corresponding theoretical problem is as follows: sources of gamma rays are distributed in a flat layer of an absorber. The detector is located in the air above the layer.

3. Action of gamma rays from the fragments, which settle from the radioactive cloud on the earth (Figure 1c).

The equivalent theoretical problem is as follows: the sources of the gamma rays are distributed over the surface of the earth, i.e., on the boundary between two semi-infinite media, the earth and the air. The detector is located in the air above the earth.

The foregoing examples pertain to the action of gamma rays in an open locality.

In shielded structures, the gamma rays are attenuated by the absorbing layers. Let us give three typical examples of the action of gamma rays in shelters.

4. Action of gamma rays passing through the protective shielding of the shelter (Figure 1d).

The theoretical problem is as follows: a broad parallel beam of gamma rays passes through an absorbing layer. The detector is located behind the absorbing layer.

5. Action of gamma rays scattered from dense layers of matter. This case takes place inside shelters which have openings or have weak spots in the shielding, through which a beam of gamma rays enters inside the shelter. After being scattered by the inner surface of the shielding layers, the gamma rays act in places which do not lie on the path of the initial beam of the gamma rays (Figure 1e).

The theoretical problem is: the gamma rays are incident at a definite angle on a dense layer of matter. The detector is protected against the direct radiation and senses only the radiation that is scattered from the layer. This is the problem of the albedo of gamma rays.

6. Action of gamma rays scattered in the atmosphere. This action occurs in pure form when the detector is protected against rays that travel directly from the source but is exposed to radiation in a definite solid angle (for example, the detector is located in a ditch -- Figure 1f).

From the theoretical point of view, this case reduces to the problem of the azimuthal distribution of gamma rays scattered by an infinite medium.

The greater part of the foregoing schematized problems has been solved in the theory of multiple scattering of quanta or in simulation experiments. Under real conditions of explosion, many complicating factors arise, and these prevent the exact solution of the problems involved in the gamma radiation from an atomic explosion.

However, the solutions of schematized problems can nevertheless be used to explain the physical picture of the appearance of gamma radiation from explosions and for approximate quantitative estimates of the doses.

CHAPTER I

MAIN SOURCES OF GAMMA RADIATION IN ATOMIC EXPLOSIONS

1. SOURCES OF GAMMA RADIATION AND THE TIME OF THEIR EMISSION.

Components of the gamma radiation from the explosion. The gamma radiation observed during the explosion of an atomic bomb consists of many components, which differ in their radiation time, in their origin, in their quantum energy, and in their radiated energy. During the time of emission, it is convenient to distinguish among the following groups of radiations.

Prompt -- acting within 0 to 10^{-5} second. This gamma radiation is released during the time of the chain reactions that make up the atomic explosion and during the time following, prior to the scattering of the bomb material. Its components are the gamma radiation due to the fission and to the fission products, and the gamma radiation due to inelastic scattering of neutrons and due to capture of neutrons in the materials of the bomb.

Short-lived -- from 10^{-5} to 3×10^{-1} sec. This is essentially the radiation produced from the capture of the explosion-induced neutrons by the nitrogen in the air (an idea advanced by P. A. Yampol'skii). It is emitted after the scattering of the bomb material. Radiation from the fragments is also possible (see Section 2).

Second -- from 3×10^{-1} to 15 seconds. This is essentially the radiation from the fission products, released during the time following the explosion up to the time when the fragments are carried upward by the incandescent air.

Residual -- from 15 seconds to ∞. This radiation is due to activity induced by neutrons in the earth and other substances in the region of the center of the explosion and to the long-period fission fragments that settle in the region of explosion and in the trail.

In the region of explosion, the greatest contribution to the dose is made by the radiation in the second range, and partially by the short-lived radiation.

As a result of the short radiation time, the role of the prompt radiation in the formation of the dose is insignificant, although this radiation produces the greatest dose power.

As regards its origin, the gamma radiation in the atomic explosion can be divided into the following groups.

Gamma radiation of fission fragments. A distinction is made in this group between the gamma radiation due to the fission and the gamma radiation of the fragments proper, although both radiations belong to the fragments. The difference lies in the emission time. The gamma radiation due to the fission follows immediately the instant of fission and is separated from it by a time that

cannot be measured with the instruments employed, i.e., within less than 10^{-8} sec, and probably 10^{-11} sec. Therefore the gamma radiation due to fission, like the emission of fission neutrons, is associated as far as terminology goes with the fission act.

By gamma radiation of the fragments proper is meant the radiation occurring within measurable time intervals after the fission. Detailed data on the gamma radiation of the fragments are given in Section 2.

Gamma radiation connected with the action of the neutrons. This gamma radiation is due to various neutron reaction with nuclei, and manifests itself in all the emission time groups.

Let us recall the following forms of gamma radiation due to neutrons.

Gamma radiation due to inelastic scattering of fast neutrons in the materials of the bomb and in the surrounding media -- air, earth, etc. This radiation belongs to the prompt group.

Inelastic scattering in the bomb takes place within the time of existence of the bomb and of its shell, i.e., within $\sim 10^{-5}$ sec.

In the surrounding media, inelastic scattering can be expected within the time of slowing down of the fast neutrons in the air to an energy ~1 Mev, i.e., within several microseconds.

Gamma radiation occurring during the capture of neutrons. The following types of radiation can be noted here:

1. Radiation occurring during capture of neutrons in the bomb, i.e., from the main nuclear fuel, from the structural materials, and from the explosive. In the latter, the neutrons are captured by hydrogen to form deuterium and by the nitrogen to form N^{15}.

This radiation is classified as prompt, i.e., it is emitted within the time of existence of the bomb and its shell, i.e., within 10^{-5} sec.

2. Radiation occurring during the capture of neutrons by the nitrogen of the air with formation of N^{15}. The life time of the neutrons in the air (with respect to the reaction N^{14} (n, p) C^{14} at P = 760 mm. Hg and T = 0°C) is approximately 60×10^{-3} sec).

Thus, by the time 0.3 second has elapsed after the time of the explosion, practically all the neutrons are captured and the emission of capture gamma radiation ceases. This gamma radiation is classified as short-lived.

3. Radiation occurring during the capture of neutrons in the earth. The life time of the neutrons in the earth is $\sim 0.5 \times 10^{-3}$ sec, i.e., it is considerably less than in the air. However, the earth "draws" neutrons from the air. Therefore the time during which capture of neutrons in the earth can take place with emission of gamma rays is equal to the time of existence of the neutrons in the air, i.e., ~0.3 sec.

This radiation, too, is classified as short-lived.

Gamma radiation of the artificial radioactive elements, formed as a result of neutron-nucleus reactions of the type (n, γ), (n, p), (n, α), and (n, 2n). Notice should be taken here of the artificial radioactive isotopes produced during the capture of neutrons in the earth and other different materials in the explosion region.

In ordinary soils, the greatest significance is the gamma radiation of Al^{28} (half life $T_{1/2}$ = 2.3 minutes), Mn^{56} ($T_{1/2}$ = 2.6 hours), Na^{24} ($T_{1/2}$ 15 hours), Fe^{59} ($T_{1/2}$ = 47 days). The gamma radiation of the known artificial radioactive elements is classified as residual radiation.

In addition to the activation of elements as a result of the (n, γ) reaction, it is possible to form radioactive products via other reactions such as (n, p), (n, α), and (n, 2n). Gamma rays can also be emitted as a result of production of short-lived isomers.

Secondary sources of gamma rays. In this group we can include bremsstrahlung (β particles, Compton electrons), thermal X-rays in the initial stage of development of the explosion, and X-rays produced by filling of the internal shells of heavy atoms ionized during the explosion.

The contribution of these sources through the overall gamma rays of the explosion is small, and is therefore disregarded here.

All the foregoing types of gamma-rays sources appear during atomic explosions. But the harmful action is connected only with a few of these. In the explosion region, harmful action is produced by gamma rays essentially from fission fragments and short-lived gamma radiation due to capture of neutrons by the nitrogen of the air (the gamma radiation from the fragments being predominant). In the region of the trail, the harmful action of gamma rays is determined by gamma radiation due to fragments and to a small degree the gamma radiation of the activated earth (the principal one is the gamma radiation from the fragments).

2. GAMMA RADIATION DUE TO FISSION FRAGMENTS OF U^{235} AND Pu^{239}.

The only gamma radiation from the fragments that can be effective is that emitted after the scattering of the material of the bomb.

The energy of the fission gamma radiation (7.8 Mev per fission event) is practically equal to the energy of the gamma radiation of the fragments (8.4 Mev per fission event), but the gamma radiation of the fission is absorbed in the matter of the bomb and therefore does not influence the magnitude of the dose and will not be considered further.

The fission of U^{235} and Pu^{239} results directly in approximately 60 isotopes. Figure 2 shows the mass distribution of the fragments produced by the fission of U^{235} and Pu^{239} by slow neutrons.

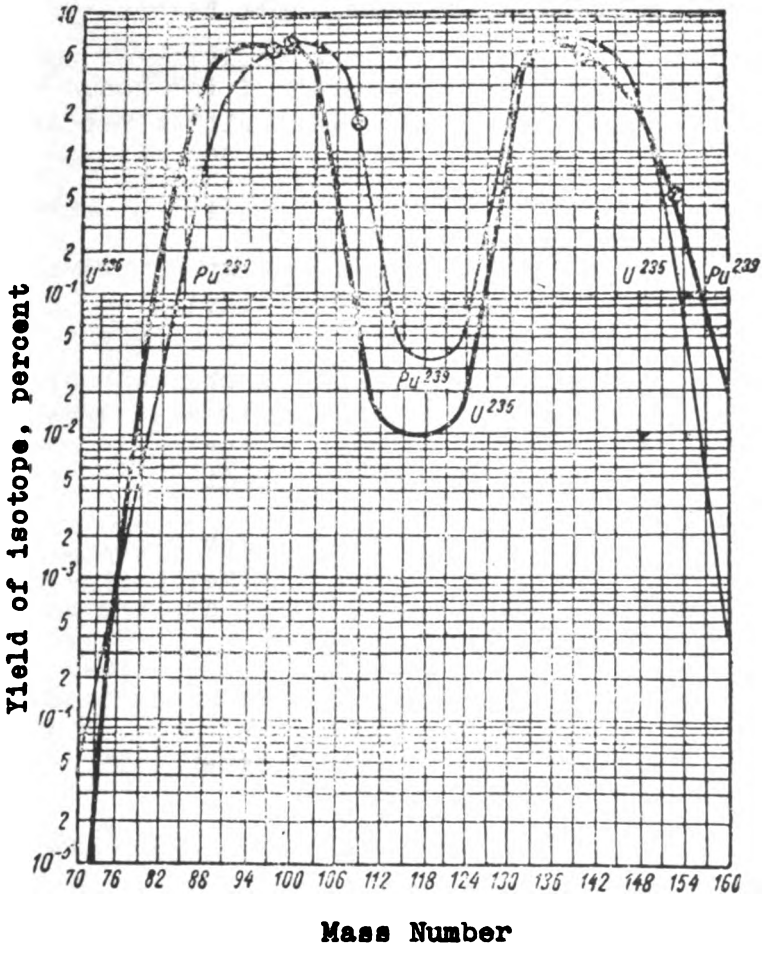

Figure 2. Distribution of fission fragments of U^{235} and Pu^{239} by masses.

Each fragment produced experiences subsequently, on the average, three β decays with different periods. Thus, there are approximately 200 radioactive nuclei involved in the fission products, with decay periods ranging from fractions of a second to several times ten years. The greater part of the decays is accompanied by gamma radiation, in which the quantum energy varies from 0.002 Mev (Tc^{99}) to 2.9 Mev (Rb^{88}).

At each given instant of time, the gamma radiation is determined by the decay of 10 - 30 fragments and only within a time longer than one year after the fission is the main part of the gamma activity produced by 1 or 2 isotopes. Since the nuclei participating in the radiation have different half-lives, the law of decrease of the gamma activity of the radiation with time is not a simple exponential law.

The effective decay period increases with time, because the short-period isotopes decay and fragments with every increasing periods remain active. The radiation becomes softer with time,

but a substantial softening takes place only within the first hour after the fission.

Table 1 lists the values of gamma activity of the fragments, i.e., the rates of emission of the energy of the gamma radiation u(t) in Mev/sec-fission for U^{235} and Pu^{235} within different instances of time in the intervals $0 < t < 60$ seconds and 1 hour $< t <$ < 1000 hours [1].

The accuracy of the given values of u(t) is estimated ± 25 percent.

An atomic explosion of 1 megaton energy gives rise to 1.45×10^{23} fissions. The overall gamma activity of the fission products of an explosion of energy E_{mt} is $G = 1.45 \times 10^{23} E_{mt} u(t)$ Mev/sec. The gamma activity of the fission products of a 20-megaton bomb (i.e., nominal bomb) is 2.9×10^{24} u(t) Mev/sec and is equivalent to the gamma activity of the following sources:

8.1×10^{13} u(t) curie of arbitrary radiation with quantum energy of 1 Mev;

3.24×10^{13} u(t) curie of Co^{60} (2.5 Mev/decay);

5.8×10^{13} u(t) curie of radium (1.4 Mev/decay).

Table 2 lists the values of $G_{20_{mt}}$ for different instants of time.

Table 1

Gamma activity of fission fragments per fission event

t, sec	u(t) Mev/sec-fission	t, hours	u(t) Mev/sec-fission
0	0,82	0.9	$1,7 \cdot 10^{-4}$
0,2	0,64	1	$1,5 \cdot 10^{-4}$
0,4	0,52	1,25	$1,1 \cdot 10^{-4}$
0,6	0,45	1,5	$9,0 \cdot 10^{-5}$
0,8	0,41	2	$6,3 \cdot 10^{-5}$
1	0,37	3	$3,5 \cdot 10^{-5}$
2	0,26	5	$1,6 \cdot 10^{-5}$
3	0,20	10	$5,9 \cdot 10^{-6}$
4	0,16	25	$1,7 \cdot 10^{-6}$
5	0,13	50	$7,8 \cdot 10^{-7}$
6	0,12	100	$3,5 \cdot 10^{-7}$
8	0,09	200	$1,8 \cdot 10^{-7}$
10	0,074	300	$1,2 \cdot 10^{-7}$
15	0,052	400	$8,5 \cdot 10^{-8}$
20	0,043	500	$6,9 \cdot 10^{-8}$
30	0,031	800	$4,6 \cdot 10^{-8}$
40	0,023	1000	$3,8 \cdot 10^{-8}$
60	0,016	—	—

Table 2

Gamma activity of fission fragments in the explosion of a 20-megaton bomb -- G_{20mt}, Mev/sec, and G_{20mt}, curie

t	G_{20mt}, Mev/sec	G_{20mt}, curie, at the following quantum energy, Mev
1 sec.....	$1{,}1 \cdot 10^{24}$	$3 \cdot 10^{13}$
2 minute.....	$4{,}8 \cdot 10^{22}$	$1{,}3 \cdot 10^{18}$
1 hour.....	$44 \cdot 10^{20}$	$1{,}2 \cdot 10^{10}$
1 day.....	$5{,}1 \cdot 10^{18}$	$1{,}4 \cdot 10^{8}$
1 week.....	$6 \cdot 10^{17}$	$1{,}6 \cdot 10^{7}$
1 month.....	$1{,}5 \cdot 10^{17}$	$4 \cdot 10^{6}$
1 year.....	$1{,}4 \cdot 10^{15}$	$3{,}8 \cdot 10^{4}$
10 years.....	$6{,}6 \cdot 10^{13}$	$1{,}8 \cdot 10^{3}$
100 years.....	$1{,}0 \cdot 10^{13}$	$2{,}7 \cdot 10^{2}$

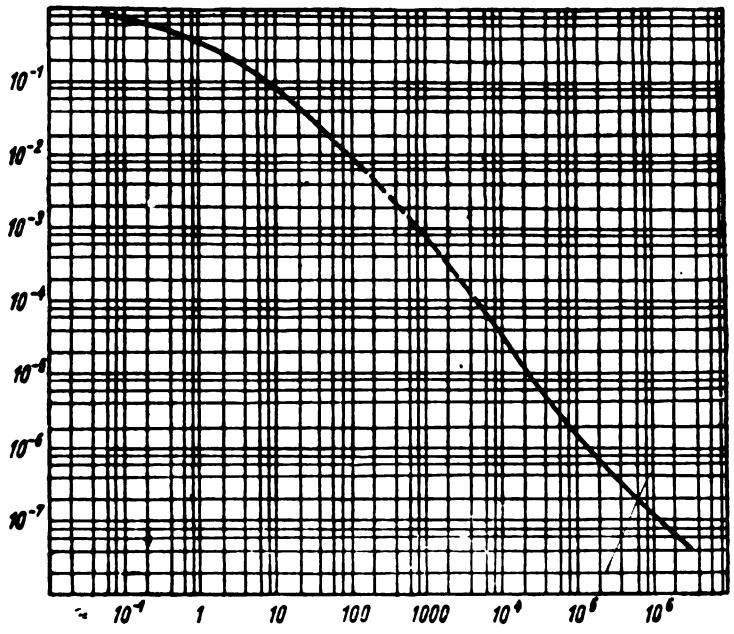

Figure 3. Activity of fission fragments u(t) Mev/sec-fission, at different instants of time after fission calculated per fission event.

A plot of dependence of u(t) on the time, plotted according to the data of Table 1, is shown in Figure 3. The value of the gamma activity of the fission fragments u(t), can be written in the form of a formula

$$u(t) = At^{-\nu} \text{ Mev/sec-fission} \qquad (2.1)$$

The values of A and ν for different intervals of time are listed in Table 3. The last column of the table indicates the maximum deviation of the values of u(t), calculated from formula (2.1) from the values given in Figure 3. The effective period of reduction of gamma activity is

$$T_{eff} = -\frac{1}{\frac{1}{u} \cdot \frac{du}{dt}} = \frac{t}{\nu}. \qquad (2.2)$$

Table 3

Values of the coefficients in the interpolation formulas for the calculation of the gamma activity of fragments at different time (2.1)

$$u(t) = At^{-\nu} \text{ Mev/sec-fission}$$

Time intervals for which the formula is applicable	Unit of measurements of time in the formula	A	ν	Some deviation from the data of Figure 3, percent
0.05 sec<t<1 sec	sec	0,4	0,27	10
1 sec<t<20 sec	"	0,4	0,72	10
20 sec<t<10 min	"	0,95	1,01	10
10 min<t<10 hr	"	7,1	1,32	10
10 hr<t<100 hr	"	5,9	1,31	10
100 hr<t<1000 hr		0,0276	0,89	10
10 hr<t<100 hr	hr	$1,3 \cdot 10^{-4}$	1,31	10
100 hr<t<1000 hr	"	$1,9 \cdot 10^{-5}$	0,89	10
10 min<t<200 hr	sec	7,1	1,33	15
20 sec<t<1000 hr	"	2	1,20	30

Inasmuch as γ is close to unity when t > 1 second, we have $T_{eff} \approx t$, i.e., it is approximately equal to the time elapsed from the instant of fission. For example, within one month T_{eff} is equal approximately to 1 month. When t > 1 year, the law of decrease of the gamma activity becomes nearly exponential, since the

gamma radiation is due essentially to the Cs^{137}, which has a half-life of 47.6 years. Many workers have noted that when $t < 1$ second the decrease in gamma activity is exponential with a half-life of 0.64 second.

Special experiments have shown that there is no gamma radiation with half-lives ranging from 10^{-3} to 0.5 second.

The radiation within the time interval from 10^{-8} to 10^{-3} second has not been investigated in detail. There are indications that radiation exists in the microsecond region [2].

Knowing u(t), one can calculate the energy radiated in individual time intervals t_1 - t_2 and during the entire time of decay

$$W_{t_1, t_2} = \int_{t_1}^{t_2} u\ (t)\ dt,$$

Table 4

Amount of gamma-radiation energy in the fission fragments after various time intervals

Time interval, seconds	0—1	0—2	0—5	0—10	0—20	0—3600	3600—∞	0—∞
Energy liberated, Mev/fission	0,54	0,82	1,35	1,80	2,35	6,8	1,6	8,4

Remark. The energy of the fission gamma radiation is 7.8 Mev/fission.

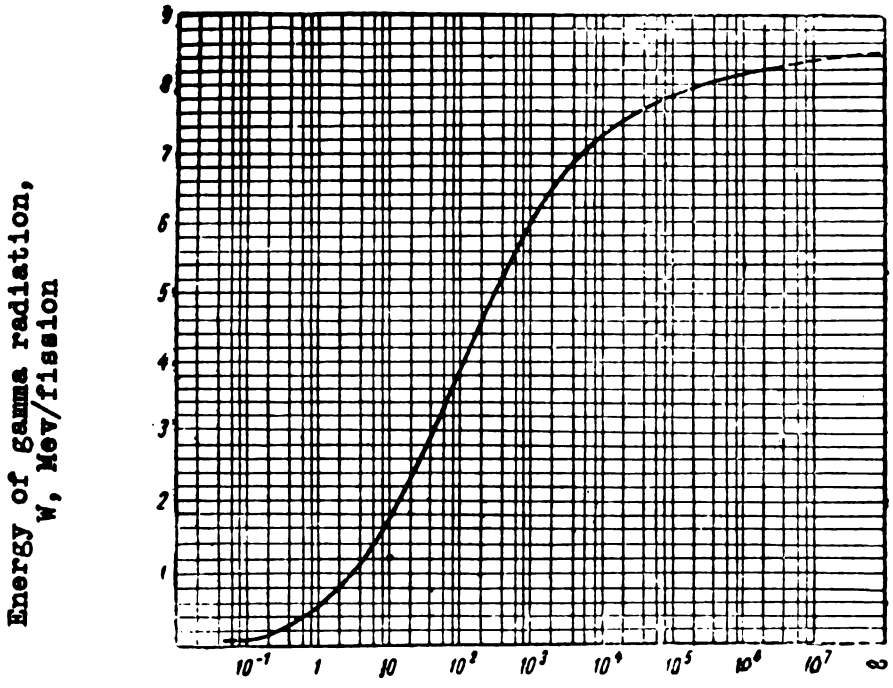

Figure 4. Amount of energy of gamma radiation of the fission fragments during different time intervals.

If we express u(t) by the power law (2.1), we get:

$$W_{t_1, t_2} = \frac{A}{\nu - 1}\left(\frac{1}{t_1^{\nu-1}} - \frac{1}{t_2^{\nu-1}}\right). \qquad (2.3)$$

The energy radiated during the total decay of the radioactive fragments is

$$W = \int_0^\infty u(t)\, dt = 8{,}4 \text{ Mev/fission.} \qquad (2.4)$$

The energy radiated during different time intervals is given in Table 4 and in Figure 4.

The spectrum of gamma rays of the fission products consists of a large number of lines. In Table 5 we give the available data on the average gamma radiation energy per quantum in different instants of time.

Table 5

Average energy per quantum of fragment gamma radiation

Radiation time, t	Average quantum energy, $\bar{\varepsilon}$, Mev	Method of determination
0—1 sec	2,2	Measurement with luminescent spectrometer [3]
1 sec–7 .	1,6	Measurements by the absorption method [4]
1 hr	1,2	
3 .	1,0	
20 .	0,7	
3 days	0,8	Calculated from data on the radiation spectrum of individual isotopes (see Appendix I)
30 days	1,0	
200 .	0,7	
3 years	0,7	
20 years	0,7	
100 .	0,7	

Note: The average energy per quantum of fission gamma radiation is 1.1 Mev.

Figure 5 shows the form of the spectral distribution of gamma rays of fission products (according to data of M. Ya. Gen, E. I. Intezarova, and M. S. Ziskin).

The characteristics of the gamma radiation of the fragments pertain to the overall gamma radiation of a mixture of all the formed fragments.

Information on the gamma radiation from individual fragments is given at the end of the book, in Appendix I, which contains a summary of the literature data on the energy and on the number of quanta and the half-life of the fragments, taken from the survey work by M. Ya. Gen, E. I. Intezarova and M. S. Ziskin.

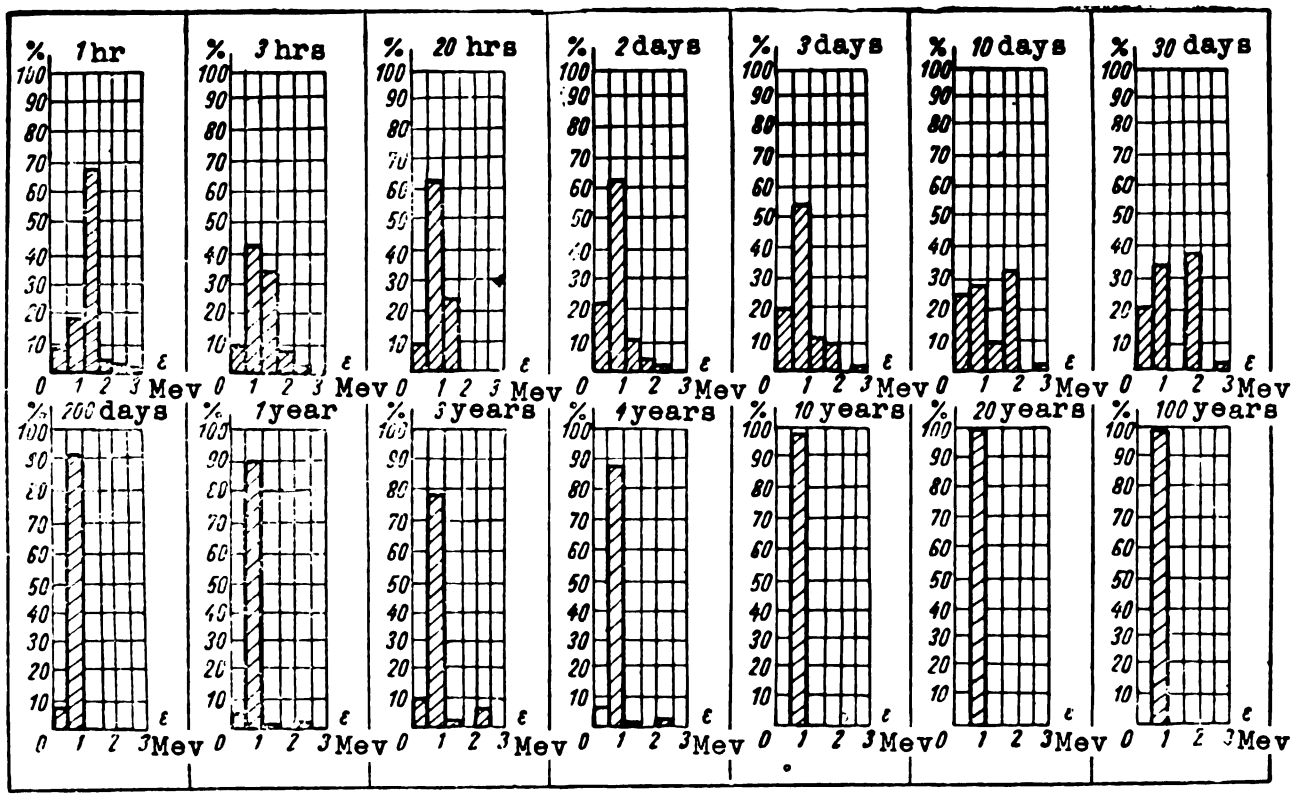

Figure 5. Spectral distribution of gamma radiation of fission fragments in different instants of time after fission. The abscissa represent the quantum energy. The ordinates represent the percentage of energy radiated in a given spectral interval.

3. GAMMA RADIATION IN THE CAPTURE OF NEUTRONS BY NITROGEN.

Part of the short-lived gamma radiation in an atomic explosion represents radiation released upon capture of neutrons by nitrogen, N^{14}. According to data by Kinsey, Bartholomew, and Walker [5] 10.82 Mev are liberated per fission event in the form of gamma quanta (determined by the mass defect). The capture cross section is 0.1 barn $\pm$ 0.05 [6], i.e., it is 16 times smaller than the cross section of the competing reaction N^{14} (n, p) C^{14}. Thus, each neutron absorbs in air causes the radiation of 10.82/17 = = 0.64 Mev of gamma-ray energy. Since 1.5 free neutrons (U^{235}) or 2 neutrons (Pu^{239}) are released during one fission event, if all the neutrons are absorbed by the nitrogen of the air, a total of 0.96 -- 1.28 Mev/fission of gamma radiation is released. The data on the spectrum of the gamma radiation are given in Reference [5]. The measurements were carried out with the aid of a paired spectrometer, so that the data on the spectrum are available only for quantum energies > 4 Mev. The question of the presence of gamma radiation with energy of 4 Mev or less remains open. It is therefore not known what fraction of the energy from the 10.82 Mev is for the hard gamma radiation measured in Reference [5]. There are grounds for assuming, that the greater part of the radiation energy is in the measured part of the spectrum.

Table 6 gives information on the energy of the quanta and the relative intensity of the capture radiation from nitrogen.

Table 6

Spectrum of gamma radiation of the reaction N^{14} (n, γ) N^{15} (hard part of the spectrum)

Quantum energy, Mev	4,48	5,29	5,55	6,32	7,16	7,36	8,28	9,16	10,82
Relative intensity, percent	18,3	30,5	2,44	12,2	0,6	4,9	2,4	0,6	6,1

Remarks:
1) 45 percent of the hard part of the spectrum is due to quanta with energy 5.3 - 6.3 Mev;
2) 15 percent of the energy is due to quanta with energy greater than 7 Mev.

4. GAMMA RADIATION FROM ACTIVATED EARTH.

The upper layer of the earth becomes a source of gamma rays as a result of capture of neutrons and accompanying formation of

radioactive isotopes of the elements contained in the earth.

The gamma radiation from the earth is released during the instant of neutron capture (~8 Mev per captured neutron for all elements with the exception of hydrogen, which releases 2.2 Mev upon capture of a neutron) and during the subsequent decay of the artificial radioactive nuclei. We shall consider henceforth only radiation from the decay of radioactive isotopes, which make up a substantial part of the residual gamma radiation in the region of the epicenter of the explosion.

For a given neutron flux, the intensity and the energy of the gamma quanta is determined by the elements contained in the upper layer of the earth. It can differ in different places, but a list of elements of practical importance is not long: 99.4 percent of the weight of the earth's crust is made up of 15 elements.

Table 7* gives the average composition by elements of the earth's crust. The same table gives also data on the gamma radiation from the radioactive isotopes obtained by neutron capture, the capture cross sections, and other information.

The values of G_i and λ_i given in Table 7 make it possible to determine g -- the specific gamma activity of the earth during the instant of time t after irradiation

$$g = \rho \Pi \sum_i G_i \lambda_i e^{-\lambda_i t} \text{ Mev/sec·cm}^3, \qquad (4.1)$$

where Σ -- sum over all the elements contained in the earth;

ρ -- specific gravity of the earth, g/cm^3;

G_i -- activity of the element per gram of earth;

Π -- flux of slow neutrons in the place of activation, over the entire time of irradiation on neutrons, neutrons/cm^2.

The column Σ contains the sum of all the activation cross sections in one gram of dry earth, which amounts to 8.9×10^{-4} cm^2/g, and the neutron capture cross section in one gram of earth, which amounts to 5×10^{-3} cm^2/g. Thus, only one-sixth of the total amount of neutrons absorbed in dry earth leads to activation of the soil. In moist earth, the capture cross section is increased (owing to the hydrogen in the water), so that the fraction of neutrons which produce artificial radioactivity is decreased.

The value of g may vary, depending on the composition of the earth. For a considerable part of the surface of the earth's sphere these variations are not large enough to influence greatly the gamma radiation, but in individual localities the deviations from the average composition may be considerable and may produce a unique pattern of gamma radiation.

By way of an example, let us calculate g for a locality in which the soil has an element composition that coincides with the average element composition of the earth's crust, as given in Table 7.

*Table 7 was made up by V. N. Sakharov.

The specific gravity of dry earth is assumed to be 1.7 g/cm^3, the water contents -- 0.1 g/cm^3, the overall specific gravity -- 1.8 g/cm^3. The neutron capture cross section per gram of such earth is 6.1 x 10^{-3} cm^2/g,* and the activation cross section is 0.9 x 10^{-3} cm^2/g.

Figure 6 shows the values of g(t) at different instants of time.

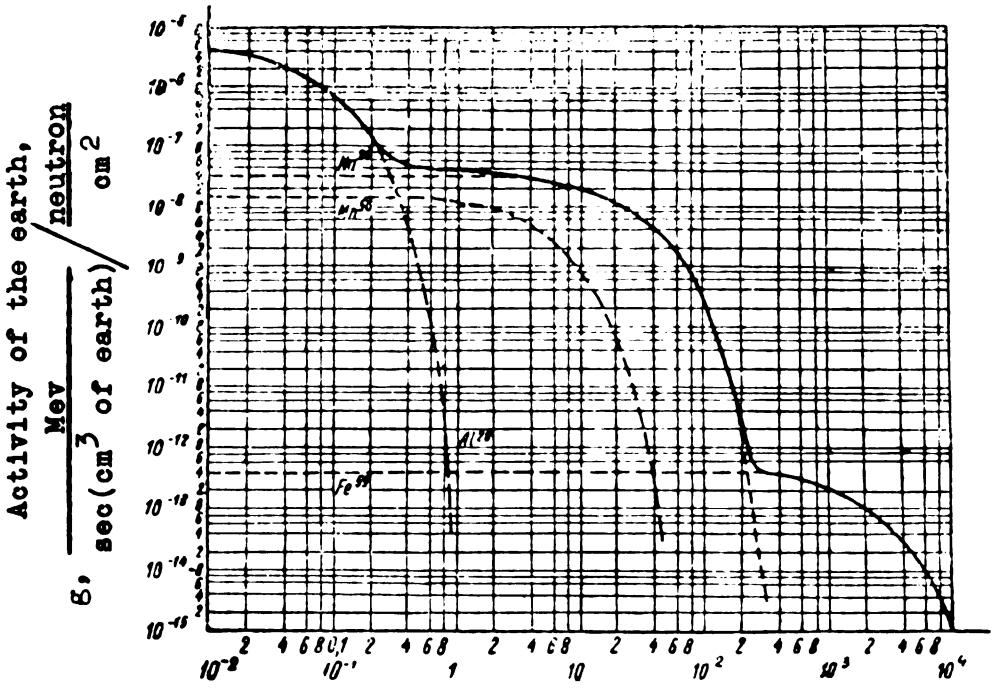

Figure 6. Activity of the earth, g, due to activation by neutrons at different instants of time after instantaneous irradiation. The dashed curves denote the specific activity of different elements of the earth in accordance with the chemical composition of the earth's crust (Table 7).

It is seen from Table 7 and Figure 6, that gamma radiation from Al^{28} predominates within time intervals from 0 to 15 minutes, Na^{24} predominates from 15 minutes to 200 hours, and Fe^{59} predominates above 300 hours.

During the time interval from 2 - 3 hours to 5 - 10 hours, gamma radiation from Mn^{56} appears against the background of the gamma radiation of Na^{24}.

*Including the capture in the water, the contents of which is 0.1 g/cm^3.

Let us determine what fraction of neutrons captured in the earth activates the foregoing characteristic elements. For this purpose it is necessary to divide the activation cross section of each element in one gram of earth by the sum of the capture and activation cross sections of the earth, 7×10^3 cm^2/g.

The formation of Al^{28} requires 5.4×10^{-2} of all the neutrons captured in the earth, while the fractions for Na^{24}, Mn^{56}, and Fe^{59}, are 5.4×10^{-2}, 1.5×10^{-2}, and 1.8×10^{-4}, respectively.

Figure 6 shows the intervals of time in which gamma radiation from individual elements predominates.

Owing to the presence of a small number of elements forming isotopes with long half-lives in the earth (for example, Co^{60} with $T_{1/2} = 5.3$ years), prolong radioactivity may occur, which is noticeable after the decay of Fe^{59}.

The residual gamma radiation in the region of the epicenter may be due not only to the activation of the earth, but also to fission fragments settling on the earth.

To clarify the role of the induced activity of the earth (particularly in a surface explosion) it is of interest to estimate the largest possible gamma radiation from the earth, i.e., that obtained when half of the neutrons of the earth are absorbed and there is no self absorption of gamma radiation in the earth, and to compare it with the gamma radiation of the fragments.

It is assumed that the earth captures one neutron per fission. Data on the composition of the earth and on the activation cross sections are listed in Table 7. The most important contribution to the gamma radiation of such an earth is made, up to 200 hours, by the following:

during the first minutes -- aluminum ($T_{1/2} = 2.3$ minutes, 1.8 Mev/decay),

during the first hours -- manganese ($T_{1/2} = 2.57$ hours, 1.2 Mev/decay),

during the first hours -- sodium ($T_{1/2} = 15$ hours, 4.2 Mev/decay),

after 200 hours -- iron ($T_{1/2} = 47$ days, 1.2 Mev/decay).

The gamma ray energy radiated starting after ten seconds (the arbitrary termination of the action of the fragment cloud) to infinity, is 6.6 Mev/fission from the fragments (Table 4) and 0.48 Mev per fission from the earth (Table 7). The contributions from sodium, aluminum, manganese, and iron are 0.31, 0.13, 0.02, and 3×10^{-1} Mev per captured neutron, respectively.

Thus, even under conditions most favorable for the activation of the earth, when half of all the neutrons are absorbed, the energy radiated from the earth as a source of residual radiation is one order of magnitude less than the energy of the fragments.

The only elements that participate in the production of residual radiation from the earth, lasting over several days, are sodium and iron, which radiate 0.31 and 3×10^{-4} Mev per fission, respectively. The radiation of the fragments in the interval from one hour to infinity amounts to 1.6 Mev/fission, i.e., during the 10 - 200 hours that the sodium is active, the energy radiated by the earth is closer (although it is several times smaller) to the energy radiated by the fragments.

Average Composition by Elements of the Earth's

Characteristic of Element	O	Si	Al
Abundance in the earth's crust, percent	46,5	27,7	7,85
Mass number	18	—	27
Content and natural isotope mixture, percent	0,2	Does not yield γ-rays	100
Half life $T_{1/2}$	27 sec	—	2,3 min
Decay constant λ, sec^{-1}	$2,57 \cdot 10^{-2}$	—	$5,02 \cdot 10^{-3}$
Activation cross section of the isotope by thermal neutrons, σ_{ac}, barn	$2,1 \cdot 10^{-4}$	—	0,215
Activation cross section, calculated for the natural isotope mixture σ_{ac}, barn	$4,2 \cdot 10^{-7}$	—	$2,15 \cdot 10^{-1}$
Activation cross section per gram of earth, S_{ac}, cm^2/g of earth	$7,35 \cdot 10^{-9}$	—	$3,77 \cdot 10^{-4}$
Cross section for the capture of thermal-neutrons by the natural mixture of isotopes, σ_{cap}, barn	$2 \cdot 10^{-3}$	—	$2,15 \cdot 10^{-1}$
Cross section for the capture per gram of earth, S_{cap}, cm^2/g of earth	$3,7 \cdot 10^{-5}$	—	$3,77 \cdot 10^{-4}$
Energy of emitted gamma quanta, Mev	1,7 (70%)	—	1,8 (100%)
Energy of gamma radiation per decay of the isotope, Mev/decay	0,85	—	1,8
Energy of gamma radiation per neutron capture in the earth, Mev/cap. neutron	$1,25 \cdot 10^{-6}$	—	$1,36 \cdot 10^{-1}$
Energy of gamma radiation emitted from gram of the element by an active neutron flux of 1 neutron cm^2, Mev/g element neutron/cm^2	$1,35 \cdot 10^{-8}$	—	$8,6 \cdot 10^{-3}$
Energy of gamma radiation emitted from 1 gram of earth, activated by a neutron flux of 1 neutron/cm^2, Mev/g of earth neutron/cm^2 (G_1)	$6,25 \cdot 10^{-9}$	—	$6,8 \cdot 10^{-4}$
Gamma activity on individual elements per gram of earth (G_1) at different instants of time			
t = 0 hours	$1,6 \cdot 10^{-10}$	—	$3,4 \cdot 10^{-6}$
t = 1 hour	—	—	$5,3 \cdot 10^{-14}$
t = 4 hours	—	—	—
t = 20 hours	—	—	—
t = 200 hours	—	—	—
t = 2000 hours	—	—	—

Table 7

Crust and Gamma Radiation from Activated Earth.

Fe	Ca	Na	K	Mg	Ti
4,85	3,75	2,8	2,62	2,25	0,75
58	46	23	41	26	50
0,34	0.0032	100	6,9	11,3	5,34
47,1 days	4,3 days	15 hrs	12,5 hrs	9,4 min	6 min
$1,7 \cdot 10^{-7}$	$1,87 \cdot 10^{-6}$	$1,28 \cdot 10^{-5}$	$1,55 \cdot 10^{-5}$	$1,23 \cdot 10^{-3}$	$1,92 \cdot 10^{-3}$
0,7	0,25	0,51	1,0	0,05	0,14
$2,4 \cdot 10^{-3}$	$8 \cdot 10^{-6}$	$5,1 \cdot 10^{-1}$	$6,9 \cdot 10^{-2}$	$5,65 \cdot 10^{-3}$	$7,5 \cdot 10^{-3}$
$1,26 \cdot 10^{-6}$	$4,5 \cdot 10^{-9}$	$3,74 \cdot 10^{-4}$	$2,8 \cdot 10^{-5}$	$3,15 \cdot 10^{-6}$	$7,1 \cdot 10^{-7}$
2,43	$0,43 \cdot 10^{-1}$	$5,1 \cdot 10^{-1}$	1,97	$5,9 \cdot 10^{-2}$	5,6
$1,27 \cdot 10^{-3}$	$2,42 \cdot 10^{-4}$	$3,74 \cdot 10^{-4}$	$8,0 \cdot 10^{-4}$	$3,3 \cdot 10^{-5}$	$5,3 \cdot 10^{-4}$
0,2 (2,8%) 1,1 (56%) 1 28 (43%)	1,4 (81%)	1,4 (100%) 2,8 (100%)	1,5 (25%)	0,84 (100%) 1,05(20%)	0,32 (70%)
1,2	1,1	4,2	0,37	1,05	0,22
$3 \cdot 10^{-4}$	$1 \cdot 10^{-6}$	$3,15 \cdot 10^{-1}$	$2,05 \cdot 10^{-3}$	$6,6 \cdot 10^{-4}$	$3,15 \cdot 10^{-5}$
$3,1 \cdot 10^{-5}$	$1,3 \cdot 10^{-6}$	$5,6 \cdot 10^{-2}$	$4 \cdot 10^{-4}$	$1,45 \cdot 10^{-4}$	$2,05 \cdot 10^{-5}$
$1,5 \cdot 10^{-6}$	$5 \cdot 10^{-9}$	$1,57 \cdot 10^{-3}$	$1,05 \cdot 10^{-5}$	$3,3 \cdot 10^{-6}$	$1,56 \cdot 10^{-7}$
$2,55 \cdot 10^{-13}$	$9,35 \cdot 10^{-15}$	$2,0 \cdot 10^{-8}$	$1,6 \cdot 10^{-10}$	$4,0 \cdot 10^{-9}$	$4 \cdot 10^{-8}$
$2,55 \cdot 10^{-13}$	—	$1,9 \cdot 10^{-8}$	—	—	—
$2,55 \cdot 10^{-13}$	—	$1,65 \cdot 10^{-8}$	—	—	—
$2,53 \cdot 10^{-13}$	—	$8 \cdot 10^{-9}$	—	—	—
$2,53 \cdot 10^{-13}$	—	$2 \cdot 10^{-12}$	—	—	—
$7,5 \cdot 10^{-14}$	—	—	—	—	—

Characteristic of Element	P	H	Mn
Abundance in the earth's crust, percent	0,11	0,11	0,075
Mass number	—	—	55
Content and natural isotope mixture, percent	Does not yield γ-rays	Does not yield γ-rays	
Half life $T_{1/2}$	—	—	2.57 hrs
Decay constant λ, sec^{-1}	—	—	$7,47 \cdot 10^{-5}$
Activation cross section of the isotope by thermal neutrons, σ_{ac}, barn	—	—	12,7
Activation cross section, calculated for the natural isotope mixture σ_{ac}, barn	—	—	12,7
Activation cross section per gram of earth, S_{ac}, cm^2/g of earth	—	—	$1,05 \cdot 10^{-4}$
Cross section for the capture of thermal-neutrons by the natural mixture of isotopes, σ_{cap}, barn	$1,9 \cdot 10^{-1}$	$3,3 \cdot 10^{-1}$	12,7
Cross section for the capture per gram of earth, S_{cap}, cm^2/g of earth	$4,1 \cdot 10^{-6}$	$2,2 \cdot 10^{-4}$	$1,05 \cdot 10^{-4}$
Energy of emitted gamma quanta, Mev	—	—	0,85 (69%) 1,8 (18,5%) 2,13(12,5%)
Energy of gamma radiation per decay of the isotope, Mev/decay	—	—	1,2
Energy of gamma radiation per neutron capture in the earth, Mev/cap. neutron	—	—	$2,55.10^{-2}$
Energy of gamma radiation emitted from gram of the element by an active neutron flux of 1 neutron/cm^2, Mev/g element neutron/cm^2	—	—	$1,7 \cdot 10^{-1}$
Energy of gamma radiation emitted from 1 gram of earth, activated by a neutron flux of 1 neutron/cm^2, Mev/g of earth neutron/cm^2 (G_i)	—	—	$1,27 \cdot 10^{-4}$
Gamma activity on individual elements per gram of earth (G_i) at different instants of time			
t = 0 hours	—	—	$9,5 \cdot 10^{-9}$
t = 1 hour	—	—	$7,2 \cdot 10^{-9}$
t = 4 hours	—	—	$3,2 \cdot 10^{-9}$
t = 20 hours	—	—	—
t = 200 hours	—	—	—
t - 2000 hours	—	—	—

Table 7 (continued)

F	Cl	S	Sum	g/ρ
0,075	0,037	0,037	—	—
19	37	37	—	
100	24,6	0,017	—	—
10,7 sec	37,3 min	5,04 min	—	—
$6,5 \cdot 10^{-2}$	$3,1 \cdot 10^{-4}$	$2,3 \cdot 10^{-3}$	—	—
0,009	0,56	0,14	—	—
$9 \cdot 10^{-3}$	$1,4 \cdot 10^{-1}$	$2,4 \cdot 10^{-5}$	—	—
$2,14 \cdot 10^{-7}$	$8,8 \cdot 10^{-7}$	$1,7 \cdot 10^{-10}$	$8,9 \cdot 10^{-4}$	—
$1 \cdot 10^{-2}$	31,6	$4,9 \cdot 10^{-1}$	—	
$2,4 \cdot 10^{-7}$	$2 \cdot 10^{-4}$	$3,4 \cdot 10^{-6}$	$5,0 \cdot 10^{-3}$	—
1,63 (93%)	1,6 (31%) 2,12 (47%)	2,75 (90%)	—	
1,6	1,5	2,5	—	
$6,9 \cdot 10^{-5}$	$2,63 \cdot 10^{-4}$	$8,5 \cdot 10^{-6}$	0,478 Mev/ captured neutrons	
$4,6 \cdot 10^{-4}$	$3,5 \cdot 10^{-3}$	$1,1 \cdot 10^{-6}$	—	—
$3,42 \cdot 10^{-7}$	$1,32 \cdot 10^{-6}$	$4,25 \cdot 10^{-10}$	—	—
$2,2 \cdot 10^{-3}$	$4,1 \cdot 10^{-10}$	$1,0 \cdot 10^{-12}$		$3,4 \cdot 10^{-6}$
—	—	—	—	$2,6 \cdot 10^{-8}$
—	—	—	—	$1,97 \cdot 10^{-6}$
—	—	—	—	$8 \cdot 10^{-9}$
—	—	—	—	$2,2 \cdot 10^{-12}$
—	—	—	—	$7,5 \cdot 10^{-14}$

In the case of a surface explosion of a pure hydrogen bomb, the number of neutrons released per unit energy is one order of magnitude greater than that produced by an explosion of a fission bomb. One can therefore expect that the radiation

[something missing in Russian in the transition from p. 30 to p. 31.]

This does not mean in itself that the surface explosion of a pure hydrogen bomb can contaminate tremendous areas of "trail" to the same extent as a surface explosion of a fission bomb. The energy of the activated soil, given above, is radiated by elements which are contained in a layer of earth 30 centimeters thick. To produce a "trail" with the same amount of energy as liberated in a fragment "trail" it is necessary that this entire layer of activated soil be carried away and settled in the same manner as the fragments are carried away and settled.

The mass of the earth is less dispersed than the dust on which the fragments are condensed. Therefore the conditions under which earth carried away and settled are not favorable to the formation of a trail of the same extent and activity as a fragment "trail," even if the activity of the earth is equal to the activity of the fratments, as may happen in the case of an explosion of a pure hydrogen bomb. The difference in the formation of a "trail" from the earth and from the fragments is difficult to estimate quantitatively, and we shall therefore confine ourselves only to the foregoing estimate of the radiated energy.

Let us compare the kinetics of the gamma radiation from earth and from fragments.

Table 8 gives the intensity of emission radiation of fragments and earth under the assumption that the earth captures one neutron per fission.

Table 8

Intensity of gamma radiation from the earth, $u_e(t)$, and of fragments $u(t)$

Time after explosion, hours	Intensity of radiation, Mev/sec-fission		$\frac{u_e(t)}{u(t)}$ 100
	Of the earth	Of the fragments	
1/6	$4{,}7 \cdot 10^{-6}$	$1{,}4 \cdot 10^{-3}$	0,3
1	$5 \cdot 10^{-7}$	$1{,}5 \cdot 10^{-4}$	0,3
2	$4{,}5 \cdot 10^{-7}$	$6{,}3 \cdot 10^{-5}$	0,7
5	$3{,}4 \cdot 10^{-7}$	$1{,}6 \cdot 10^{-5}$	2,1
10	$2{,}5 \cdot 10^{-7}$	$5{,}9 \cdot 10^{-6}$	4,2
18	$1{,}7 \cdot 10^{-7}$	$2{,}75 \cdot 10^{-6}$	6,2
26	$1{,}2 \cdot 10^{-7}$	$1{,}6 \cdot 10^{-6}$	7,5
50	$4 \cdot 10^{-8}$	$7{,}8 \cdot 10^{-7}$	5,1
100	$4 \cdot 10^{-9}$	$3{,}5 \cdot 10^{-7}$	1,1
150	$4 \cdot 10^{-10}$	$2{,}4 \cdot 10^{-7}$	0,2

It is seen from the table that up to 5 hours after the explosion, u_e does not exceed 2 percent of u. From 5 to 50 hours u_e is approximately 20 times smaller than u; after 50 hours the value of u_e again diminishes rapidly compared with u. In a pure hydrogen explosion $u_e(t)$ can increase by approximately by one order of magnitude.

It is seen from the table that in the interval from 1 to 10 hours the fragments decay more rapidly than the active soil, u_e/u increases with increasing t; in the interval from 10 to 50 hours, the law of decrease of activity with time is practically the same for the soil and for the fragments u_e/u = const; after 50 hours the induced activity diminishes more rapidly than the activity of the fragments (u_e/u decreases with increasing t).

In the interval from 10 to 50 hours it is difficult to distinguish between the induced activity and the fragment activity, judging from the kinetics of the decrease in activity. These activities can be distinguished by the kinetics of the decrease by means of measurements before 10 hours after 50 hours. For example, the ratio of the one-hour and five-hour activities of the soil and the fragments, which differ greatly from each other, are:

$$\frac{u_e(1\text{ hr})}{u_e(5\text{ hr})} = 1.5; \quad \frac{u(1\text{ hr})}{u(5\text{ hr})} = 9.1.$$

In the case of explosions in the air, the residual radiation is determined by the induced activity of the earth.

In surface explosions, near the epicenter, i.e., in the region where the fragments settle, the residual radiation is determined by the fragments. It is seen from Table 8 that if 1 percent of the fragments settles in the region of the epicenter, then the residual radiation is determined by the fragments and not by the earth.

Away from the epicenter (the distance depends on the explosion energy), the residual radiation is determined in the case of surface explosion by the induced activity.

At intermediate distances, the earth and the fragments produce comparable contributions.*

In those cases when the residual radiation is determined by the activity of the earth, the dose power can be connected with the specific activity of the earth or with the neutron flux, and it can be calculated. This calculation will be given in Section 9.

---

*It must be noted that the radiation of the fragments can appear not only where they have settled, but also in neighboring places where they are not located, at a distance compared with the range of the quanta. In this region the decrease in the dose power may be of either a fragment or a mixed character.

CHAPTER II

PROPAGATION OF GAMMA RADIATION IN ABSORBING MEDIA

5. "GOOD" AND "POOR" GEOMETRY.

For almost all cases of action of gamma rays of atomic explosion, it is characteristic that the doses of gamma rays are produced not only by direct radiation of the sources, which has passed through the absorption layer without interacting with the matter, but also by the scattered quanta, which have experienced single or multiple scattering in the matter.

In many atomic explosions the scattered radiation is of decisive significance in the formation of the gamma-ray doses.

The important role of the scattered radiation is due to the fact that the gamma radiation propagates in an atomic explosion in a broad beam, and passes through thick layers of absorber.

Figure 7 illustrates the features of the propagation of gamma rays in broad and narrow beams.

Figure 7a shows the passage of a narrow parallel beam of gamma rays through a thin absorber. The detector receives only the direct radiation, i.e., radiation which passes through the absorber without interacting with the atoms, i.e., it is neither absorbed or scattered. The scattered radiation drops out of the beam and does not enter the detector. Such conditions of propagation of radiation are called "good" geometry. In these conditions when the radiation passes through the absorber, there is no change in the spectral composition and in the directivity of the radiation striking the detector, the number of gamma quanta in the beam N, changes in accordance with the well-known law

$$N = N_0 e^{-\mu x},$$

N_0 -- flux of gamma quanta ahead of the absorber; N -- flux of gamma quanta passing through the absorber;

μ -- linear coefficient of absorption of radiation.

Accordingly, the intensity of radiation J varies as

$$J = J_0 e^{-\mu x}. \qquad (5.1)$$

These formulas are valid for absorption of monochromatic radiation. When the radiation has a complicated spectral composition, the intensity of each spectral opponent attenuates in accordance with analogous exponential law, with a different value of μ.

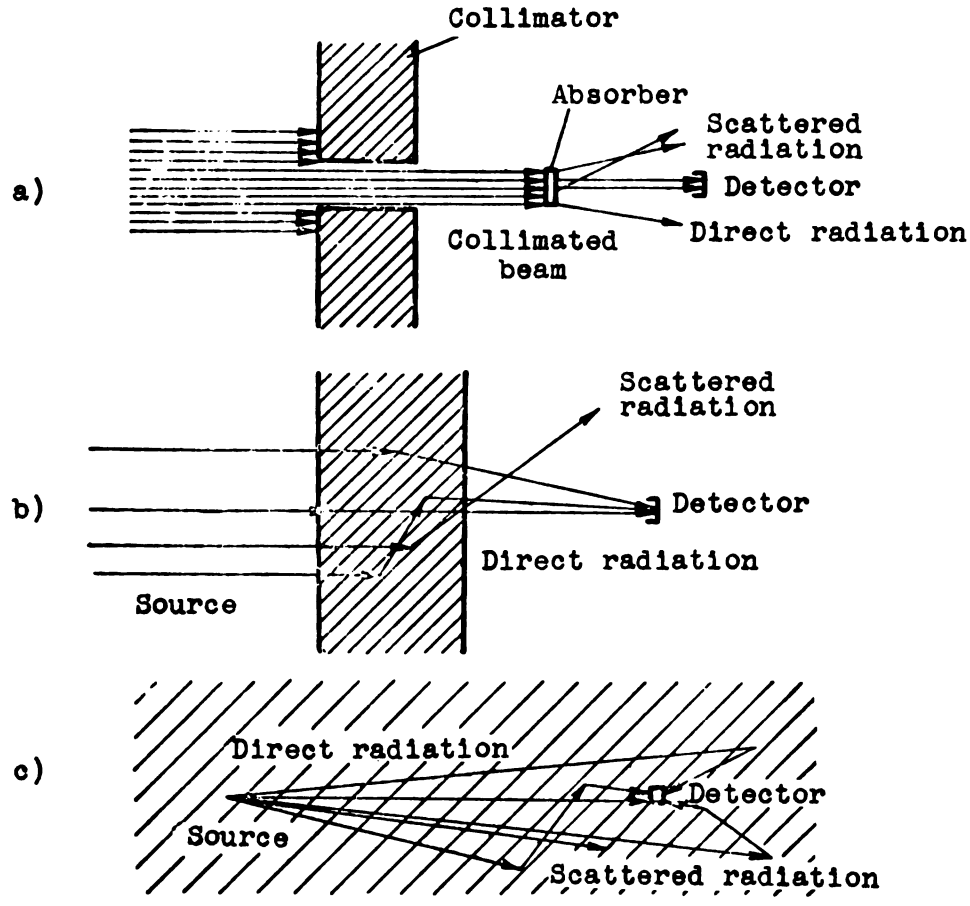

Figure 7. Passage of a narrow beam of gamma rays through a thin scatterer (a) and of a broad beam of gamma rays through a thick scatterer (b) and inside an absorbing medium (c). Case a -- "good" geometry. Case b and c -- "poor" geometry.

Figures 7b and 7c show the characteristic features of the propagation of a broad beam of gamma rays through a thick layer of absorber (b) and inside an absorbing medium (c). In these cases the detector receives not only the direct beam, but also scattered radiation. Such conditions of propagation of radiation are called "poor" geometry.

Under conditions of "poor" geometry, the attenuation of the intensity of radiation with absorber thickness is slower than according to the exponential formula (5.1), since fluxes of scattered radiation are added to the flux of radiation of the direct beam in the absorber.

With this, the spectral composition and the directivity of the radiation do not remain constant along the path of the radiation in the absorber, because the scattered radiation, adding to the

direct radiation, differs from the latter in spectral composition and in direction of propagation.

The amount of scattered radiation added to the direct radiation, its spectral composition, and its angular distribution, all depend on the relative placement of the sources of the gamma rays, the absorbing media, the detectors, and the properties of the absorbing media.

A complete solution of the problem of propagation of radiation under conditions of "poor" geometry should contain information on the intensity, spectral composition, and angular distribution of radiation in any point of space.

To obtain the solution it is necessary to know the geometrical locations of the sources and absorbers, the spectral composition of the primary radiation, and the atomic number and density of the absorbers. The solution of this problem is treated in the theory of multiple scattering of gamma quanta.

The problem can be solved both theoretically and experimentally. Theoretically, knowing the probability of the elementary processes of interaction of the quanta with the matter, it is possible in principle to solve any problem of multiple scattering of gamma rays. What is entailed here is usually a large volume of computation. The use of electronic computers makes it possible to solve the kinetic equations that describe multiple scattering of quanta.

By now there exist a large amount of computational data on the propagation of broad beams of gamma rays in absorbing media, and information keeps on accumulating.

In many cases it is possible to prepare an experimental model, in which the investigated conditions of propagation of gamma rays are produced either on the natural scale or on some reduced scale. With the aid of such models it is possible to solve experimentally particular problems in the propagation of gamma rays and verify the theoretical results obtained by computational methods.

6. ELEMENTARY PROCESSES OF INTERACTION OF GAMMA QUANTA WITH MATTER.

Forms of interaction of radiation with matter. Elementary processes of interaction of gamma quanta with matter have been discussed in sufficient detail in the physical literature and in textbooks; we shall therefore confine ourselves only to an exposition of a minimum of information, necessary to designate the quantities and necessary for convenience in understanding the less universally known sections of the book.

The passage of gamma radiation through matter is accompanied by absorption and scattering of gamma quanta. In the problems of interest to us, the following three types of interaction between radiation and matter are basic: photoelectric absorption, Compton scattering, and formation of electron-positron pairs. The remaining processes -- coherent scattering, nuclear photoeffect, nuclear scattering, and others, can be neglected.

The foregoing processes lead to absorption of gamma-quantum energy and simultaneously produce in the medium various secondary gamma radiations: fluorescence, bremsstrahlung of electrons, and annihilation radiation.

All the secondary sources are considerably softer than the primary source. An estimate has shown that in the problems of interest to us, the secondary radiation can be neglected, and will therefore be disregarded here.

Photoelectric absorption. In photoelectric absorption, the gamma quantum, whose energy exceeds the binding energy of the electron in the atom, causes an electron to be removed from the atom.

The energy of the quantum is converted fully into kinetic energy of the knocked-out electron less the binding energy of the electron in the atom.

Thus, a quantum which experiences photoelectric absorption drops out completely from the beam of gamma rays. The consequence of the photoabsorption of a gamma quantum is secondary fluorescent radiation of the excited atoms. The probability of the photoeffect is particularly large compared with the probabilities of other processes at small values of quantum energies and at high atomic numbers Z of the absorber. For a given quantum energy, the photoeffect cross section increases with increasing atomic number approximately as $Z^{4.5}$. For a specified atomic number Z, the cross section of the photoeffect increases with decreasing energy [7] as $1/\varepsilon$ when $\varepsilon > 0.5$ Mev, and as $1/\varepsilon^3$ when $\varepsilon < 0.2$ Mev.

Table 9 gives the values of the energies of the gamma quanta, at which the photoeffect cross section σ_{ph} becomes equal to the Compton scattering cross section $a\sigma_C$, and the energies at which $\sigma_{ph} = (1/5)\, a\sigma_C$.

When the quantum energy is smaller than indicated in the column for $\sigma_{ph} = a\sigma_C$, the photoeffect becomes the predominant type of absorption.

In Table A15 of Appendix II we give the cross sections of the photoeffect σ_{ph}, calculated for one atom of matter. For comparison, the table gives also the cross section of the Compton scattering $a\sigma_C$, also calculated per atom.

Compton scattering. The Compton scattering takes place on the electrons of the atom. As a result of the scattering the quantum loses part of its energy and changes the direction of its initial motion.

Table 9

Quantum energy ε at which the cross section of the photoeffect is equal to and is 1/5 as small as the scattering cross section

Substance	ε, Mev, with	
	$\sigma_{ph} = a\sigma_C$	$\sigma_{ph} = 1/5\ a\sigma_C$
Nitrogen.....	0.02	0.04
Aluminum.....	0.05	0.08
Iron.....	0.12	0.2
Lead.....	0.5	1.5

The energy lost by the gamma quanta is converted into kinetic energy of the electron on which the scattering takes place. In the gamma-quantum energy region in which the Compton scattering is more probable than the photoeffect, it is possible to neglect the binding energy of the electron in the atom compared with the quantum energy. It can therefore be assumed that the Compton scattering occurs on the free electrons.

The values of the energy ε_e acquired by the recoil electron and of the energy ε_γ retained by the scattered quantum depend on the angle θ of deflection of the quantum from the initial direction:

$$\varepsilon_e = \frac{\varepsilon\alpha\,(1-\cos\theta)}{1+\alpha\,(1-\cos\theta)}\,,\quad \varepsilon_\gamma = \frac{\varepsilon}{1+\alpha\,(1-\cos\theta)} \tag{6.1}$$

(here α is the energy of the initial quantum, expressed in units mc^2 = 511 kev).

Thus, a quantum that experiences Compton scattering does not drop out of the gamma radiation in the matter, and merely loses part of its energy and changes its direction of motion. The energy lost in the scattering of a gamma quantum is equal to ε_e, i.e., the same energy that is transferred to the recoil electron.

The greatest energy $(\varepsilon_e)_{max}$ which can be transferred to an electron and hence lost by the gamma quantum, is

$$\varepsilon_{e\ max} = \frac{\varepsilon}{1+\dfrac{1}{2\alpha}}\,. \tag{6.2}$$

This occurs when the quantum is scattered by 180°, i.e., "backward" (the electron is emitted "forward" in this case). The energy of a quantum scattered by 180° is at a minimum and is equal to

$$\varepsilon_{\gamma\,min} = \frac{\varepsilon}{1+2\alpha} = mc^2\,\frac{\varepsilon}{mc^2+2\varepsilon}\,. \tag{6.3}$$

When $\varepsilon \gg mc^2$, this quantity cannot be greater than $mc^2/2$ = 250 kev, and when ε = 0.5 Mev, we have $\varepsilon_{\gamma min}$ = 170 kev, i.e., $\varepsilon_{\gamma min}$ depends little on the quantum energy when $\varepsilon > 0.5$ Mev.

At small scattering angles ($\cos\theta \approx 1$), i.e., when a quantum is scattered "forward," the energy of the scattered quantum differs little from the energy of the initial quantum, and the absorption of energy during the scattering is small. In this case the electron is emitted in a direction close to perpendicular to the motion of the quantum.

In Compton scattering, the gamma quantum may be scattered in all directions and the recoil electrons can be emitted only within the limits $\pi/2 \geq \theta \geq -\pi/2$, i.e., only in the "forward" direction.

The quanta are scattered preferably "forward."

The greater the quantum energy, the lower the probability of its scattering by a large angle. This can be seen from Figure 8, where the differential cross section of scattering of the quantum

by an angle θ is shown in relative units, as a function quantum energy (the differential "forward" scattering cross section is taken to be 1).

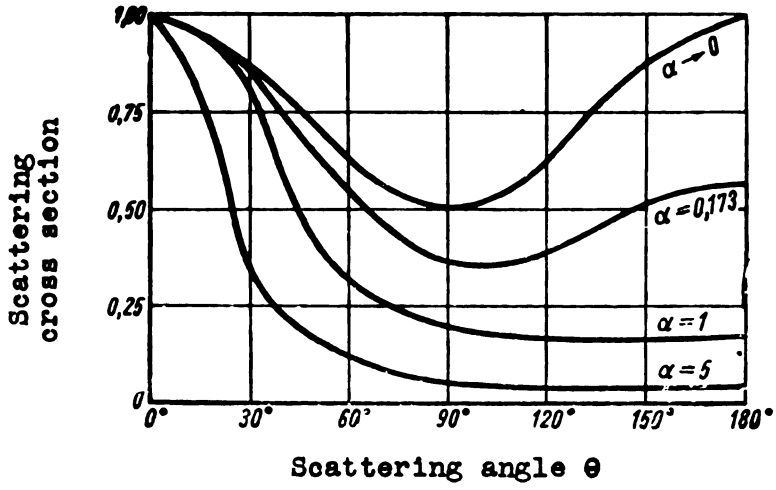

Figure 8. Differential cross section of scattering of quanta as a function in the scattering angle θ for different quantum energies $\varepsilon = \alpha mc^2$ [19].

The probability of "forward" scattering is independent of the quantum energy; with increasing quantum energy the probability of scattering by angles other than 0 decreases.

The probability of scattering of a quantum that passes through matter is characterized by the scattering cross section and is equal to the scattering cross section per square centimeter of square area (S, cm^2) for each square centimeter perpendicular to the quantum flux

$$S = N_e \sigma_C. \tag{6.4}$$

where σ_C is the scattering cross section per electron, and N_e is the number of electrons along the quantum path in a volume having a transverse cross section of 1 cm^2.

The scattering cross section per atom, $_a\sigma_C$, is Z times greater than the section per electron (Z -- atomic number of the substance):

$$_a\sigma_C = Z\sigma_C. \tag{6.5}$$

The distribution of the energy of a quantum that has experienced scattering, between the recoil electron and the scattered quantum, is characterized by cross sections σ_e and σ_γ, the energy transferred to the electron being $\varepsilon\sigma_e/\sigma_C$, and the energy remaining with the scattered quantum being $\varepsilon\sigma_\gamma/\sigma_C$ (ε -- initial energy of the quantum). It is obvious that

$$\sigma_C = \sigma_e + \sigma_\gamma. \qquad (6.6)$$

The scattering cross section decreases with increasing quantum energy. In Figure 9 and in Table A16 of Appendix II are given the values of σ, σ_e, and σ_C per electron as functions of the quantum energy.

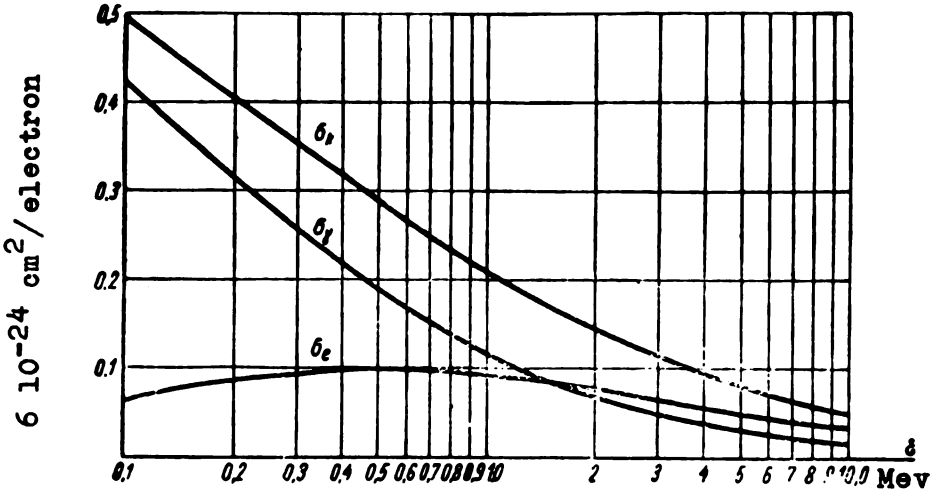

Figure 9. Cross section for Compton scattering, σ_C, for the transfer of energy to the electron σ_e, and for the transfer of energy to the quantum σ_γ, at different quantum energies.

If the dimensions of the scattering medium are sufficiently large, then a quantum scattered once can experience secondary, etc., scattering. Thus, multiple scattering of the quanta takes place in media whose dimensions are sufficiently large compared with the mean free path of the quanta. In each scattering the quantum loses part of its energy and changes its direction. As a result quanta with lower energies appear in the scattering medium, in addition to the primary quanta. The greater the scattering experienced by the quantum, the smaller these energies are.

Figure 10 shows the ratio of the average quantum energy after a single scattering to the initial energy of the quantum, as a function of ε. It is seen from the figure the smaller the quantum energy, the smaller the fraction of the energy that the quantum loses on the average in the scattering.

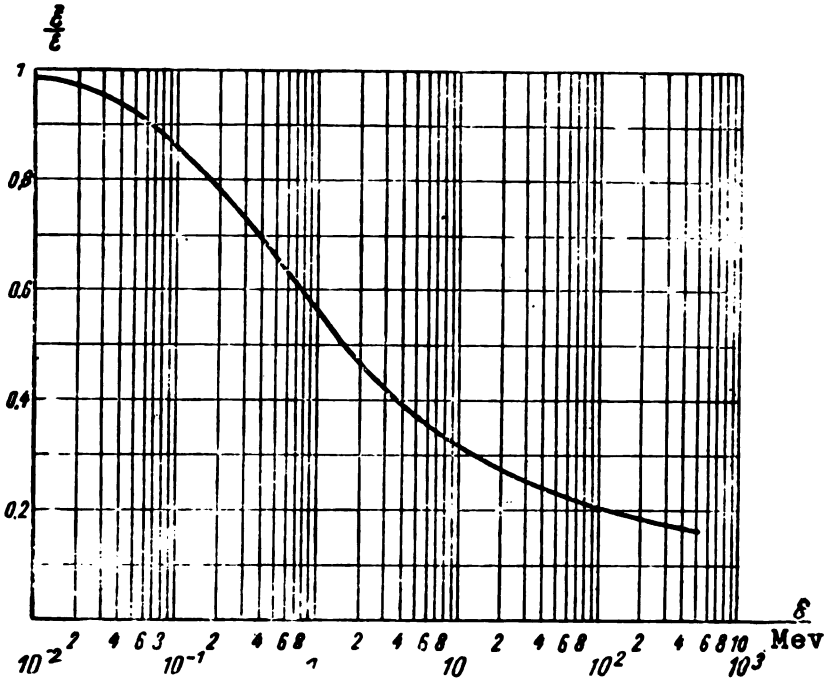

Figure 10. Ratio of the average quantum energy $\bar{\varepsilon}$ after single Compton scattering to the energy of the quantum prior to the scattering, for different quantum energies ε [20].

A limit on multiple scattering of the quantum in the medium is imposed by the photoeffect. When the quantum energy decreases to such a value that the photoeffect is more probable than Compton scattering, the gamma quantum is absorbed as a result of the photoeffect.

In air, the probability of the photoeffect becomes comparable with the probability of the Compton scattering (Table 9) at ε = 30 kev. A quantum with an initial energy ε = 3 Mev should experience on the average ~20 scatterings prior to being absorbed. In air the lifetime of such a quantum is $\sim 4 \times 10^{-6}$ sec, and in water it is $\sim 5 \times 10^{-9}$ sec.

Production of electron-positron pairs. Pairs are produced as a result of interaction between the gamma radiation and the Coulomb field of the nucleus. The process becomes possible only at a quantum energy in excess of the energy corresponding to the sum of the rest masses of the electron and the positron, i.e., $\varepsilon > 2m_0c^2 = 1.02$ Mev. In this process, the gamma quantum loses all its energy which, after subtracting $2m_0c^2$, goes into the kinetic energy of the electron and positron.

When a pair is produced, the gamma quantum drops out completely from the composition of the gamma radiation in the

matter. This process, however, leads to the formation of secondary radiation, occurring during the annihilation of the positron. Annihilation occurs with the maximum probability when the energy of the positron is close to zero. Upon annihilation, two gamma quanta of energy by 511 kev each are emitted.

The cross section for pairs production σ_p increases with increasing gamma-radiation energy and with increasing atomic number of the absorber ($\sim Z^2$).

The process of pair production predominates over other processes at high gamma-ray energies. Table 10 gives the values of the gamma-ray energies at which σ_p becomes equal to $a\sigma_C$ and $a\sigma_C/5$.

Table 10

Quantum energy ε, at which the cross section for pair production is equal to and is 5 times smaller than the scattering cross section

Substance	ε, Mev	
	$a\sigma_p = a\sigma_C$	$a\sigma_p = 1/5 a\sigma_C$
Nitrogen.....	23	7.5
Aluminum.....	15	5.3
Iron.....	9.5	4.0
Lead.....	4.7	2.3

Summary linear coefficients of interaction between radiation and matter. When a parallel beam of gamma quanta passes through matter, any interaction between the quantum and the matter causes the quantum to drop out from the parallel beam, either by absorption or by a change in the direction of motion through scattering. Therefore the total interaction cross section σ_t, with respect to dropping out of a quantum from a parallel beam of quanta, is equal to the sum of the cross sections of all the three individual processes

$$\sigma_t = \sigma_{ph} + \sigma_C + \sigma_p. \tag{6.7}$$

The number of quanta dropping out from the parallel beam of the gamma quanta of density N quantum/cm^2 when the beam passes through a layer of absorber of thickness dx, in the case of normal incidence of the quanta on the absorber, is

$$dN = -N\sigma_t\, n\, dx = -N\mu\, dx = -N\frac{\mu}{\rho}dm = -N\frac{dx}{\lambda}. \tag{6.8}$$

Here σ_t -- summary cross section of interaction, referred to a single atom; n -- number of atoms in 1 cm^3 of medium; ρ -- density

of medium in g/cm^3; dm -- mass of matter obtained in a layer of area 1 cm^2 and thickness dx; ($dm=\rho dx\ \frac{г}{см^2}$); $\mu=\sigma_t n$ -- linear coefficient of absorption of radiation, with a dimensionality cm^{-1}. This coefficient is equal to the probability of interaction of a quantum with the substance per unit path length of quantum in the absorber.

The coefficient μ/ρ is called the mass coefficient of absorption and has a dimensionality cm^2/g. It is equal to the probability of interaction of the quantum with the matter per unit mass, located on the path of radiation in a layer of area 1 cm^2.

The quantity $\lambda = 1/\mu$ is the mean free path of the gamma quanta in the substance.

All these quantities characterize the total probability of interaction between the radiation and the substance, which leads both to absorption and to the scattering of quanta. The cross section σ_t and the coefficients μ and λ characterize the total probability of interaction between the quanta and the matter, but do not characterize the value of the gamma-ray energy absorbed thereby.

The absorbed gamma-ray energy is the part of the energy transferred to the electron by photoeffect, scattering, and pair production, and consumed by the electron in ionization and optical excitation of the atoms. That part of the energy which remains in the form of gamma quanta, naturally, is not the absorbed energy of the gamma radiation (this is the energy of the scattered quantum, of the X-ray quanta, and of fluorescence following the photoeffect, the quanta of annihilation of the positron after pair production, and the bremsstrahlung of the recoil electron). Therefore the cross section of absorption of the gamma-quantum energy in interaction with matter is

$$\sigma_{te} = f_1\sigma_{ph} + f_{2a}\sigma_e + f_3\sigma_p. \qquad (6.9)$$

The coefficient f_1 takes account of the fact that in photoabsorption part of the absorbed gamma-quantum energy is radiated in the form of secondary fluorescence.

The coefficient f_2 takes account of the fact that secondary bremsstrahlung is produced in the bremsstrahlung of the recoil electrons.

The coefficient f_3 takes into account the annihilation radiation and the bremsstrahlung of the electron and positron. All coefficients $f < 1$.

An approximation of σ_{te} with the aid of the coefficient f is made in reference [8] in order to take account of the secondary sources of radiation in the problem of the absorption of gamma rays in the process of multiple scattering.

In the cases of interest to us, the role of fluorescent, bremsstrahlung and annihilation radiations is small and the expression for σ_{te} assumes the usual form

$$\sigma_{te} = \sigma_{ph} + a\sigma_e + \sigma_p = \sigma_t - a\sigma_\gamma. \qquad (6.10)$$

The reduction in the energy of gamma radiation which passes through a layer of matter of thickness dx is equal to

$$dE = -N\varepsilon\sigma_{te}\, n\, dv = -N\varepsilon\mu_e\, dx = \\ = -N\varepsilon\frac{\mu_e}{\rho}\, dm = -N\varepsilon\,\frac{dx}{\lambda_e}. \qquad (6.11)$$

here ε -- energy of the primary quanta, μ_e, $\frac{\mu_e}{\rho}$, and λ_e are coefficients that characterize the probability of process of absorption of the energy by the gamma rays by the medium:

$$\left.\begin{aligned} \mu_e &= \sigma_{te}\, n,\ cm^{-1} \\ \lambda_e &= 1/\mu_e,\ cm \end{aligned}\right\} \qquad (6.12)$$

In Tables A17 -- A21 of Appendix II are given the quantities μ, μ_e, λ, λ_e, μ/ρ, and μ_e/ρ for water, air, aluminum, iron, and lead for ε from 0.1 to 10 Mev. The values for air are obtained from the corresponding values for water by multiplying by the ratio of the electron densities ($\rho/\rho_0 = 860$).

Figure 11 shows the values of μ for air. The dotted line shows the values of μ_ε without allowance for secondary radiations (fluorescence, annihilation, bremsstrahlung). The values of μ_e are given with allowance for the secondary radiations. In Appendix II (Table A17 - A21) are given the values of μ for water, aluminun, iron, ald lead. Figure 11 gives the values of μ_e, μ_{ph}, μ_C, and μ_p, i.e., the linear coefficients of absorption of radiation energy, photo-absorption, Compton scattering, and absorption of radiation during the process of pair production.

Figure 12 gives the values for λ for air at different quantum energies.

From these figures and tables it is seen that μ_e of air and of water vary little in the quantum energy interval from 0.1 to 2 Mev, and it can be considered constant, with the limits of error not exceeding ± 12 percent, at a value 3.4×10^{-5} cm^{-1} for air and 0.029 cm^{-1} for water, ± 12 percent.

As the radiation energy increases the coefficient μ first decreases and reaches a certain value of μ_{min} at ε_{min}, and then increases again. The reduction in the coefficient μ is connected with the reduction in the probability of the photoabsorption and Compton scattering processes with increasing gamma-radiation energy.

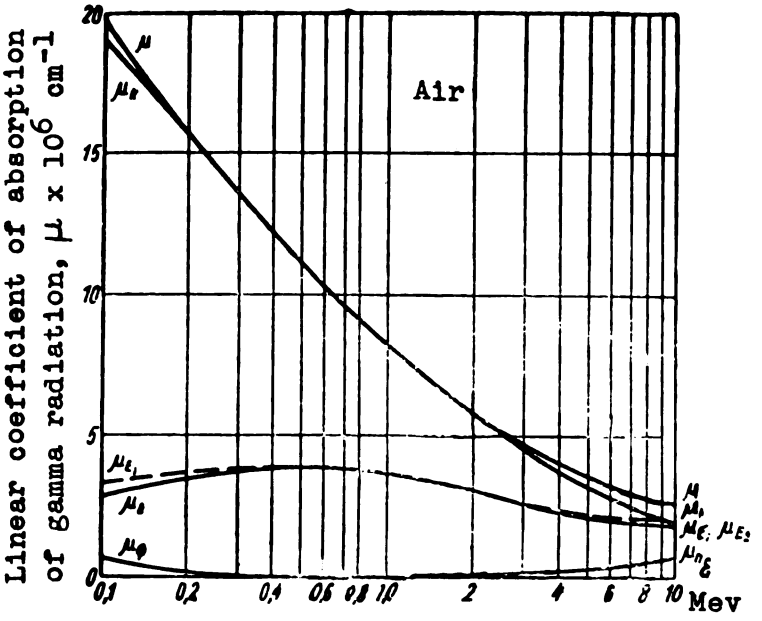

Figure 11. Linear coefficients of absorption of gamma radiation in air (NTP) for different quantum energies. The dotted line gives the values of μ_ε without allowance for secondary radiations (fluorescence, annihilation, bremsstrahlung). The values of μ_e are given with allowance for the secondary radiation.

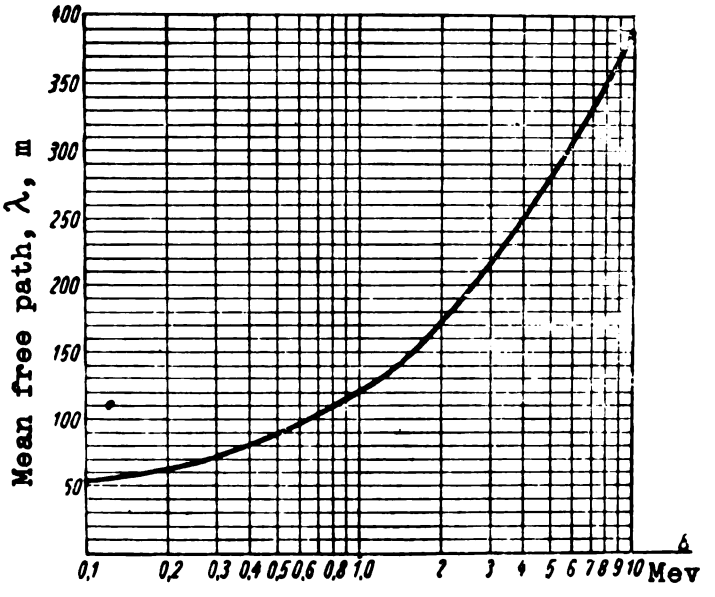

Figure 12. Mean free path λ in air (normal temperature and pressure) for different quantum energies.

The increase in the coefficient μ at high energies of radiation is connected with the appearance of pair production at $\varepsilon > 2m_0c^2$ and with the increase of the probability of this process upon further increase in ε.

The quantity ε_{min} depends on the atomic number of the substance; the smaller Z, the greater ε_{min}. Table 11 lists the values of ε_{min} for different substances.

Table 11

Quantum energy at which μ assumes a minimum value.

Element	Be	B	C	N	O	Al	Fe	Zn	Cd	W	Pb	U
ε_{min}, Mev..	94	70	56	46	39	21	9	7,6	4,4	3,5	3,4	3,3

The role of the pair-production and photoeffect processes in absorption of gamma rays is significant only when the radiation interacts with heavy elements. For light elements the predominating process is Compton scattering. For example, for air, at least within the limits of Compton energies from 100 kev to 3 or 4 Mev (Figure 11), the interaction between the radiation and matter is determined only by the Compton scattering.

Table 12 gives the intervals of gamma-quantum energy, in which one of the three basic processes of interaction between quanta and matter predominates.

Table 12

Value of quantum energy at which one of the three processes of interaction between the quanta and matter predominates in the absorption.

Substance	Photoeffect ε, kev	Compton scattering	Pair production, ε, Mev
Air	< 20	30 kev < ε < 23 Mev	> 23
Aluminum	< 50	50 " " 15 "	> 15
Iron	< 120	120 " " 10 "	> 10
Lead	< 500	500 " " 5 "	> 5

It is seen from the table that in air, aluminum, and iron, in the gamma-quantum energy range from 100 kev to 10 Mev, the predominating process is Compton scattering. In Compton scattering,

the linear coefficient of absorption is determined by the density of the electrons in the matter

$$\mu = {}_a\sigma_C n = \sigma_C n Z = \sigma_C n_e. \tag{6.13}$$

Here $n_e = nZ$ is the density of the electrons in the matter, electron/cm^3,

$$n = \frac{N\rho}{A} \tag{6.14}$$

(N is the Avogadro number; ρ -- density of the substance; A -- the atomic weight).

Substituting (6.14) in (6.13) we obtain

$$\mu = \sigma_C \rho N \frac{Z}{A}. \tag{6.15}$$

or

$$\frac{\mu}{\rho} = \sigma_C N \frac{Z}{A}. \tag{6.16}$$

For light elements the value of Z/A is close to 1/2 (with the exception of hydrogen, which Z/A = 1).

Table 13 lists the value of Z/A for several elements and chemical compounds.

Table 13

Magnitude of ratio $\frac{Z}{A}$

Substance	Z/A	Substance	Z/A
Carbon.....	0.50	Wood.....	0.52
Nitrogen.....	0.50	Sodium.....	0.48
Oxygen.....	0.50	Aluminum.....	0.48
Air.....	0.50	Silicon.....	0.50
Water.....	0.55	Iron.....	0.46

According to these data and formula (6.15), the linear coefficients of absorption μ of the light elements and their compounds (i.e., most of the structural material) are proportional to the density of the matter and are practically independent of Z. The mass coefficients of absorption μ/ρ are independent of the density of the substance. Therefore, knowing μ for one substance, we can readily determine μ for any other substance by multiplying by the ratio of the densities of the substances.

This simple rule is valid only when the quantum energy is

such that the predominating process is Compton scattering, and it is therefore approximate. The degree of accuracy of this rule is determined by the constancy of the ratio Z/A (Table 13) on going from one substance to the other. It is the exact only for substance with the same ratio Z/A. For example, the two substances water and air do not have the same values of Z/A, therefore the rule of proportionality of μ and ρ is not exact for these substances:

$$\frac{\rho \text{ water}}{\rho \text{ air}} = \frac{1}{0.00129} = 770.$$

This ratio differs somewhat from the ratio of the coefficients of absorption, which is equal to the ratio of the electron densities

$$\frac{\mu \text{ water}}{\mu \text{ air}} = \frac{n_e \text{ water}}{n_e \text{ air}} = 860.$$

The Roentgen. The ultimate purpose of a physical estimate of the action of gamma radiation is to determine the gamma ray energy absorbed by 1 cm^3 of air. This quantity called the dose,* characterizes the biological action of the radiation. The dose can be expressed in units of energy absorbed in the air and in units of amount of electricity released as a result of ionization of the air upon absorption of the gamma-ray energy. The dose is measured in roentgens (r). By definition, a dose of one roentgen is the amount of absorbed radiation, which produces in 0.00129 grams of air the number of ions necessary to make up one cgs electrostatic units of each polarity.

The roentgen is related to other units used in the calculation of doses by the following connections:

1 roentgen corresponds to ionization in air, equivalent to:

a) 1 cgs esu/cm^3 of air,

b) 2.08×10^9 pairs of ions per cubic centimeters of air,

c) 1.61×10^{12} pairs of ions per gram of air;

1 roentgen corresponds to an absorbed gamma-ray energy equal to:

a) 6.86×10^4 Mev/cm^3 of air,

b) 0.11 erg/cm^3 of air,

c) 84 erg/g of air,

d) 5.3×10^7 Mev/g of air,

e) 93 erg/g of tissue.

*In the official definition of the dose, one refers to the radiation dose and not to the absorbed radiation energy. But since the biological action is produced by the absorbed radiation energy and not by the radiation passing through a given place, we speak here of a dose of absorbed energy, all the more since in the official definition the radiation dose is measured, in final analysis, by the energy absorbed in air.

Table 14

Density of quantum flux and intensity of radiation producing a dose of 1 roentgen at different quantum energies [27]

ε, Mev	$N_0 \cdot 10^{-9}$ $\frac{\text{quantum}}{\text{cm}^2}$	$N_0\varepsilon \cdot 10^{-9}$ $\frac{\text{Mev}}{\text{cm}^2}$	ε, Mev	$N_0 10^{-9} \cdot \frac{\text{quantum}}{\text{cm}^2}$	$N_0 1^{-9} \cdot \frac{\text{Mev}}{\text{cm}^2}$
0,020	4,7	0,094	1,2	1,7	2,05
0,060	26	1,55	1,8	1,3	2,35
0,120	19	2,3	2,4	1,0	2,4
0,300	6	1,8	3,0	0,9	2,7
0,600	3	1,8	4,5	0,73	3,3
0,900	2,1	1,9	12	0,4	4,3

1 Mev/cm^3 of air equals 1.48 x 10^{-5} r,

1 Coulomb/cm^3 of air equals 3 x 10^9 r.

Table 14 lists the values of the density of the flux of gamma rays (N_0, quanta/cm^2) and the corresponding energy flux density ($\varepsilon = N_0\varepsilon$, Mev/cm^2), which produces a dose of 1 roentgen.

The intensity of gamma radiation necessary for the formation of a dose of 1 roentgen in the gamma-ray energy interval from 0.1 to 2.5 Mev, is practically independent of the energy (since μ_e in air is approximately constant) and amounts to 2.1 x 10^9 Mev/cm^2 ± 15 percent.

7. PROPAGATION OF GAMMA RADIATION FROM A POINT SOURCE IN A HOMOGENEOUS INFINITE MEDIUM.

Distribution of dose intensity of gamma rays at different distances from the source. This problem is basic for all practical applications, since the action of any configuration of sources can be made up of the sum of the action of point sources. It corresponds to the scheme of action of gamma radiation from explosion as described in Item 1 of the introduction (page 10 [of source], Figure 1a).

This problem has been the subject of many theoretical and experimental investigations. The most complete theoretical results were published by Fano and Spenser [9] and by Goldstein and Wilkins [10]. By using the method of simulation in water, the most complete results were obtained by Leipunskii and Sakharov (quantum energy 0.41, 1.25, and 2.8 Mev), by White [11] (quantum energy 1.25 Mev),

and by Roys and others [22] (quantum energy 6 Mev).

It can be stated that the problem of the three-dimensional distribution of doses and of the intensity of gamma radiation from a point source in an infinite medium has been completely solved.

Little attention has been paid to the following problems, which are also of practical importance: the case of an inhomogeneous medium (for example, variable density of the medium, the boundary between two half spaces of earth and air), angular distribution of doses, spectral distribution of intensity of the scattered radiation in various solid angles, etc.

This problem considered has spherical symmetry. Therefore the distribution of the intensity and of the doses of the gamma rays in space depends only on one space coordinate -- the distance R from the source.

The intensity of radiation from an isotropic point source attenuates with increasing R, owing to increased distance from the source and owing to the interaction with matter.

In vacuum, the attenuation is produced only by the geometrical factor and therefore

$$J_V = \frac{G}{4\pi R^2} \tag{7.1}$$

(G is the activity of the source, Mev/sec).

In a medium, the intensity decreases also as a result of absorption of energy in the substance.

A definite fraction of the quanta passes through the substance without being scattered or absorbed. These constitute the so-called direct radiation, unlike the scattered radiation, the composition of which is determined by the multiple scattering (diffusion) of the quanta. Inasmuch as the probability of a quantum passing through a distance R without interacting is equal to $e^{-\mu R}$, the intensity J_0 of the direct radiation is

$$J_0 = \frac{G}{4\pi R^2} e^{-\mu_0 R}. \tag{7.2}$$

It is obvious that the sought J(R) is less than $J_V(R)$, since no absorption is taken into account in (7.1), but is greater than $J_0(R)$, since the absorption has been over-estimated in (7.2) (scattered quanta not taken into account in (7.2), are added to the direct-radiation quanta). Thus,

$$J(R) > J(R) > J_0(R). \tag{7.3}$$

According to (7.1), (7.2), and (7.3), the expression for J(R) can be written in form

$$J = \frac{G}{4\pi R^2} K_J, \tag{7.4}$$

where K_J is the intensity attenuation factor ($K_J < 1$), equal to the

ratio, at the given point in space, of the intensity of the gamma rays in the presence of an absorber to the intensity in the absence of an absorber, or else in the form

$$J = \frac{G}{4\pi R^2} e^{-\mu R} B_J = J_0 B_J, \qquad (7.5)$$

where B_J is the intensity build-up factor, equal to the ratio of the intensity of radiation to that part of the radiation due only to the direct radiation

$$B_J = \frac{J_s + J_0}{J_0} \qquad (7.6)$$

J_s -- intensity of scattered radiation. It is obvious that

$$K_J = B_J e^{-\mu R}. \qquad (7.7)$$

The expressions (7.3), (7.4), (7.5), (7.6), and (7.7) are written for the intensity of the gamma radiation, but they can be generalized for all effects connected with the action of the quanta. Then, in accordance with (7.6), the coefficient B can in general be taken to mean the ratio of the result of a definite action of the total flux of gamma-ray quanta to the result of the action of the flux of quanta due only to the direct radiation. The subscript of the coefficient B will indicate in this case the particular radiation action referred to. For example, B_N is the ratio of the total number of quanta to the number of quanta in the direct beam; B_J -- ratio of the total intensity to the intensity of the direct beam; B_r -- ratio of the total dose power to the power produced by the direct beam. One can introduce also coefficients B for the ratio of the readings of certain instruments, etc.

Similar symbols are used also for the attenuation coefficient K.

According to (6.11), the dose power of interest to us, P, i.e., the power of the absorbed energy, is connected, in the case of a monoenergetic radiation, with the intensity J (in Mev/cm^2) by the following relation

$$P = \mu_e J \cdot 1{,}48 \cdot 10^{-5}, \text{ r/sec} \qquad (7.8)$$

(1.48×10^{-5} is the conversion factor from absorbed energy in Mev/cm^3 to the dose, r).

In the case non-monoenergetic radiation, the expression (7.8) must be replaced by

$$P = 1{,}48 \cdot 10^{-5} \int \mu_e(\varepsilon) J(\varepsilon)\, d\varepsilon, \text{ r/sec}. \qquad (7.9)$$

After passing through the matter, the gamma radiation becomes

non-monoenergetic, even if the source itself, with a quantum energy ε_0, is monoenergetic. In this case the factor $\mu_e(\varepsilon_0)$ is taken outside the integral sign

$$P = 1{,}48 \cdot 10^{-5} \mu_e(\varepsilon)_0 \int \frac{\mu_e(\varepsilon)}{\mu_e(\varepsilon)_0} J(\varepsilon)\, d\varepsilon. \qquad (7.10)$$

In accordance with (7.10), (7.4), (7.5) and with consideration of the general meaning of the coefficients B and K, we can write down the following expressions for the dose power from a monoenergetic source with quantum energy ε_0:

$$P = 1{,}48 \cdot 10^{-5} \frac{G\,\mu_e(\varepsilon_0)}{4\pi R^2} K_r, \text{ r/sec}; \qquad (7.11)$$

$$P = P_0 B_r = 1{,}48 \cdot 10^{-5} \frac{G\,\mu_e(\varepsilon_0) B_r}{4\pi R^2} e^{-\mu(\varepsilon_0) R}, \text{ r/sec}; \qquad (7.12)$$

$$K_r = B_r e^{-\mu(\varepsilon_0) R} \qquad (7.13)$$

As already indicated, in a wide range of quantum energy ε - $\mu(\varepsilon)_e$ is practically independent of ε, therefore $J \approx P$, $K_r \approx K_J$ and $B_r \approx B_\gamma$.

The determination of the coefficients K_r (R, ε_0) or B_r (ε_0) is a problem in the theory of multiple scattering of quanta or of model experiments.

Theoretical determination of B_r. Figure 13 and Table A22 of Appendix II give the calculated values of B_r [10]. In these data the distance from the source R is expressed in units of mean free path of the primary radiation in the medium $\lambda_0 = 1/\mu(\varepsilon_0)$. With the space coordinate expressed in this manner, the magnitude of the coefficient of attenuation of the radiation per unit length of absrober is independent of its intensity, and all the laws of absorption of radiation in media with equal values of Z, but with different densities, assume the same form. This rule is retained also for substances with different Z in the case when only the scattering by the free electrons is of importance in the interaction between the quanta and the substance (Table 12).

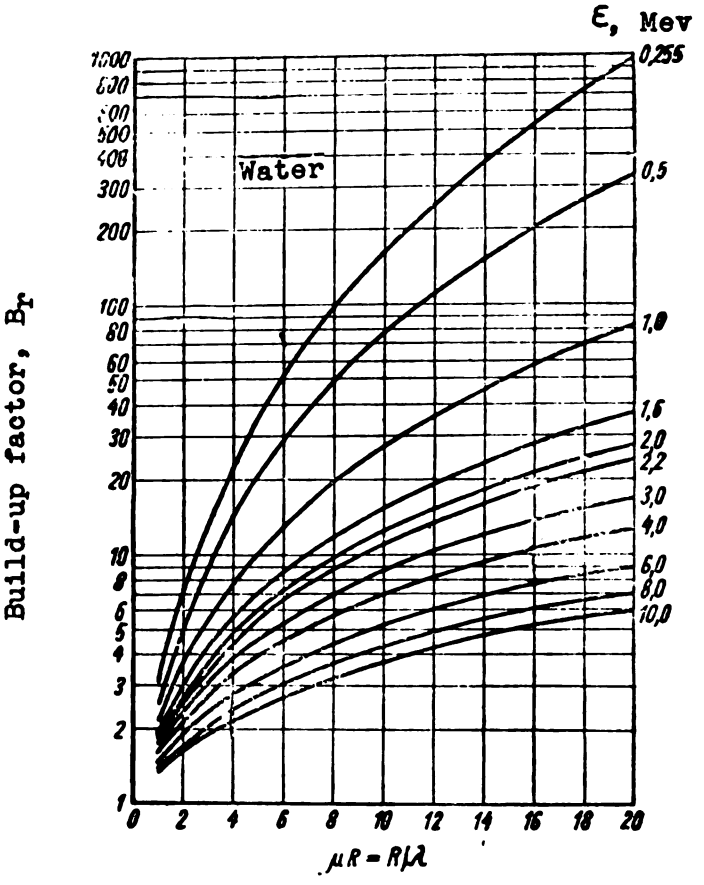

Figure 13. Dose build-up factor B_r (ε_0, μR) for gamma radiation from a point source in water at different values of quantun energy ε_0 [10].

According to this rule, the coefficients B for two absorbing media are equal, if the thickness of the absorber is expressed in units $\lambda_0 = I/\mu$ (ε_0).

The ratio of the quantities λ_0 for water and air at 0°C and a pressure 760 mm is 860. When measuring distances in ordinary units of length, the coefficients B for water and for air are equal at distances from the source differing by a factor of 860. This rule serves as the basis for the possibility of simulating the conditions of propagation gamma rays in air with the aid of small-size water models.

The accuracy of the calculation of B_r and B_J is estimated by the authors at ± 5 percent for the case of iron and lead at short distances from the source and at ± 15 percent for long distances. In the case of light elements such as water and aluminum, the estimates are ± 10 percent for short distances and ± 25 - 30 percent for long distances.

Figure 13 shows the values of B_r in water for different distances from the source (the values of ϵ are marked on the end of each curve). From Table A22 of Appendix II and from Figure 13 it is seen that as the distance from the source is increased, the coefficients B_r are continuously increased and that consequently the role of radiation in the production of the gamma-ray dose also increases continuously.

For primary radiation $\epsilon_0 = 0.5$ Mev, at a distance from the source of 10 R/λ_0 in water, the dose produced by the scattered radiation is 80 times greater than the dose produced by the direct radiation. By interpolating the data of Table A22 of Appendix II we can obtain values of B_r for elements with different values of Z and for different quantum energy ϵ_0. Thus, values of B_r have been obtained for $\epsilon_0 = 1.6$ and 2.2 Mev, which are characteristic of gamma-ray sources produced in the region of an atomic explosion. The values of B_r can be calculated also from interpolation formulas.

The values of B_r given in Figure 13 and in Table A22 of Appendix II make it possible to calculate the doses of gamma rays up to $\mu_0 R = 15$ or 20. At greater distances from the source it is difficult to solve the kinetic equation for the distribution of gamma rays with a sufficient degree of accuracy even with the aid of electronic computers.

At large values of $\mu_0 R$, an asymptotic form has been derived for the attenuation of the intensity and the power of the gamma-ray dose [9].

Experimental determination of K_r. Figure 14 shows a comparison of the results of an experimental determination of the coefficients of attenuation in simulation experiments in water (according to the data of references [11, 21, 22]) with the theoretical values obtained by formula (7.13).

The laws of attenuation of gamma-ray doses thick layers are not simple exponential laws. The observed effective linear coefficients of absorption of the dose power of gamma rays, μ_{eff} (the change in the logarithm of coefficient of attenuation or the dose power per unit length of absorber) is not constant, but depends on the distance to the source. At small distances, μ_{eff} is close in magnitude to μ_{0e} -- the coefficient that determines the absorption of the energy from the direct radiation. This is natural, for at small distances from the source the double or multiple scattering has low probability, and the energy loss in single scattering of radiation is determined by the coefficient μ_{0e}.

For soft radiation, the coefficient μ_{eff} at small distances from the source may be even less than μ_{0e}, when the flux of the backward-scattered radiation from deep layers of the absorber is added to the direct and singly-scattered radiation traveling from the source.

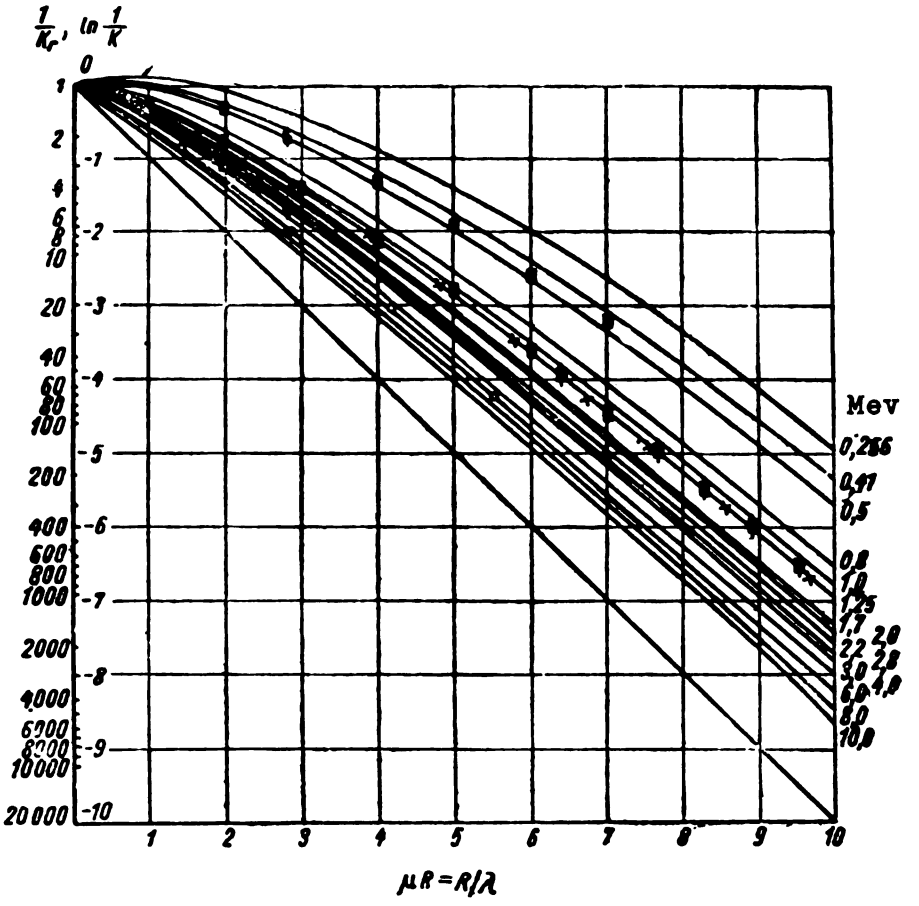

Figure 14. Coefficient K_r (ε_0, $\mu_0 R$) of attenuation of the dose of gamma radiation from a point source in water at different quantum energies.

For example, with ε_0 = 0.41 Mev and less, at a distance $\mu_0 R = 1$ from the source, the gamma-ray dose not only is not attenuated by the absorber but, to the contrary, is intensified. As the distance from the source is increased, μ_{eff} increases and approaches μ_0, i.e., the linear coefficient of absorption of the primary radiation.

It can be seen that, over a wide range of source quantum energies, the experimental and theoretical methods of investigation give identical results within the limits of errors of calculation and measurement. Since the accuracy of the theoretical calculations of the value of K for ε_0 = 0.41 Mev is less than the accuracy of the experiment, we shall use the experimental data in further calculations for this energy.

From Figure 14 it is seen that within a definite interval of distances from the source the laws of attenuation of the gamma-ray doses can be represented approximately by means of the empirical formula

$$P = 1{,}48 \cdot 10^{-5} \frac{G\,\mu_e(\varepsilon_0)}{4\pi R^2}\,\alpha\, e^{-\mu_{eff}R}, \text{ r/sec.} \qquad (7.14)$$

Using this notation, we introduce two coefficients α and μ_{eff}, which depend little on the distance, in lieu of the coefficient B_r, which depends very strongly on the distance, and $\mu(\varepsilon_0)$, which does not depend on the distance. The coefficient α is independent of the density of the substance, while the coefficient μ_{eff} is proportional to the density ρ. Therefore the expression for the coefficient of attenuation K_r can be written in the form

$$K_r = \alpha e^{-\mu_{eff}R} = \alpha e^{-R/\lambda_{eff}} \qquad (7.13')$$

instead of (7.13).

Formulas (7.13') and (7.14) are convenient to use in the case when they can be employed in the interval of distances in which α and μ_{eff} can be considered constant.

Figure 15 shows the values of α and μ_{eff} for air for two distance intervals in which α and μ_{eff} were assumed constant.

The distance intervals 400 - 1000 and 1000 - 2000 meters were chosen such as to make formula (7.14) give a result accurate to ± 10 percent. If the permissible error is greater, the width of the interval with constant α and μ_{eff} where (7.14) is valid* can be increased.

Intensity of gamma radiation in the presence of a spherical cavity around the source. A spherical cavity around the source is the simplest model of inhomogeneity of air, occurring in atomic explosion along the path of the gamma rays, as a result of the propagation of the shock wave.

Information on the propagation of radiation in air, is obtained in this case with the aid of simulation experiments in water. The region of rarefaction around the source was simulated in water with the aid of 10 empty aluminum spheres, the center of each of which a source was placed. The radii of the spheres were 18.5, 29.5, and 40 centimeters, equivalent to rarefaction regions in air with radii 160, 254, and 342 meters. The measurements were carried with three gamma-ray sources with ε_0 = 0.41, 1.25, and 2.8 Mev.

*In Chapter III we shall use formula (7.14) instead of (7.12).

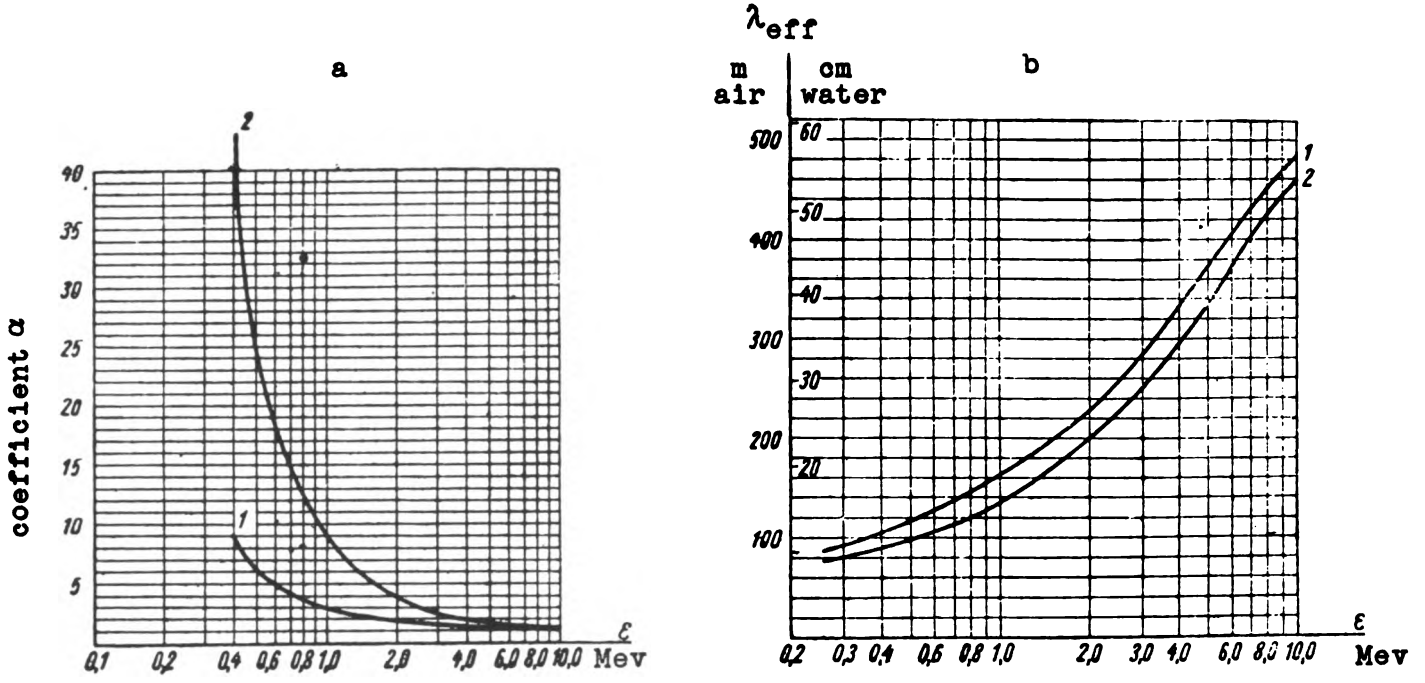

Figure 15. Coefficients α and λ_{eff} of the interpolation formula (7.14) for the calculation of the dose power of a point source of gamma radiation in air (normal temperature and pressure) and in water at different quantum energies: 1 -- interval of applicability for formula (7.14) is 400 - 1000 meters of air (46.5 - 116.3 centimeters of water); 2 -- interval of applicability is 1000 - 2000 meters of air (116.3 - 232.6 centimeters of water).

Figure 16 shows the result of the experiments, with the abscissa axis representing the thickness of the layer of water (R - L) along the path of the gamma rays, i.e., a quantity numerically equal to the "optical thickness" Δ (since ρ = 1). The energy of the quanta, in Mev, is marked on the end of each curve in the figure. The approximate agreement between the coefficients of attenuation in the experiments with and without cavity shows that K_r, and consequently also B_r and μ_{eff}, are functions of the "optical thickness" R - L.

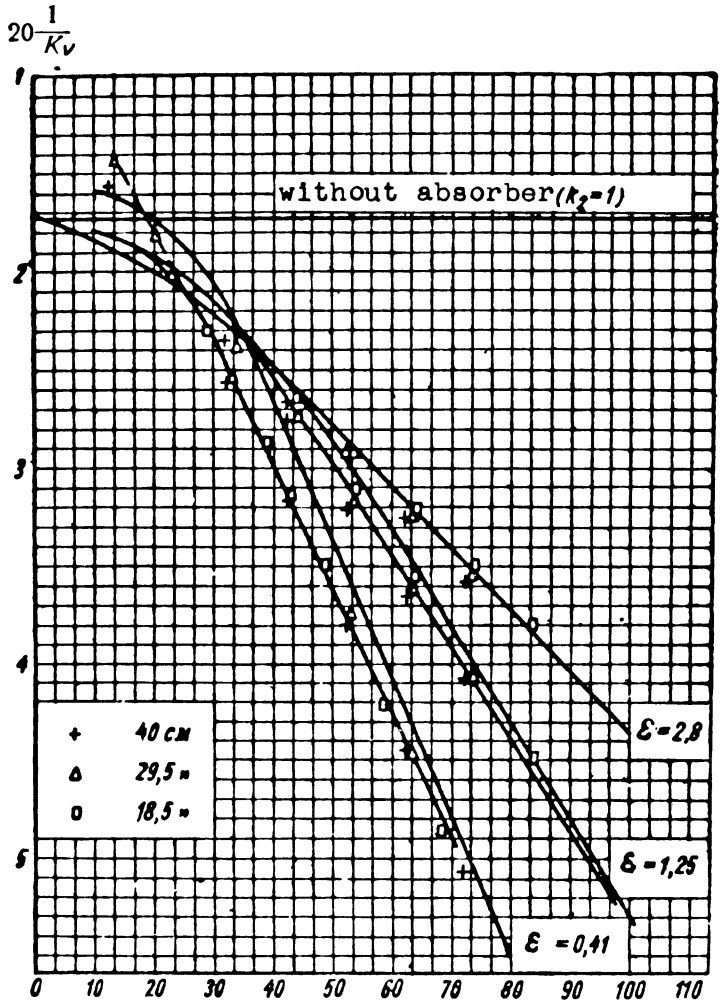

Thickness of water layer along path of γ rays, R-L, cm

Figure 16. Coefficient of dose attenuation K_r of gamma radiation in water in arbitrary units in the presence of a spherical cavity of radius L around a point source, for different quantum energies: ——— — measurements without cavity, +++ - for L = 40 centimeters; ΔΔΔ - for L = 29.5 centimeters; □ □ □ - for L = 18.5 centimeters.

The results of the experiments is the conclusion that the coefficient of attenuation of the radiation K_r, both in a homogeneous absorbing medium and in a medium in which the absorber becomes rarefied around the source, is almost the same for equal thickness of absorber R - L along the path of the gamma rays. This follows from the approximate agreement between the values of K_r in experiments with and without cavity. Thus, the value of K_r, which is equal to

$$B_r(\mu R)\, e^{-\mu R},$$

is a function of $\mu(R - L)$.

The result obtained can be interpreted in a more general form. The coefficients characterizing the attenuation of the radiation of the absorber B_r and K_r at a point located a distance R from a point source, are determined not by the value of μ_r or R/λ, but by a quantity analogous to the so-called "optical thickness" Δ:

$$\Delta = \int_0^R \mu\, dR. \tag{7.15}$$

If the density of the matter is variable and depends on R in accordance with a law $\rho(R)$, then the coefficient $\mu(\rho)$ changes, depending on ρ, in accordance with the law

$$\mu(\rho) = \mu(\rho_0)\frac{\rho(R)}{\rho_0}, \tag{7.16}$$

and then

$$\Delta = \int_0^R \mu\, dR = \int_0^R \mu(\rho_0)\frac{\rho(R)}{\rho_0}\, dR. \tag{7.17}$$

If the density of the substance is constant, then

$$\int \mu(\rho_0)\frac{\rho(R)}{\rho_0}\, dR = \mu(\rho_0)\, R,$$

i.e., the "optical thickness" in this case is equal to the parameter μR.

If this source is surrounded by a cavity of radius L, then we have $\rho = 0$ when $R < L$ and $\rho = \rho_0$ when $R > L$, and consequently

$$\Delta = \int_0^R \mu\,(\rho_0)\,\frac{\rho\,(R)}{\rho_0}\,dR = \mu\,(\rho_0)\,(R-L) = \frac{R-L}{\lambda}. \qquad (7.17')$$

Figure 16 shows that in the case when the medium does not have a homogeneous density it is necessary to use as the parameter determining the value of the coefficients B and K the values (7.15) and (7.17') -- the "optical thickness," instead of μR or R/λ. This operation is approximate. The degree of approximation can be seen in Figure 16.

The concept of "optical thickness" is used in Chapter III in the estimate of the effect of the shock wave on the intensity of the gamma radiation.

Notes on the propagation of gamma radiation in air near the earth. If an atomic bomb explodes near the surface of the earth, then the propagation of the gamma radiation occurs under conditions of an inhomogeneous medium, i.e., of two half spaces -- the earth and the air.

The effect of the earth on the propagation of gamma rays in earth has been investigated little.

The interaction between the radiation and the earth is particularly important when calculating the gamma-ray doses on the surface of the earth -- on the boundary between the earth and the air.

Let us consider the possible difference between this case and the case of propagation of gamma rays in a homogeneous air medium.

In a homogeneous medium at large distances from the source, the intensity of the gamma rays is determined essentially by the scattered radiation, which is produced by a broad beam of primary gamma rays.

In the presence of earth, part of this broad of gamma rays is absorbed by the earth in the direct vicinity of the source and does not participate in the creation of scattered radiation.

If the point source and the point at which the radiation is investigated are located at the level of the earth, then half of the broad beam of the gamma rays traveling in the direction from the source strikes the earth and is absorbed in it. One can therefore expect that in this case the total intensity of the gamma radiation at large distances from the source is approximately half as small as in the case of a homogeneous air medium. At small distances from the source one can expect, to the contrary, a certain increase in the intensity of the gamma rays, by 10 or 20 percent, owing to the presence of radiation scattered backward from the earth.

The characteristic features of the propagation of gamma rays in air over the earth are shown in Figure 17. The radiation scattered in the air, making up the main contribution to the dose at large distances, occurs only on the upper half of the space, whereas in the case of a homogeneous air medium it would also come from the lower half space (dotted). Therefore in the case shown in Figure 17 the dose is approximately half the dose in an infinite

homogeneous medium. If the source is located not on the earth, but above it, then as its distance from the earth increases, the influence on the gamma-ray doses on the surface should decrease.

The foregoing qualitative considerations concerning the propagation of gamma rays in air over the earth have been confirmed by experimental data.

Figure 18 shows curves in the attenuation of the gamma-ray dose intensity according to the data of the author and V. N. Sakharov. The experiments were carried out with a source of Co^{60}, located at a height of 1 meter above the earth.

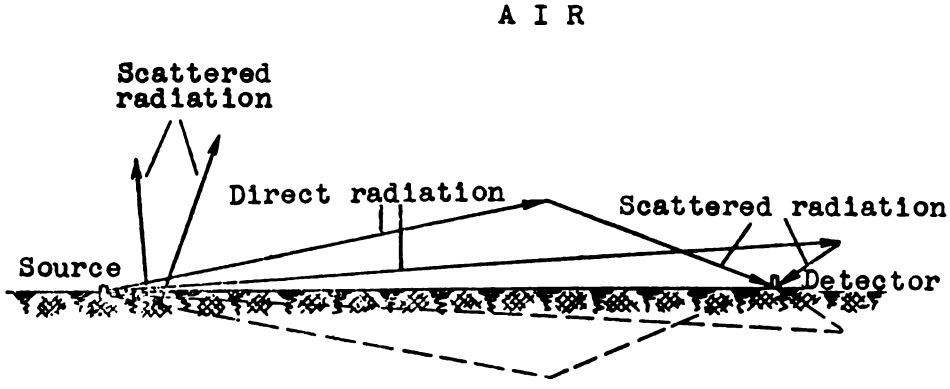

Figure 17. Features of the propagation of gamma radiation in the case when the source and detector are located in the boundary of the air -- earth half spaces.

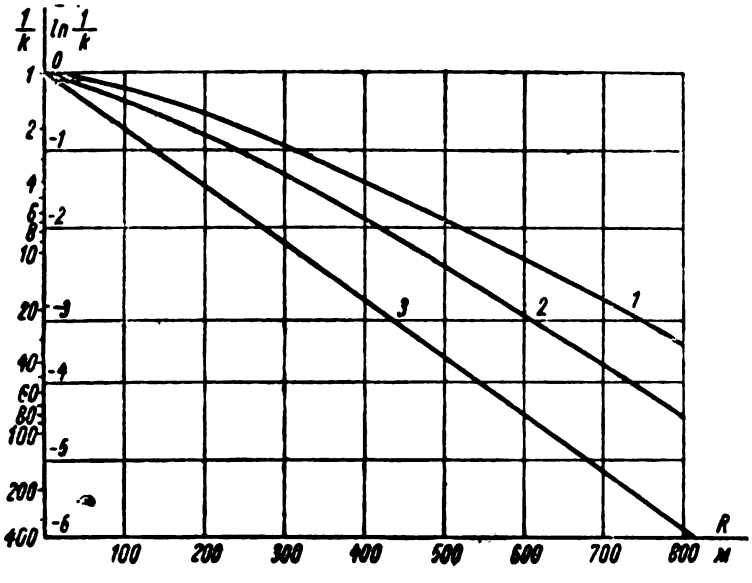

Figure 18. Coefficient of attenuation of the dose of gamma radiation from a Co^{60} point source when the source and the detector are located on the earth -- air boundary at a height of 1 meter above the earth (curve 2). For comparison, the figure shows the attenuation coefficients in a homogeneous air medium (curve 1) calculated from the measurements in water and the coefficients of attenuation of the direct ray (curve 3).

Spectral composition of gamma radiation. In reference [10] the spectral distribution of gamma radiation in an absorbing medium was calculated for different distances of the point source. Figure 19 shows the spectral composition of the gamma radiation of a monochromatic point source of unit activity (G = 1 Mev/sec) with ε_0 = 2 Mev in water. The spectral distribution is expressed by the function

$$f[\varepsilon, \mu(\varepsilon_0) R] = \frac{dJ}{d\varepsilon}. \tag{7.18}$$

Along the abscissa axis is plotted the quantum energy in Mev, while the ordinates represent the values of the function (7.18), referred to the intensity of the direct radiation of the source, i.e., the values $f[\varepsilon, \mu(\varepsilon_0)R]/J_0$.

$$\frac{1}{J_0}\frac{dJ}{d\varepsilon} = \frac{f[\varepsilon, \mu(\varepsilon_0) R]}{J_0[\mu(\varepsilon_0) R]} = \frac{f[\varepsilon, \mu(\varepsilon_0) R]}{G} 4\pi R^2 e^{\mu(\varepsilon_0) R};$$

The function $f[\varepsilon, \mu(\varepsilon_0)R]$ makes it possible to calculate the intensity of the gamma rays at different energy intervals over different distances from the source

$$\left.\begin{aligned} &\int_{\varepsilon_1}^{\varepsilon_2} f[\varepsilon, \mu(\varepsilon_0) R]\, d\varepsilon = J_{\varepsilon_1, \varepsilon_2} \\ &\text{(in the interval } \varepsilon_1 \text{ to } \varepsilon_2 \text{ at a distance from the source } \mu(\varepsilon_0)R); \\ &\int_0^{\varepsilon_0} f[\varepsilon, \mu(\varepsilon_0) R]\, d\varepsilon = J[\mu(\varepsilon_0) R]; \\ &\int_0^{\varepsilon_0} \frac{f[\varepsilon, \mu(\varepsilon_0) R]\, d\varepsilon}{J_0} = \frac{J}{J_0} = B_J; \\ &\int_0^{\varepsilon_0} \frac{f[\varepsilon, \mu(\varepsilon_0) R] d\varepsilon}{J[\mu(\varepsilon_0) R]} = 1. \end{aligned}\right\} \tag{7.19}$$

In Table 15 and in Figure 19 are given the values of the intensity in different spectral intervals $J_{\varepsilon_1, \varepsilon_2}$ in percent of the overall gamma-ray intensity J for $\mu(\varepsilon_0)R$ = 4.7 and 15.

In Figure 20 we compare the form of the spectral distribution

of gamma rays in water and different $\mu(\varepsilon_0)R$ with energy 2 Mev. The curves shown in this figure coincide in the soft part of the spectrum.

As can be seen from Figure 20 and Table 15, the relative spectral distribution established as a distance (2 - 4) R/λ_0 from the source changes little with further increase in R/λ_0. Approximately 1/4 of the entire radiation energy belongs to the soft radiation with energy $\varepsilon < 0.25$ Mev.

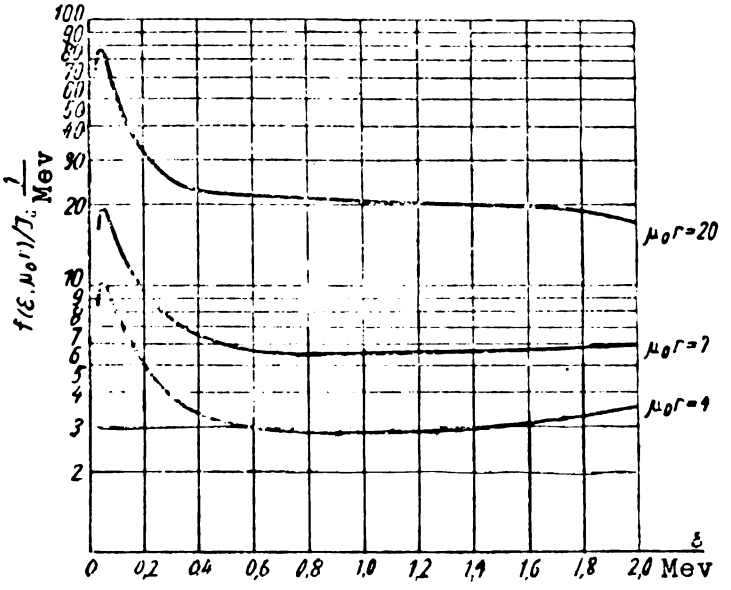

Figure 19. Spectral distribution of the intensity of gamma radiation in water at different distances at μR from a point source of quanta with energy ε = 2 Mev. The values of the intensity of radiation are expressed in units of intensity of direct ray J_0, at the given place [10].

Figure 20. Comparison of the spectral distribution of the intensity of gamma radiation in water at different distances $\mu_0 r$ from a point source of quanta of 2 Mev energy. The curves for $\mu_0 r$ = 4 and 20 on Figure 19, coincide with the curve $\mu_0 r$ = 7, to which the scale on the ordinate axis refers.

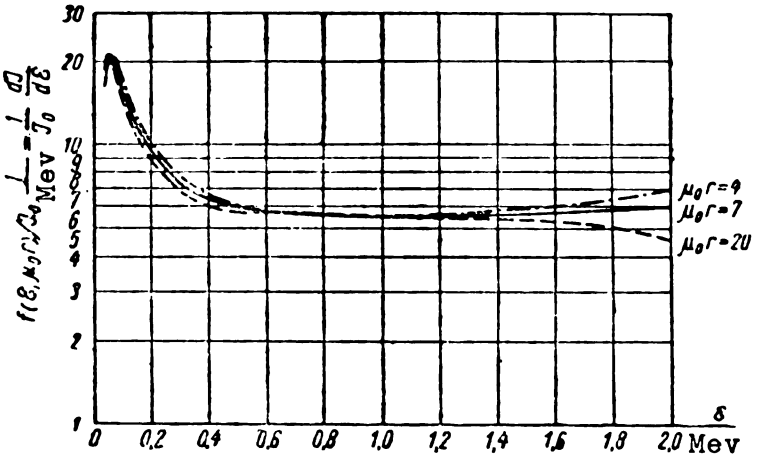

As $\mu(\varepsilon_0)R$ changes from 4 to 20, the ratio of the intensities of the individual spectral components in the soft part of the spectrum, for $\varepsilon < 1.5$ Mev, remains almost unchanged, while when

$\varepsilon > 1.5$ Mev it changes by not more than 30 percent.

Table 15

Spectral distribution of gamma radiation in water from a quantum source with energy 2 Mev, percent

Energy interval, Mev	$\mu(\varepsilon_0)$ $R = 4$	$\mu(\varepsilon_0)$ $R = 7$	$\mu(\varepsilon_0)$ $R = 15$
0—0,050	3,5	3,6	3,6
0—0,100	10,5	10,5	10,5
0—0,25	22,9	22,9	22,9
0—0,5	35,9	35,6	35,6
0—1,0	56,4	57	57,5
0—1,5	77	78	79,1
0—2,0	100	100	100

Note. The intensity of radiation in the energy interval is given as a percentage of the overall intensity $J[\mu(\varepsilon_0)]$ R

Angular distribution of gamma radiation. The question of the angular distribution of radiation arises in cases when part of the radiation is held back by a shield, and the detector receives only the gamma rays traveling from the scattering medium in a definite solid angle. Such a problem is encountered in all schemes of action of gamma rays.

There is no published theoretical solution of this problem. The available experimental data are given below.

The angular distribution of the radiation of a point source in a homogeneous medium depends, in view of the symmetry of the considered problem, only on two space coordinates: the distance to the source and the angle Θ between the directions to the point source and to the radiating volume in the medium. Corresponding to the "forward" half space is the interval of Θ from 0 to $\pi/2$, while corresponding to the "backward" half space is the interval of Θ from $\pi/2$ to π. When the source and the detector are both located on the earth surface, the solid angles of the forward and backward half spaces are equal to π steradians instead of 2π as in a homogeneous medium.

The dose $D(\omega)$ produced by the radiation from the space occupying a solid angle ω, is equal to

$$D(\omega) = D \int_{\omega} \delta(\Theta)\, d\omega, \tag{7.20}$$

where D is the total dose in the given place, $\delta(\Theta)$ is the dose

produced by the radiation traveling in a unit solid angle at an angle Θ and expressed in fractions of the total dose, i.e.,

$$\delta(\Theta) = \frac{1}{D} \frac{dD(\omega)}{d\omega},$$

$$\int_{\Theta=0}^{\pi} \delta(\Theta)\, d\omega = 1. \qquad (7.21)$$

There exist separate data on the dose produced by the radiation from the entire "backward" half space, i.e., concerning the quantity

$$\delta_b = \int_{\pi/2}^{\pi} \delta(\Theta) d\omega,$$

and separate information on the quantity $\delta(\Theta)$ in the "forward" half space.

The author and V. N. Sakharov, and also A. A. Voevodskii, have determined the amount of radiation reaching the measurement point from the scattering medium in a wide angle Θ, from $\pi/2$ to π, i.e., from the "backward" half space of the scattering medium. In one of the investigations, the experiments were carried out in water with point sources of quanta with $\varepsilon_0 = 0.41$ and 1.25 Mev, while in the other -- in the case of propagation of a parallel beam of quanta with $\varepsilon_0 = 1.25$ Mev in concrete.

In both investigations, in order to estimate the amount of radiation going from the "backward" half space in a solid angle of 2π steradians, a comparison was made of the gamma-ray dose measured in a homogeneous medium, with the gamma-ray dose measured after removal of the "backward" half space of water or concrete, respectively.*

The angular distribution of the radiation from a point source of Co^{60} in air over the earth was determined in reference [12] (the source and the detector were located at a height of one meter above the earth). The "backward" half space occupied an angle of π steradians, and not 2π steradians.

Reference [12] also gives data on the dose of gamma rays going from the "backward" half space, and on the angular distribution of the gamma rays within the limits of the "forward" half space.

The results obtained in work on the angular distribution of doses in the "backward" half space are given in Table 16, in which is listed the percentage ratio of the dose of the gamma rays from

*Such a method of measurement gives a somewhat excessive value of dose from the "backward" half space, in view of the possible multiple passage of radiation from the "backward" half space into the "forward" one and vice versa.

the "backward" half space to the total gamma-ray dose, i.e., δ_b.

Table 16

Dependence on the dose of gamma rays in the "backward" half space (δ_b, percent) on the thickness of the absorber R/λ_0

Medium and type of source	R/λ_0	δ_b, %
1. Concrete. Parallel beam of gamma rays with ε_0 = 1.25 Mev.....	1,42	5,6
	2,88	9,1
	4,32	11,5
	5,75	13,8
	7,8	26
2. Water. Point source of gamma rays		
a) With ε_0 = 0.41 Mev.....	4,18	33
b) With ε_0 = 1.25 Mev.....	3,8	13
3. Air. Point source of gamma rays on the air -- earth boundary with ε_0 = 1.25 Mev.....	0,66	5,1
	1,33	7,6
	2,00	9,4
	2,66	10,2

Note. The values of δ_b for the case of propagation of gamma rays in air over the earth are closed over the values of δ_b in homogeneous medium.

The fraction of the dose from the "backward" half space increases with increasing R/λ_0 and with decreasing quantum energy.

The limiting value of this fraction can obviously not exceed 50 percent of the total dose of gamma rays. In view of the absence of detailed data on the spectral and differential angular distributions of the radiation within the limits of the "backward" half space, one can start out in practical calculations from the following estimates:

1. The angular distribution of radiation within the limits $\pi/2 < \theta < \pi$ is uniform, i.e., is independent of θ and consequently it is given for a homogeneous medium by the formula

$$\delta(\theta) = \delta_b \frac{\omega}{2\pi} \qquad (7.22)$$

and for the case when the source and the detector are located on the earth -- air boundary, it is given by the formula

$$\delta(\theta) = \delta_b \frac{\omega}{\pi} \qquad (7.23)$$

(the values of δ_b are indicated in Table 16).

2. An analogy spectrum of radiation in backward scattering (Section 11), the energy of radiation going from the "backward" half space lies essentially in the interval ε = 100 - 300 kev.

The angular distribution of the doses from the radiation going from the "forward" half space can be determined from the data of [12], which pertains to a Co^{60} source and to a small interval of R/λ_0 values.

In Table 17 are given the values of $\delta(\theta)$ in the "forward" half space with $R/\lambda_0 = 2.66$, calculated from the data of reference [12].

Table 17

Angular distribution of doses produced by radiation from the "forward" half space

Interval of angle of measurement of radiation θ, deg	$\frac{D\omega^*}{D} \cdot 100\%$	$\delta(\theta)$ 100%**.
0—5	45,7	—
5—10	5,1	157
10—20	8,8	61,4
20—30	7,2	31,6
30—40	5,9	18,9
40—50	4,9	12,6
50—60	4,0	9,0
60—70	3,3	6,7
70—80	2,7	5,1
80—90	2,2	4,0
90—180	10,2	3,2***

*$D(\omega)/D$ -- ratio of doses produced by the radiation arriving at the measurement point within the limits of the given angles θ to the total dose of gamma rays.

**$\delta(\theta)$ -- ratio of dose which arrives on the average per unit solid angle within the given limits of θ to the total gamma-ray dose.

***Average value over the solid angle π.

It is seen from Table 17 that the angular distribution of the gamma rays is highly anisotropic.*

Within the limits of θ from 7.5 to 90°, with $R/\lambda_0 = 2.661$, we have

$$\delta(\theta) = \frac{0{,}04}{1{,}035 - \cos\theta}, \text{ 1/steradian.}$$

Within the limits θ from 90 to 180° we have

$$\delta(\theta) = 0{,}032, \text{ 1/steradian} \qquad (7.24)$$

The fact that the average value of $\delta(\theta)$, taken over the "backward" half space [$\delta(\theta) = 3.25 \times 10^{-2}$] is close to the value of $\delta(\theta)$ for $\theta = 80 - 90°$ [$\delta(\theta) = 4 \times 10^{-2}$], as determined in a solid angle which is 1.3 as large as the angle of the "backward" half space, indicates that the angular distribution of the radiation in the "backward" half space is much more isotropic than the "forward" half space.

8. POWER OF GAMMA-RADIATION DOSE IN AIR OVER AN EARTH SURFACE COVERED WITH GAMMA-RADIATION SOURCES.

This problem corresponds to case "c" (see introduction and Figure 1c).

Any surface distribution of the gamma activity can be considered as consisting of individual point sources and the dose power over the earth can be calculated as the sum of the doses from these individual point sources.

Let us give the results of the calculation of the dose power of gamma rays over sections of the earth, uniformally covered by monoenergetic sources of gamma rays.

The doses of gamma rays in air from the point source were determined from data obtained with sources of gamma quanta of three different energies ($\varepsilon_0 = 0.41$, 1.25, and 2.8 Mev) in model experiments in water, pertaining to the propagation of gamma rays in an infinite homogeneous medium. In these calculations we disregard the inhomogeneity of the medium, i.e., the influence of the earth on the dose in the air.

The results of the calculations are given in the form of the formula**

$$P = 1{,}48 \cdot 10^{-5} \mu_e \sigma f(\varepsilon_0, H, r), \text{ r/sec,} \qquad (8.1)$$

where P is the dose power of the gamma rays in air and altitude H above the center of an area on earth with radius r, on which the gamma ray sources are uniformly distributed. The activity of these sources is σ Mev/sec-cm^2, and μ_e is the linear coefficient of absorption of energy in air.

---

*One should expect the anisotropy of the angular distribution of the doses to decrease with increasing R/λ.

**The calculations were performed by V. N. Sakharov.

Table 18

Values of the coefficient $f(H, \varepsilon_0, r)$ for the calculation of gamma radiation

ε_0, Mev	Altitude H of the point of measurement of the surface, meters	$f(H, \varepsilon_0, r)$ when the radius of the gamma-active surface is r meters					
		25	50	100	200	500	∞
0,41	0,7	—	—	—	—	—	2,87
	1	1,6	1,95	2,79	2,555	2,695	2,7
	25	—	—	—	—	—	1,1
	50	0,55	0,165	0,38	0,605	0,74	0,75
	100	—	—	—	—	—	0,405
	200	0,00205	0,00825	0,0305	0,085	0,14	0,1435
	250	0,00105	0,00425	0,016	0,0435	0,081	0,085
	300	—	—	—	—	—	0,0485
	500	$0,435 \cdot 10^{-4}$	$1,75 \cdot 10^{-4}$	$6,4 \cdot 10^{-4}$	0,00215	0,00525	0,00625
	1000	—	—	—	—	—	0,00006
1,25	0,7	—	—	—	—	—	2,9
	1	1,6	1,95	2,28	2,535	2,71	2,73
	25	—	—	—	—	—	1,125
	50	0,0535	0,165	0,37	0,585	0,76	0,78
	100	—	—	—	—	—	0,45
	200	0,0022	0,00875	0,0375	0,093	0,18	0,193
	250	0,00125	0,005	0,0185	0,0525	0,1165	0,13
	300	—	—	—	—	—	0,09
	500	$1 \cdot 10^{-4}$	$3,9 \cdot 10^{-4}$	$14,5 \cdot 10^{-4}$	0,005	0,0135	0,018
	1000	—	—	—	—	—	0,0005
2,8	0,7	—	—	—	—	—	2,9
	1	1,6	1,93	2,25	2,525	2,735	2,785
	25	—	—	—	—	—	1,19
	50	0,053	0,16	0,365	0,595	0,8	0,855
	100	—	—	—	—	—	0,535
	200	0,0024	0,0095	0,0375	0,1	0,215	0,26
	250	0,0015	0,006	0,0225	0,06	0,15	0,19
	300	—	—	—	—	—	0,145
	500	$1,65 \cdot 10^{-4}$	$6,5 \cdot 10^{-4}$	$25 \cdot 10^{-4}$	0,009	0,035	0,052
	1000	—	—	—	—	—	0,0055

As was shown in Section 6, μ_e depends little on ε and it can be set at $3.4 \times 10^{-5} \pm 12$ percent for quanta with ε ranging from 0.1 to 2 Mev.

The values of the coefficient $f(H, \varepsilon_0, r)$, needed for calculations by means of formula (8.1) of doses over a surface which is uniformly covered by gamma sources of energy ε_0 Mev, are listed in Table 18 (the radius r of the gamma activity of the surface is given in meters).

The values of the coefficient $f(H, \varepsilon_0, r)$ for values of ε_0, H, or r different from those given in Table 18, can be obtained by interpolation.

Figure 22 shows, for convenience in interpolation, the values of $f(H, \varepsilon_0)$ as functions of ε_0. It follows from Table 18 and Figure 22 that at low altitudes above the earth ($H < 200$ meters) the magnitude of the dose of the gamma rays depends only on the surface density of the radiation of the energy and is practically independent of the energy of the gamma quanta, ε_0, in an interval of ε_0 from 0.41 to 3 Mev. This circumstance makes it possible to determine, on the basis of dosimetric measurements carried out on altitudes up to 200 meters, the density of the surface contamination of the earth or the dose power of the surface of the earth, independently of the energy of the quanta radiation from the sources covering the earth.

Table 18 shows that for $H \approx 0.7 - 1$ meter the intensity and the dose power of the gamma rays can be calculated from the following simple formulas:

$$J \approx 3\sigma, \text{ Mev/sec} \cdot \text{cm}^2, \tag{8.2}$$

$$P \approx 1{,}5 \cdot 10^{-9}\sigma, \text{ r/sec}. \tag{8.3}$$

Figure 21 shows the values of the coefficient $f(H, \varepsilon_0, r)$ as a function of the magnitude of the radius of gamma activity on the earth's surface (the values of the quantum energy are marked at the end of each curve. At the end of each group of three curves, pertaining to the quantum energies 0.41, 1.25 and 2.8 Mev, there is indicated the height of the detector H above the earth).

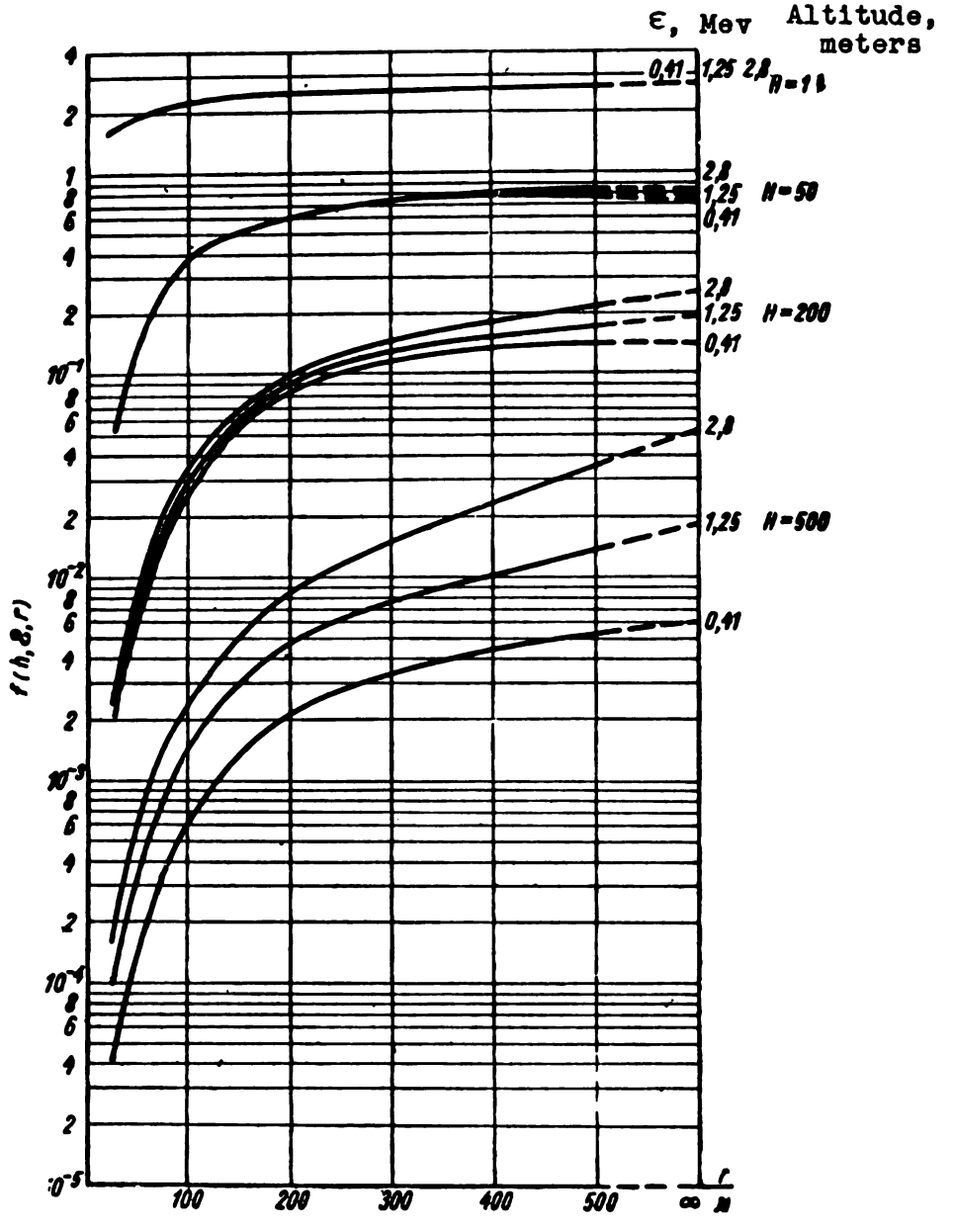

Figure 21. Dependence of the coefficient $f(\varepsilon_0, H, r)$ in formula (8.1) on the radius r of a surface uniformly covered by sources of gamma radiation.

Altitude, meters

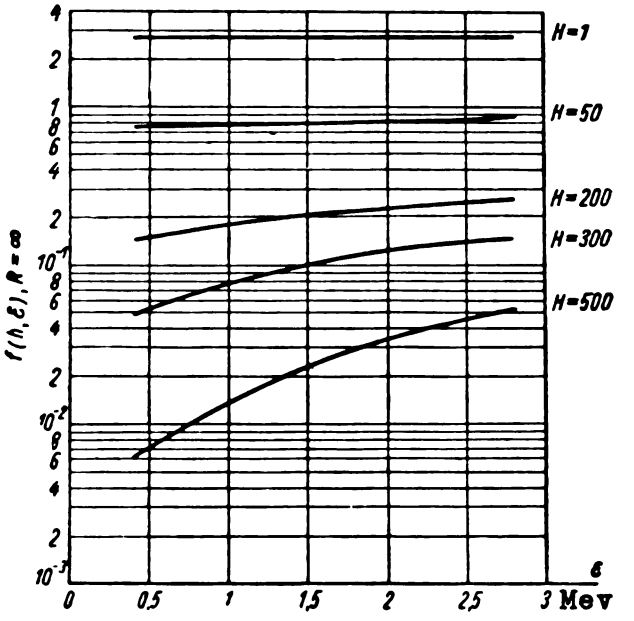

Figure 22. Values of the coefficient $f(\varepsilon_0, H, r = \infty)$ for different quantum energies ε, determining according to (8.1) the dose power in air at an altitude H above an infinite area, uniformly covered with sources having a surface activity σ Mev/cm^2 sec.

As can be seen from the figure, at small heights above the earth ($H \approx 1$ meter) the dose of gamma rays is determined essentially (up to 90 percent), by sources located not farther than 200 - 300 meters from the measurement source. The gamma activity of more remote portions produces only an insignificant fraction of the total dose.

As the height of the point of dose measurement above the earth is increased, the role of the remote portions becomes more important. Table 19 gives the radii of sections, whose gamma activity determines 50, 80, and 90 percent of the total dose of the gamma radiation above an infinite surface of the earth, uniformly covered by gamma-ray sources.

The table makes it possible to estimate the influence of contamination sections located at various distances from the measurement point on the gamma-ray dose. This is important to know when doses are measured over regions with nonuniform radiation energy density σ.

Table 19

Radii of sections (r, meters) producing a definite fraction of the total gamma-ray dose

Height of measurement point above the earth, H, meters	ε_0 = 0.41 Mev			ε_0 = 1.25 Mev			ε_0 = 2.8 Mev		
	50%	80%	90%	50%	80%	90%	50%	80%	90%
1	15	75	140	15	85	160	15	95	130
50	100	200	290	110	230	325	130	270	370
200	140	300	375	210	340	460	260	475	—
250	200	370	450	250	370	470	300	500	—
500	280	460	—	325	550	—	450	—	—

If the distribution of the activity above the earth is uniform within several hundred meters, i.e., if σ = const, then it is possible to determine the dose at not too high an altitude above the earth from the values of the coefficient f calculated for an infinite plane, i.e., the coefficient $f(H, \varepsilon, r = \infty)$.

9. DOSE POWER OF GAMMA RADIATION ABOVE A PLANE LAYER OF ABSORBER, CONTAINING SOURCES OF GAMMA RADIATION.

This problem corresponds to case "b" (see Introduction, Figure 1b) of the action of gamma rays in an atomic explosion.

When the earth becomes activated, and also when gamma activity becomes distributed in a volume of water, individual point sources of gamma rays are distributed over a layer of the absorber (earth or water). To calculate the doses of gamma radiation above the surface of a gamma active layer of absorber, it is necessary to take into account the absorption of the radiation in this layer.

As in the case described in Section 8, the dose of γ rays can be calculated as the sum of the doses from the individual point sources. The yield of γ radiation from an individual point source from an absorber layer into the air above the surface has been investigated experimentally by means of water experiments. With an error not exceeding ± 10 percent, the coefficient of attenuation of the dose power the γ rays, at an absorber layer up to $(4 - 6)\lambda_0$ can be represented in the form (7.13') [21].

$$K_r = \alpha e^{-x/\lambda_{eff}}, \qquad (9.1)$$

where x is the thickness of the layer of absorber along the path of the γ rays from the source to the point of measurement, while α and λ_{eff} are empirical coefficients.

The values of the coefficients α and λ_{eff} for the case of absorption of the radiation in water in the presence of point sources of γ-quantum energy ε_0, amounting to 0.41, 1.25, and 2.8 Mev, and of γ rays from Na^{24}, are given in Table 20.

The radiation of Na^{24}, which consists of γ rays with $\varepsilon_0 = 1.4$ and 2.8 Mev, is the most characteristic for the radiation from earth and water activated by neutrons. The values of λ_{eff} for earth, concrete, or other substances which consist of light elements can be obtained by multiplying the given values of λ_{eff} for water by the ratio of the electron densities of the substances. This has yielded the values of λ_{eff} for water given in Table 20.

Table 20

Parameters of α and λ_{eff} of the coefficient of attenuation K_r in formula (9.1)

Quantum energy ε_0, Mev	α	λ_{eff}, cm	
		in water	In earth (ρ =1.7 g/cm^3)
0.41	1.36	18	10.6
1.25	1.33	24	14.1
2.8	1.2	39	23
γ rays from Na^{24}	1.23	34	20.0

The coefficient α for absorbers made of light elements is independent of the density of the substance. The values of α and λ_{eff} for γ-quantum energies different from those given in Table 20 can be obtained by interpolation, using Figure 23.

If the distribution of the γ activity in the absorber layer is known, then by using the data of Table 20 it is possible to calculate the doses of γ rays above the surface of the absorber. With uniform distribution of the γ activity, it is possible to obtain the solution in the form of simple formulas.

Figure 24 gives the scheme of the solved problem.* The dose power of the γ rays at an altitude H above an infinite layer of absorber of thickness x, with sources uniformly distributed in such

*The calculation of the dose power was carried by V. N. Sakharov.

a way that the specific activity corresponds to g Mev/sec - cm^3, is

$$P = 1{,}48 \cdot 10^{-5}\,\mu_e \int_0^x \int_{l_o}^{\infty} \frac{2\pi\, r\,dr}{4\pi\, L^2}\; g\varepsilon\; e^{-\frac{xl}{\lambda_{eff} H}}\, dx,\ \text{r/sec.} \qquad (9.2)$$

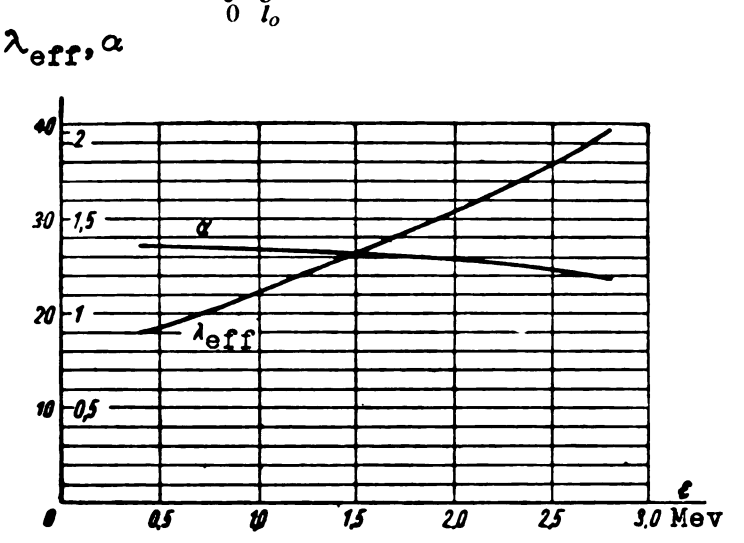

Figure 23. Attenuation of the dose power from a point source on passing through a plane layer of water. The values of the coefficient λ_{eff} and α in formula (9.1) are for different quantum energies ε.

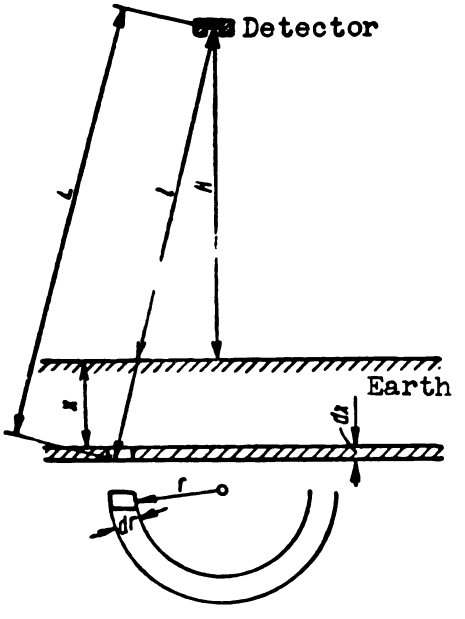

Figure 24. Scheme for calculating the dose power at an altitude H above a layer of absorber, in which the sources of γ radiation are uniformly distributed.

It is seen from Figure 24 that

$$\frac{dL}{L} = \frac{dl}{l}; \; l\,dl = r\,dr \tag{9.3}$$

(l_0 is the minimum distance from the detector to the earth, from which the integration begins, $l_0 \geqslant H$). In integrating from l_0 to infinity, one calculates the dose power of the γ rays, produced by the γ activity of the entire active layer, with the exception of those portions of this layer which are located at a distance $l < l_0$ from the detector $P(l_0)$. In integrating from $l_0 = H$ to ∞, one calculates the dose power from the entire active layer P(H). The difference between P(H) and $P(l_0)$ determines the dose power of γ rays from the γ activity, located at a distance $l < l_0$ from the detector; x is the thickness of the active layer, measured in the same units of length as λ_{eff}. The distances H and l are measured in identical arbitrary units of length. The absorption or scattering of γ quanta in air is not considered, and therefore (9.2) is valid only for small values of the height H.

By integrating with respect to x and l and using formula (9.3), we get

$$P(l_o, x, H) = 1{,}48 \cdot 10^{-5}\mu_e \alpha \frac{g}{2}\left\{ x\left[-\mathrm{Ei}\left(\frac{-xl_0}{\lambda_{eff}H}\right)\right] + \right.$$

$$\left. + \frac{\lambda_{eff}H}{l_0}\left(1 - e^{-\frac{xl_0}{\lambda_{eff}H}}\right)\right\}, \text{ r/sec.} \tag{9.4}$$

For the entire infinite activated layer of absorber of thickness x, i.e., for $l_0 = H$ we get

$$P(x, l_0 = H) = 1{,}48 \cdot 10^{-5}\mu_e \alpha \frac{g}{2}\left\{ x\left[-\mathrm{Ei}\left(-\frac{x}{\lambda_{eff}}\right)\right] + \right.$$

$$\left. + \lambda_{eff}\left(1 - e^{-\frac{x}{\lambda_{eff}}}\right)\right\}, \text{ r/sec.} \tag{9.5}$$

For an infinitely thick layer, i.e., for $x \longrightarrow \infty$, we get

$$P(l_o, x = \infty) = 1{,}48 \cdot 10^{-5}\mu_e \alpha g \frac{\lambda_{eff}}{2}\frac{H}{l_0}, \text{ r/sec.} \tag{9.6}$$

When $l_0 = H$ and when $x \longrightarrow \infty$, i.e., for an infinite uniformly activated half-space of absorber, we have

$$P = 1{,}48 \cdot 10^{-5}\mu_e \alpha g \frac{\lambda_{eff}}{2}, \text{ r/sec.} \tag{9.7}$$

A feature of formulas (9.5) and (9.7), derived for an infinite layer of absorber, is that the dose power of the γ rays does not depend on the height of the point of measurement above the layer, i.e., on H, so long as absorption of γ rays in the air can be neglected, meaning so long as the height of the measurement point above the earth is not greater than 20 - 50 meters.

Using the formulas derived we can determine the dose power not only above an infinite section of a γ-active layer of absorber, but also over a finite one.

The dose power above a layer of absorber of radius r and thickness x is

$$P(r, x) = P(H, x) - P(l_0 = \sqrt{H^2 + r^2}, x) = \\ = 1{,}48 \cdot 10^{-5} \mu_e \alpha \frac{g}{2} F(\varepsilon_0, H, r, x). \tag{9.8}$$

Figure 25 shows the values of the coefficients $F(\varepsilon_0 H, r, x)$, calculated from formulas (9.4), (9.5), and (9.8) for an altitude of 1 meter above the surface of γ-active earth with density $\rho = 1.7$ g/cm^3. The coefficients F have been calculated for γ-quantum energies ε_0 equal to 0.41, 1.25 Mev and for γ rays Na^{24} at various thicknesses and radii of the active layer of earth. On the right-hand vertical axis are shown values for an infinitely thick layer of active absorber, i.e., for the case $x \to \infty$. The values of the quantum energies ε, to which the curves pertain, are written down at the end of each group of curves. The upper group of curves pertains to non-monoenergetic γ radiation from radioactive Na^{24}, consisting of quanta with energies 2.8 and 1.4 Mev.

As can be seen from Figure 25, the upper layer of earth of thickness 5 centimeters produces approximately 50 percent of the dose produced by an infinitely thick radioactive layer.

Layers of activated ground located at depths greater than 20 centimeters, can produce not more than 50 percent of the complete dose of γ rays if the earth is uniformly activated. One can therefore assume that the dose above the surface of the earth is produced essentially only by the upper active layers, 20 - 30 centimeters thick. For the radioactive layers of thickness one can use in practice the simple formulas (9.6) and (9.7), which have been derived for infinitely thick layers. In accordance with (9.8)

$$P(\varepsilon_0 H, r) = 1{,}48 \cdot 10^{-5} \mu_e \alpha g \frac{\lambda_{eff}}{2} \left(1 - \frac{H}{l_0}\right), \tag{9.9}$$

(the dependence on ε is through λ_{eff}).

Here

$$l_0 = \sqrt{H^2 + r^2}.$$

From this formula, as well as from the data given in Figure 25, one can draw conclusions concerning the dependence of the dose

power above an active layer on the radius r of this layer. In the case of uniform activation of the ground, parts of the active ground located at a distance greater than l_0 from the measurement point, produce (H/l_0) x 100 percent of the total dose of γ rays produced by the entire infinite layer of ground. For example, when H = 1 meter, the portions of the ground more than 10 meters away from the point of measurement produce only 10 percent of the total dose, while the portions more than 20 meters away produce only 5 percent of the total dose.

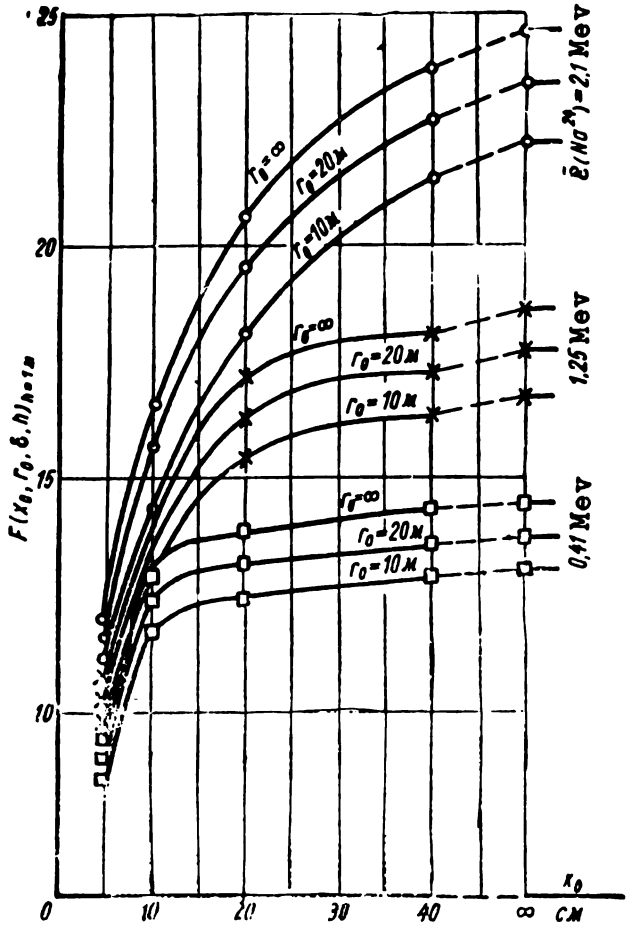

Figure 25. Values of the coefficients $F(x, r, \varepsilon_0)$, which determine, according to (9.8), the dose power above a plane around layer of absorber x centimeters thick and of radius r, in which the sources of γ radiation are uniformly distributed.

Taking into consideration the statements made above regarding

the weak dependence of the dose power above an active layer of ground on the thickness of the layer when $x > 20$ centimeters and on the radius of the layer when $H = 1$ meter and $r > 20$ meters, and recognizing that in real atomic explosions the ground is uniformly activated within the indicated limits of x and r, we can use the following formulas for the calculation of the doses from the activated ground:

$$P = 1 \cdot 48 \cdot 10^{-5} \mu_e \alpha g \frac{\lambda_{eff}}{2}, \text{ r/sec}, \tag{9.10}$$

$$J = \alpha g \frac{\lambda_{eff}}{2}, \text{ Mev/sec}, \tag{9.11}$$

i.e., the formulas derived for an activated half-space of ground.

Substituting in formula (9.10) the values of the coefficients α and λ_{eff} for sodium from Table 18 ($\alpha = 1.23$, $\lambda = 20$ centimeters, $\rho = 1.7$ g/cm^3, $\mu_e = 3 \times 10^{-5}$ cm^{-1}), we get

$$P = 5{,}8 \cdot 10^{-9} \cdot \Pi g, \text{ r/sec}, \tag{9.12}$$

where Π -- neutron flux, neutrons/cm^2.
The values of g are given in Table 7.
Immediately after the explosion we have

$$P = 3{,}35 \cdot 10^{-14} \Pi, \text{ r/sec},$$

after 1 hour

$$P = 2{,}6 \cdot 10^{-16} \Pi, \text{ r/sec},$$

after 20 hours

$$P = 7{,}9 \cdot 10^{-17} \Pi, \text{ r/sec},$$

10. ATTENUATION OF A PARALLEL BEAM OF γ RAYS IN A PLANE LAYER OF ABSORBER.

This problem corresponds to item "d" in the introduction and to Figure 1d. The paper of Hirshfelder, Adams, and Hull [13] gives an approximate solution, and in reference [10] there is a more exact solution of the problem for the case of normal incidences of the γ rays on a plane layer of absorber.

In reference [13] it is considered a plane layer of absorber finite thickness, on both sides of which there is vacuum (Figure $1d_2$). On the other hand, in reference [10] it is assumed that the layer of absorber occupies a semi-infinite space (Figure $1d_1$). Thus, the formulation of the problem is somewhat different in these two references.

In the first reference is calculated the intensity of the γ rays passing through the layer of absorber.

In the second reference is calculated the intensity of the γ rays inside the absorber, i.e., the overall intensity of the γ rays that have passed through a definite layer of absorber, and of the γ rays reflected from the deeper layers.

Thus, the doses in the case of Figures $1d_1$ and $1d_2$ should differ by the intensity of the backward-scattered radiation. From the quantitative point of view, the backward scattered radiation depends on the thickness of the absorber layer traversed by the radiation, and may amount from 10 to 50 percent of the total dose of γ radiation.

The results of an experimental investigation of the fact of parallel fluxes of γ rays through a layer of absorber were obtained by A. A. Voevodskii and L. B. Pikel'ner.

They investigated the attenuation of γ rays from Co^{60} in concrete slabs. The doses measured experimentally were found to be smaller than the doses calculated according to the data of reference [13].

The calculated dose may exceed the measured ones by 1.3 - 2 times, and then the calculated thickness of the concrete shield will exceed the correct one by 5 - 10 centimeters. Such deviations can be considered acceptable.

Thus, the measurements of Voevodskii and Pikel'ner show that in practical calculations of shields against γ rays, it is possible to employ the data of the theoretical investigations [13] and [10]. A design of shielding according to these data will contain a certain "safety factor."

The attenuation of the doses, calculated in reference [10], can be represented by means of interpolation formulas similar to (7.13'), i.e.,

$$D = D_0 K_r = D_0 \alpha e^{-x/\lambda_{eff}}. \qquad (10.1)$$

Figures 26a and 26b show the values of the coefficients α and λ_{eff} from formula (10.1), for which this formula gives an error of $\pm$ 10 percent compared with the data of reference [10].*

Everything said above pertains to normal incidence of γ rays on the layer of absorber. In the case of oblique incidence, the intensity of the γ rays attenuates more strongly than in normal incidence of the γ rays on the same layer. This is natural, since the path covered by the primary γ rays in the layer of absorber becomes longer, i.e., the thickness of the layer along the beam of the γ rays increases; we shall call this new thickness the oblique thickness of the layer.

When the γ rays are incident at an angle φ on the surface of an absorbing layer of thickness x, the oblique thickness is

$$l = \frac{x}{\cos \varphi}. \qquad (10.2)$$

*The calculation of α and λ_{eff} from the data of [10] was made by V. I. Tereshchenko.

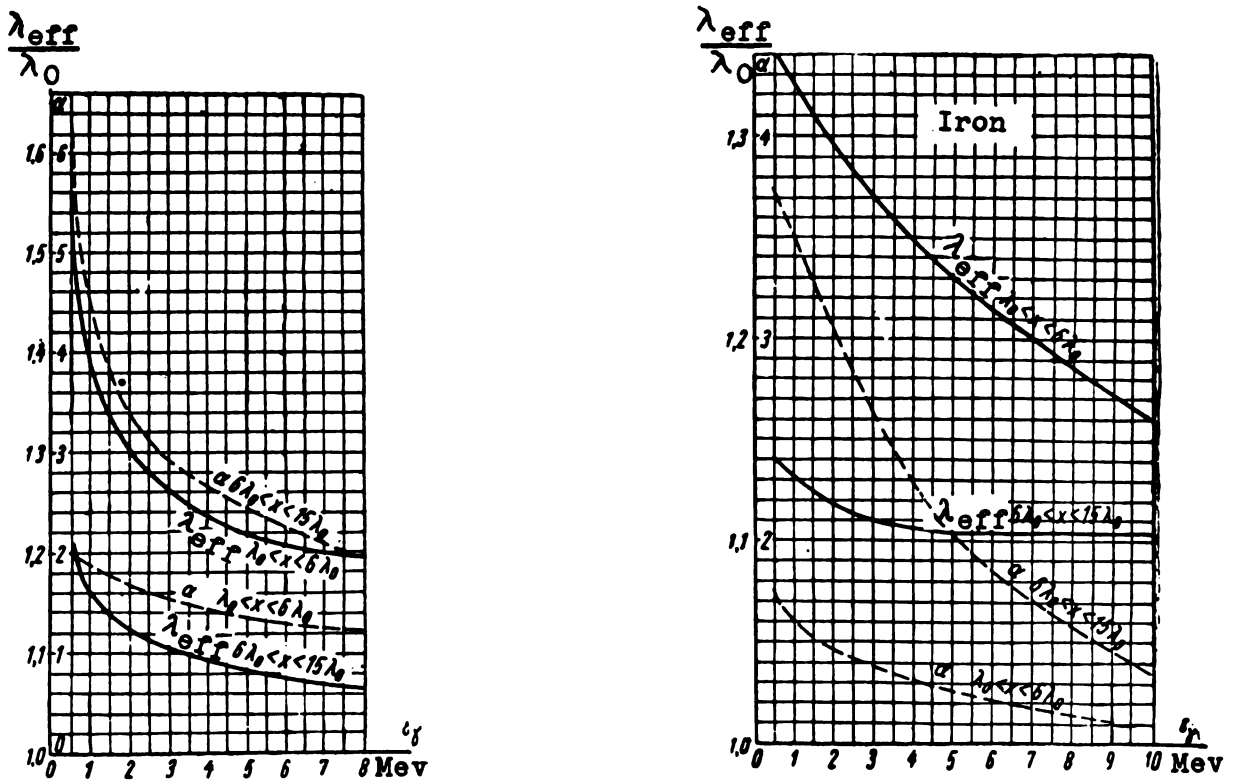

Figure 26. Attenuation of the dose power of a parallel beam of γ quanta in a semi-infinite space filled with water (a) or iron (b) in normal incidence of the quanta on interface between the vacuum and the medium [the coefficients of formula (10.1)].

It would be wrong to assume that the attenuation of the dose power of the γ rays can be calculated from the formulas for normal incidence of γ rays by substituting in these formulas the layer thickness x by the oblique layer thickness l (10.2). Such a calculation will yield too low a value of the γ-ray dose. The point is that in oblique incidence of γ rays, some of the scattered radiation can pass through the layer of absorber through a shorter path than the direct radiation, and consequently the effective thickness of the layer in oblique incidence of γ rays is less than the oblique thickness of the layer $x/\cos\varphi$, and in the case of normal incidence of the γ rays the path of the scattered γ quanta through the layer of absorber will always be greater than the path of the direct radiation.

Figure 27 illustrates the possibility of the scattered radiation passing a shorter path than the direct path in the layer.

The deviation of the effective layer thickness from $x/\cos\varphi$ was observed in the measurements of A. A. Voevodskii and L. B. Pikel'ner, and also by Wyckoff and others [14].

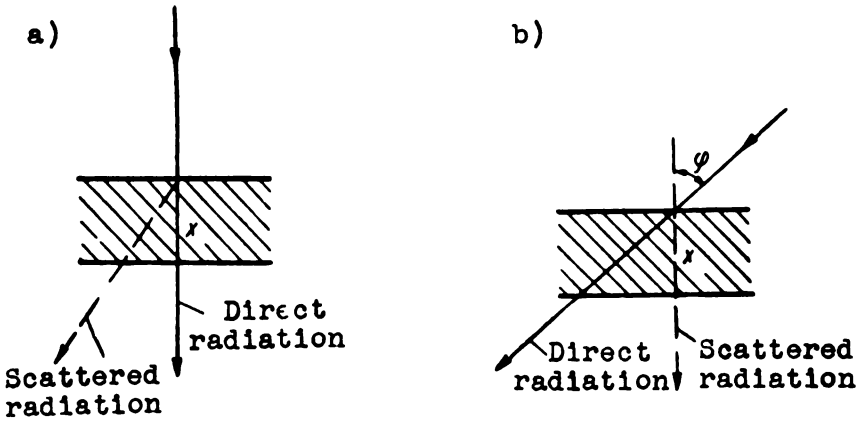

Figure 27. Incidence of quanta on a plane layer of absorber; a -- direct; b -- oblique.

The coefficient of attenuation of the dose in case of oblique incidence of the quantum flux can be expressed by means of a relation

$$K_r(l, \varphi, \varepsilon_0) = a(\varphi, \varepsilon_0, K)\, K_r(l, \varepsilon_0). \qquad (10.3)$$

The coefficient $a(\varphi, \varepsilon_0, K)$ takes into account the specific nature of the oblique incidence, $a(\varphi, \varepsilon_0, K) > 1$, while $K_r(l, \varepsilon_0)$ is the coefficient of attenuation of the dose at a thickness l obtained either by theoretical calculation or by experiment. The coefficient $K_r(l, \varepsilon_0)$ pertains theoretically and experimentally to normal incidence of a parallel beam of quanta on a layer of thickness l.

When $\varphi = 0$ we have

$$l = x;\ a\ (\varphi,\ \varepsilon_0,\ K) = 1. \qquad (10.4)$$

Table 21 gives the values $a(\varphi, \varepsilon_0, K)$, obtained in reference [14]. In that work K_r was measured inexperimentally at normal incidence of the γ rays.

Table 21

Dependence of the coefficient $a\ (\varphi, \varepsilon_0, K)$ in expression (10.3) on the quantum energy ε_0, and on the coefficient of attenuation K_r at different angles of incidence φ

Quantum energy ε_0, Mev	Coefficient of attenuation K_r for normal incidence of γ rays	Value of $a\ (\varphi, \varepsilon_0\ K)$ for		
		$\varphi = 50°$	$\varphi = 60°$	$\varphi = 70°$
0,41	0,1	1,1	1,2	1,2
	0,01	2,0	2,7	4,0
	0,001	3,7	7,0	15,0
0,66	0,1	1,2	1,2	1,3
	0,01	1,7	2,5	3,7
	0,001	2,3	5,2	10,1
1,25	0,1	1,0	1,0	1,2
	0,01	1,4	1,9	2,5
	0,001	2,0	3,5	5,6

In the interval of incidence angles from 0 to 30° it can be assumed that $a(\varphi, \varepsilon_0) = 1$, i.e., that the "oblique" thickness of the layer is equivalent to the "direct" thickness. At greater angles of incidence it is necessary to take into account the fact that "direct" and "oblique" thicknesses are not equal, and to employ in the calculations the coefficients $a(\varphi, \varepsilon_0, K)$ in accordance with (10.3).

The value of $a(\varphi, \varepsilon_0, K)$ increases with increasing φ and K and decreases with increasing ε_0. Table 21 is so far the only source of information on the values of $a(\varphi, \varepsilon_0, K)$, which can be used to estimate the doses in oblique incidence of γ rays on a shielding layer.

11. ALBEDO OF γ RADIATION.

The question of the albedo arises in the analysis of the action of γ rays from an atomic explosion (Introduction, Figure 1). Experimental data on the albedo of γ rays are scanty, in particular with respect to the spectral and angular distribution of the scattered radiation. The greater part of the information on albedo can be obtained from the theoretical papers [15] and [16], in which the calculations were performed by the "Monte Carlo" method. As regards the spectrum and angular distribution of the scattered radiation, the accuracy of the calculations is probably higher at present than the accuracy of the measurements.

The scattered quanta emerging from the surface of the absorber are formed in the concrete and in the light elements, essentially as a result of multiple scattering rather than single scattering. In scattering from concrete, the multiple scattering provides two or three times more energy than single scattering. With increasing Z, the role of multiple scattering decreases, owing to the increase in the photoelectric absorption, and the value of the albedo approaches the value determined by single scattering, particularly at low quantum energy.

Figure 28 shows the calculated values of the albedo of the γ-ray energy in the case of scattering from concrete at different energies of incident quanta and at different angles of incidence [15].

Table 22 lists the values of the albedo of the energy of γ radiation produced by quanta of energy 1 Mev. The albedo was calculated for different angles of incidence and for scattering from substances with different Z [16] (the table lists substances whose effective atomic widths correspond approximately to the indicated numbers of the elements).

The albedo increases with decreasing quantum energy and with decreasing Z. As the angle of incidence is increased the albedo increases, and the dependence of the albedo on Z is less pronounced.

Table 22

Albedo of γ quanta with energy ε = 1 Mev as a function of the atomic number Z and the angle of incidence φ

Substance	Atomic number of the element Z	Albedo of the energy			Albedo of energy of an isotropic source located on the surface of the scatterer
		$\varphi = 0°$	$\varphi = 45°$	$\varphi = 80°$	
Water	8	0,051	0,085	0,198	0,15
Concrete or earth	13	0,044	0,078	0,192	0,13
Iron or copper	29	0,027	0,061	0,175	0,12
Tin or barium	50	0,012	0,038	0.140	0,08
Lead	82	0,002	0,03	0,092	0,05

Figures 29 and 30 show the dependence of the albedo of the energy of γ quanta from Co^{60} on the atomic number of the scatterer as measured by B. P. Bulatov and E. A. Garusov [18]. The measurements pertained to experiments with normal incidence of the quanta on the surface of the scatterer.

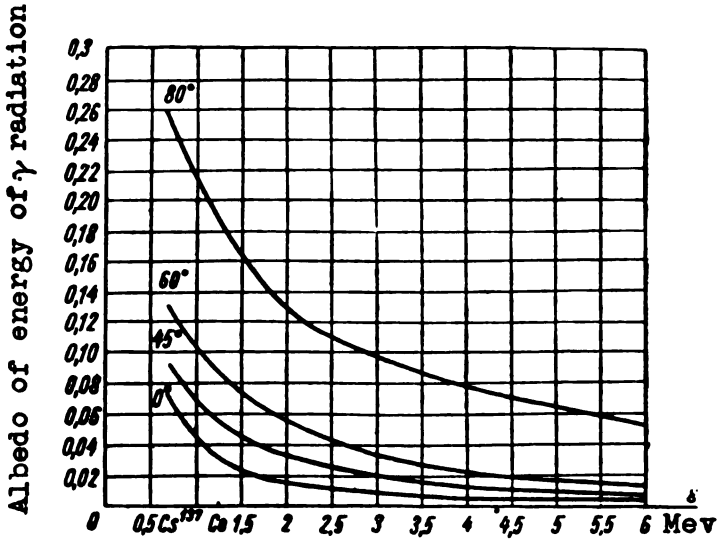

Figure 28. Calculated values of the albedo of the energy of γ radiation in scattering from concrete of γ quanta with energy ε, incident on the concrete at angles $\varphi = 0°$; 45°; 60°; and 80°; as marked at the start of each curve [15].

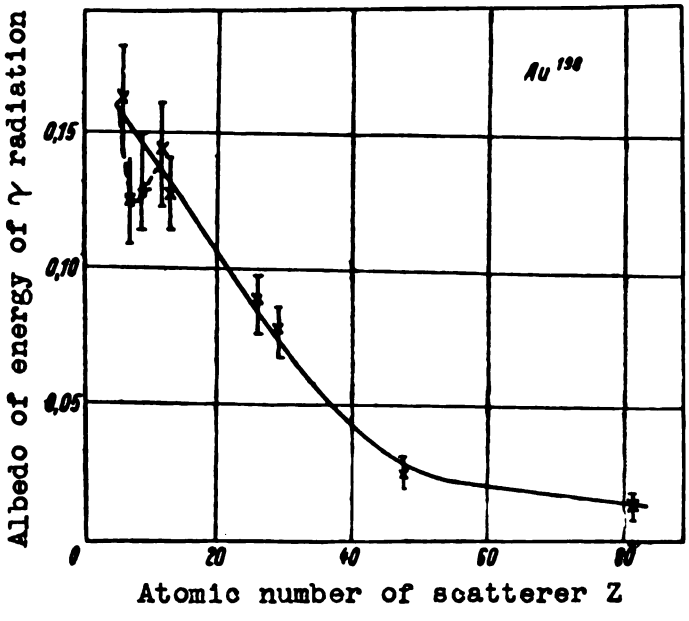

Figure 29. Measured values of the albedo of energy of γ radiation of quantum energy 0.41 Mev, incident perpendicular to the surface of scatterer with atomic number Z [18].

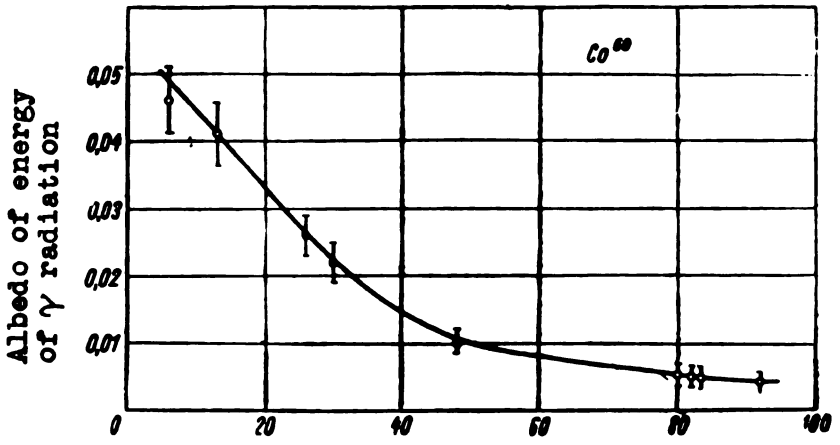

Figure 30. Measured values of the albedo of energy of γ radiation from Co^{60} (average quantum energy 1.25 Mev), incident perpendicularly to the surface of a scatterer with atomic number Z [18].

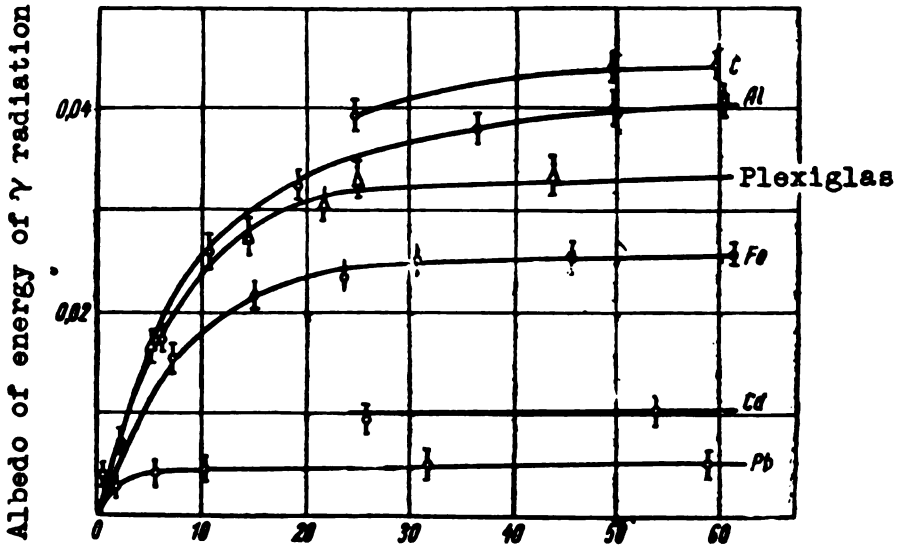

Figure 31. Dependence of the albedo of energy of γ radiation from Co^{60}, incident perpendicularly to the scattering surface on the thickness of the scatterer (average quantum energy 1.25 Mev) [18].

Figure 31 shows the radiation of the albedo with increasing thickness of the scatterer (at the end of each curve is indicated the scatterer material [18]). It is seen from Figure 31 that the albedo reaches its full value, shown in Figures 29 and 30 at a thickness equal approximately to 1 range unit for light elements and approximately 0.5 range unit for heavy elements.

Calculated information on the angular distribution of scattered radiation is available only for the case of normal incidence of γ quanta from Co^{60} source on concrete. The intensity of the scattered radiation, traveling from the surface at an angle φ to the normal, is approximately proportional to $\cos\varphi$.

In the case of oblique incidence of γ rays, the cosine law does not hold. In the "forward" direction the flux of the scattered energy is greater; a quantitative estimate is difficult to obtain at the present time.

Figure 32 shows the calculated spectrum of scattered radiation of Co^{60} from concrete at different angles of incidence. The greatest amount of scattered energy lies in the interval 100 - 300 kev. The few experiments do not contradict the values of Figure 32 and show that the interval of quantum energy at which the maximum of scattered energy occurs is practically independent of the atomic number of scatterer and is at least for normal incidence, independent of the energy of the incident of γ rays in the investigated interval 0.28 - 1.25 Mev.

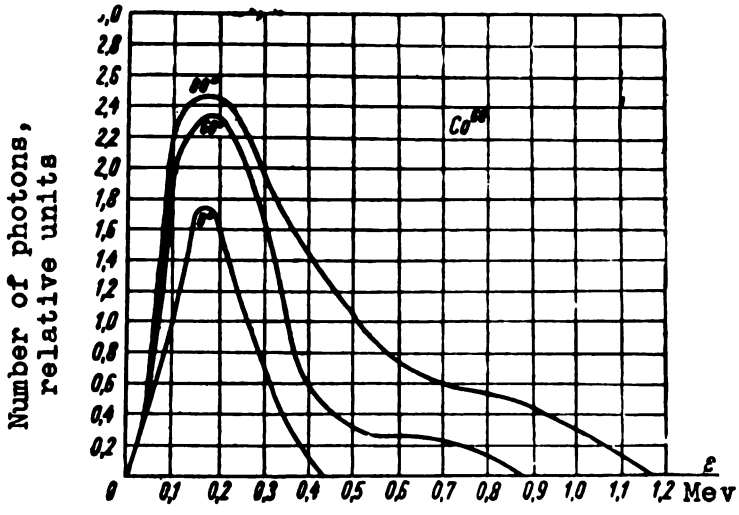

Figure 32. Calculated spectral distribution of quanta scattered from concrete on which γ radiation from Co^{60} is incident (ε_0 = 1.25 Mev) for different angles of incidence [15].

The γ radiation from an atomic explosion is scattered and becomes softer on passing through air, therefore the albedo for air is greater than that showing in Figures 29 and 30.

Inasmuch as the value of the albedo depends on the energy and

on the angle of incidence of the quanta, the albedo of γ radiation from an explosion can depend on the distance from the center of the explosion, on the angle between the flux of quanta incident on the scatterer and the direction from the center of explosion, etc. To estimate the albedo of γ radiation from an explosion it is necessary to assume approximately that it is similar to the γ radiation from Co^{60}, surrounded by a layer of paraffin several range units thick, which simulates the air. The albedo of the energy from such a radiation can be scattered by concrete amounts to approximately 0.15, according to the measurements of V. V. Miller.

Inasmuch as the calculations of the dose frequently do not require great accuracy, provided the calculated dose is not clearly underestimated, this value can be assumed as the value of the albedo for light elements in the case of γ radiation from an explosion. In a more accurate analysis it is necessary to take account of the fact that the "forward" radiation (from the center of the explosion) has a lower albedo than that moving "backward", and the radiation of the "direct ray" has a lower albedo than the scattered radiation.

CHAPTER III

γ-RADIATION DOSE OF AN ATOMIC EXPLOSION

12. INTENSITY OF FRAGMENT γ RADIATION OF ATOMIC EXPLOSION. INFLUENCE OF SHOCK WAVE.

The values of the γ-radiation intensity J(R) and the dose power P(R) can be derived by applying to the atomic explosion the results obtained on the propagation of γ radiation from a point source in an infinite air medium (Introduction, item 1). Then the dose power is given by formula (7.12) or by the equivalent formula (7.14). Let us introduce into (7.14) the coefficients that are characteristic of the γ radiation of the fission fragments (along with μ_{eff} we shall use also the reciprocal quantity $\lambda_{eff} = 1/\mu_{eff}$).

In (7.14) we express G(t) in terms of the fission fragments and the activity of the fragments per fission u(t)

$$G(t) = 1{,}45 \cdot 10^{23} \cdot E_{\text{т.т.}}\, u(t),\ \text{Mev/sec}$$

The values of u(t) are given in Table 1. The coefficients μ_{eff}, α, λ_{eff} and μ_e depend on the energy of the γ quanta emitted by the fragments. In accordance with Table 5, we assume that the time interval of interest to us (several seconds after fission) the average quantum energy is 2 Mev. Then $\mu_e = 3 \times 10^{-5}$ cm^{-1}. The values of α and λ_{eff} in two intervals of distances from the center of explosion are given in Table 23.

Substituting in formula (7.14) the numerical values of the coefficients, and expressing R in meters, we obtain

$$P(t, R) = \frac{5{,}12 \cdot 10^{8} \cdot E_{\text{т.т.}}\, u(t)\, \alpha\, e^{-R/\lambda_{eff}}}{R^2},\ \text{r/sec} \qquad (12.1)$$

In accordance with Table 23, we obtain

$$P(t, R) = \frac{9{,}32 \cdot 10^{8} \cdot E_{\text{т.т.}}\, u(t)\, e^{-R/255}}{R^2},\ \text{r/sec} \qquad (12.2)$$

Formula (12.2) can be used in a broader interval of distances, but the error in this case will be more than 10 percent.

Table 23

Values of α and λ_{eff} in formula (7.14) at a quantum energy 2 Mev ($\mu_e = 3 \times 10^{-5}$ cm^{-1})

Coefficients	Values of coefficients in the interval of distances R, meters	
	$400 < R < 1000$	$1000 < R < 2000$
α	1,82	3,9
λ_{eff}/λ_0	1,31	1,13
λ_{eff}, meters (at a pressure of 760 mm Hg and a temperature 0°C).....	231	200
λ_{eff} meters (at a pressure 760 mm Hg and a temperature 25°C).....	255	220
λ_{eff}, meters (at a density ρ, mg/cm^3	$300/\rho$	—

Expression (12.1) was found to be insufficiently accurate, since it does not take into account the essential feature of the propagation of γ rays under conditions of an atomic explosion.

Ya. B. Zel'dovich and the author have called attention to the fact that the absorption of γ rays along the path from the center of explosion to the point under consideration should be sensitive to the redistribution of the air mass caused by the passage of the shock wave. In the calculation of the propagation of the γ radiation in air it is necessary to take into account the real distribution of the air density produced by the shock wave during the time of the emission of γ radiation. Formula (12.1) is therefore highly approximate, and does not take into account the qualitative aspects of the phenomenon. We shall show below that it gives too low a value to the dose power, as a result of which the error may exceed one order of magnitude.*

Let us examine the distribution of the density of air in a shock wave, which manifests itself on the propagation of γ rays.

In a strong shock wave, which diverges from the center of explosion, all the air is concentrated practically in a narrow edge near the front of the wave and moves outward from the center. This in turn produces inside the shock wave a region with lower density, i.e., a cavity.

After the shock wave has passed by and the initial pressure

*In reference [26], which was published after this book was written, there is mention of the influence of the rarefaction of air. The mechanism of this influence was not explained in detail.

of the air has been restored, the region with lower density nevertheless remains. The entropy in the shock wave increases, the air does not return to the initial state and remains heated after the shock wave has passed and the initial pressure restored. In the region where the shock wave was strong, the residual heating is large and causes the air to glow. The fire ball that forms after the atomic explosion is the "trail" of the prior strong shock wave. The pressure in it is equal to atmospheric, and the density is low because of the high temperature of the air, i.e., the fire ball is a cavity in the air.

Table 24 gives the distribution of the density of the air at different distances in the case of explosion of a 300-kiloton bomb, at the instant 0.765 seconds, when the radius of the front of the shock wave R_f is equal to 1000 meters; Table 25 corresponds to the instant 5.35 seconds, when R_f = 3000 meters.

Table 24

Density of air in shock waves at various distances from the center of a 300-kiloton atomic explosion at an instant 0.765 second after the explosion

Distance from the center, R, meters	1000	900	800	700	600	500	400	300	200
Air density ρ/ρ_0	2,34	1,58	0,913	0,456	0,187	0,0585	0,000	0,000	0,000

The solid curve of Figure 33 shows the distribution of the air density at different distances from the center at the instant 0.765 second.

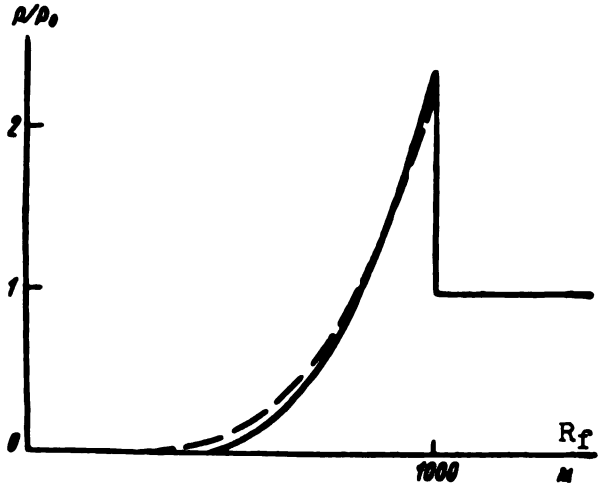

Figure 33. Distribution of the air density in a strong shock wave (E_{TT} = 300 kilotons, 0.765 second after explosion, R_f = 1000 meters).

The solid curve of Figure 34 shows the distribution of the density of the air at different distances from the center at 5.35 seconds.

It is seen from Table 24 that 0.765 second after the explosion, at a distance up to 600 meters from the center, we have $\rho/\rho_0 \ll 1$. The absorption of γ rays in this region is negligible and one can assume that inside the strong shock wave* there is a cavity the radius L of which is 600 meters.

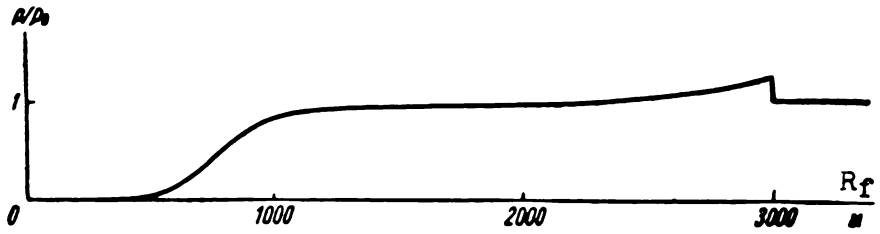

Figure 34. Distribution of the air density after passage of strong shock wave (E_{TT} = 300 kilotons; t = 5.35 seconds after the explosion, R_f = 3000 meters).

With increasing time and radius of the front, the pressure in the front of the shock wave decreases, the shock wave becomes weak, the air partially returns in the opposite direction, and the central regions, as well as all regions with the exception of a small peak on the front of the wave, return to atmospheric pressure. However, the temperature in the central region remains high and the air density remains low.

Subsequently the shock wave, propagating over an ever increasing distance, is continuously attenuated and turns again into a sound wave. The phenomenon of the shock wave terminates, but the air remains heated by its passage. The cooling of the air (and the resumption of the normal density) is by radiation and by convection over a prolonged time, much longer than the time of emission of the major part of the γ radiation.

It is seen from Tables 24 and 25 that several seconds after the explosion the radius of the cavity, determined for example from the condition $\rho/\rho_0 < 0.2$, amounts to 600 meters.

Thus, the region near the center of explosion, in which the shock wave is strong, is a region where the low air density both during the time of passage of the shock wave and afterwards, i.e., during the entire time when the γ rays are emitted by the fission fragments.

The radius of the fire ball L_{fb} fixes the extreme position at which the shock wave was still strong.

The evolution of the cavity exerts a strong influence on the

*We call a strong shock wave one in which the pressure on the front is much greater than the initial pressure.

intensity of ionization of the air at all points under consideration, inside and outside the cavity.

Table 25

Density of air in shock wave at various distances from the center of an atomic explosion of energy 300 kilotons at an instant 5.35 seconds after the explosion

Distance from the center, R, meters	3000	2700	2400	2100	1800	1500	1200	900	600	300
Air density ρ/ρ_0	1,22	1,1	1,01	0,952	0,939	0,927	0,878	0,732	0,122	0,000

The γ rays pass through the cavity practically without being absorbed; their flux decreases inside the cavity only in inverse proportion to the square of the distance from the center, as if the γ rays were to propagate in vacuum.

Let us give an example of the influence of the cavity on the intensity of ionization under the conditions of Table 24 for a point located at a distance R = 600 meters from the center of explosion, during the instant of time 0.765 second, when the shock wave has propagated at the distance R_f = 1000 meters from the center.

Figure 35 shows a diagram of this example.

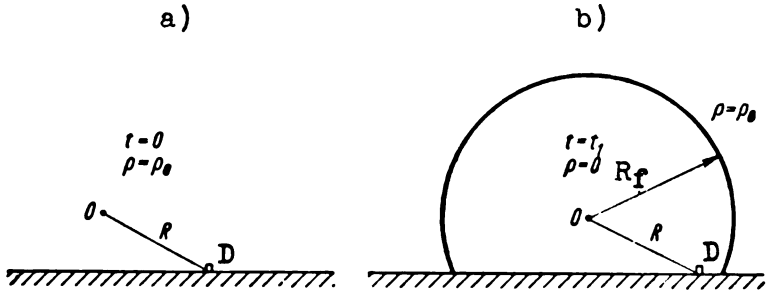

Figure 35. Reduction in the absorbing layer of the earth when the detector D enters inside the shock wave (b); a -- distance at the instant of explosion.

When the detector D (for example, an ionization chamber measuring the intensity of the ionization) is inside the cavity (Figure 35b), then obviously the intensity or the radiation dose power registered by the detector can be greater than during the first instant after the explosion (Figure 35a), because in this case (case a) an absorbing layer of air R is located between the γ ray source (fragment cloud) and the detector, and after 0.765

second (case b) a considerable part of the air between the fragment cloud and the chamber is carried away by the front of the shock wave.

According to formulas (12.4) and (12.2) as well as Table 1, the dose power is:

1) for case a

$$P(0) = \frac{5{,}12 \cdot 10^8 E_{т.т.} u(0) \alpha e^{-R/\lambda_{eff}}}{R^2};$$

2) for case b

$$P(0.765 \text{ sec}) = \frac{5{,}12 \cdot 10^8 E_{т.т.} u(0{,}76)}{R^2};$$

$$\frac{P(0)}{P(0.765 \text{ sec})} = \frac{u(0.76)}{\alpha u(0)} e^{-R/\lambda_{eff}} = \frac{0{,}41}{1{,}8 \cdot 0{,}82} e^{-600/255} = 2{,}9. \quad (12.3)$$

The intensity of ionization at the instant 0.765 second should decrease to one half, because of the decay of the fragments; however, because of the passage of the shock wave the intensity of ionization not only did not decrease, but increased by a factor of 2.9 compared with the initial instant of time.

It is seen from the foregoing example that the formation of the cavity inside the shock wave is a strong physical factor, which determines to a considerable degree the intensity of the γ radiation and the dose of the γ rays in an atomic explosion.

We have chosen for illustration an extreme case of the action of a strong shock wave on the passage of γ rays, namely the case when the front of the shock wave has moved to the position of the chamber (Figure 35b) so that there is practically no air between the center of explosion and the detector.

However, in the case when the front of the shock wave has not yet reached the detector (Figure 36a) and consequently the total amount of air between the source and the center of explosion and the detector remain the same as before the explosion, and the presence of a shock wave decreases the absorption of the γ rays.

So long as there was no cavity (i.e., no shock wave), the γ radiation from the source O passed a distance R to the detector D in the absorbing medium of density ρ_0 (Figure 36a).

When a shock wave is formed the air, filling a sphere of radius R_f (Figure 36a), is forced into an edge of thickness $\Delta R \ll R$ at the surface of the front, and a cavity is formed in a sphere of radius $R_f - \Delta R$ (Figure 36b). The length of path on which absorption of the γ rays takes place is much less in case b than in case a, because $\Delta R \ll R_f$. For example, when R_f = 1000 meters, all the air is concentrated practically in the layer approximately 300 meters thick. To be sure, the density of the air, ρ, is greater along the path ΔR than it was previously on the path R_f, but the increase of the air density in the edge of the shock wave does not compensate for the reduction in the length of the absorbing medium. It is obvious that, as the mass of the air gets distributed in the

spherical layer, the greater the radius of the sphere the smaller the thickness of the layer (Figure 37). And since the absorption of the γ rays is determined by the thickness of the layer, it is found that the same mass of air is more "transparent" to the γ rays if it is distributed in a spherical layer of large radius. Therefore the absorption of the γ rays is less in the case b than in the case a.

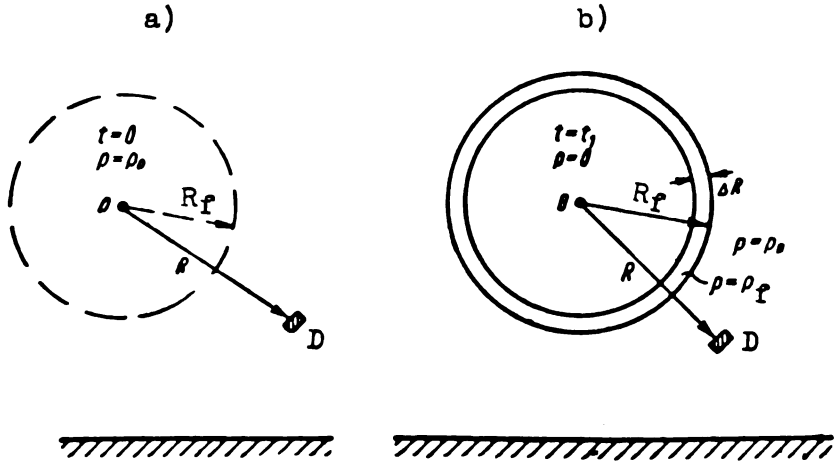

Figure 36. Reduction in absorbing thickness of air when the detector is located outside the shock wave (b); a -- state prior to explosion.

Let us illustrate the foregoing in an idealized case, when the distribution of the density in the front of the shock wave is in the form of a rectangle (Figure 38), instead of the distribution shown in Figure 33.

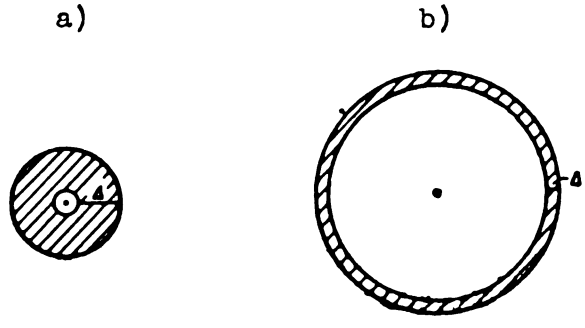

Figure 37. Absorbing thickness Δ for radiation traveling from the center of a sphere, when a constant amount of matter is distributed: a -- in a sphere of small radius (initial time) and b -- a sphere of increased radius (subsequent time).

So long as there was no short wave, the intensity of the γ radiation emitted from a sphere of radius R was proportional to the factor

$$e^{-R/\lambda_{eff}} = e^{-\mu_{eff}R}$$

[see (12.2) and (7.14)].

The appearance of a shock wave causes the medium to become inhomogeneous and the density of the air is not uniform along the ray. It was shown in Section 7 that in the case of inhomogeneity of the medium one can use approximately the "optical thickness" to describe the absorption of the γ rays, and instead of $\mu_{eff}R$ we can put in (7.14) $\int\mu_{eff}(R)dR$.

In the case under consideration (Figure 38), ρ has a value 0 everywhere, with the exception of a layer of thickness ΔR, where $\rho = \rho_f$. Therefore

$$\int_0^{R_f} \mu \frac{\rho}{\rho_0} dr = \mu \frac{\rho_f}{\rho_0} \Delta R. \qquad (12.4)$$

The intensity of the γ radiation emitted from this sphere, after formation of a cavity (i.e., a shock wave) of radius R_f, is proportional to exp $(\mu_{eff}\Delta R\rho_f/\rho_0)$. The quantity $\Delta R\rho_f$ is determined from the condition that the mass of the air contained in the volume of the cavity prior to the formation of the shock wave be equal to the mass of the air now located on the surface of a cavity of radius R_f in a layer of thickness ΔR

$$\frac{4}{3}\pi R_f^3 \rho_0 = 4\pi R^2_f \Delta R \rho_f,$$

hence

$$\rho_f \Delta R = \frac{\rho_0 R_f}{3}. \qquad (12.5)$$

Substituting (12.5) in (12.4) and (12.1) we find that as a result of the cavity produced in the air when the air is forced out of the periphery, the intensity of the γ radiation emitted from a sphere of radius R_f increases by a factor

$$\frac{e^{-\frac{\mu_{eff}R_f}{3}}}{e^{-\mu_{eff}R_f}} = e^{\mu_{eff}\cdot\frac{2}{3}R_f} = e^{\mu_{eff}L_{eff}}. \qquad (12.6)$$

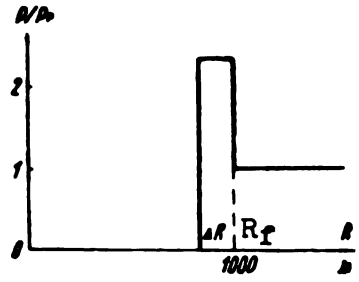

Figure 38. Schematized representation of the distribution of the air density in the front of the shock wave.

We shall henceforth call the quantity L_{eff} introduced in (12.6) the effective radius of the cavity. It is equal to the radius of usual cavity formed by the removal of the air around the source, which reduces the absorption of the γ rays by the same amount as the shock wave under consideration.

The effective radius of the cavity L_{eff} is equal to 2/3 of the radius of the front of the shock wave

$$L_{eff} = \frac{2}{3} R_f. \qquad (12.7)$$

This conclusion is valid only for an idealized distribution of densities as shown in Figure 38. If the distribution of the density in the shock wave is as shown in Figure 33, we have

$$L_{eff} < \frac{2}{3} R_f.$$

Thus, in the case when the detector is located outside the front of the shock wave (Figure 36), and consequently the same amount of air is contained between the detector and the γ-ray source as at the instant of explosion, the absorption of γ rays is still reduced as if the sources were surrounded by a cavity of radius L_{eff}. In the case under consideration (Figure 35 and 36) we have in mind the cavity formed by a strong shock wave at the instant of its passage.

After the shock wave has terminated and atmospheric pressure has been restored, the center of explosion remains surrounded by a cavity formed by the residual heating of the air -- the "fire ball".

All the foregoing statements concerning the reduction in the absorption of γ rays remain obviously true also for that stage of evolution of the cavity, whether the detector be located inside or outside the cavity.

Using the foregoing qualitative considerations concerning the effect of redistribution of air density in the shock wave on the passage of γ rays, let us estimate the dose of γ radiation P(t, R)

using the scheme proposed by Ya. B. Zel'dovich.

We assume here that:

1) The source of γ radiation is practically a point source and is stationary.

2) The absorption of the γ rays is determined by the "optical thickness"

$$\int_0^R \mu_{eff} \frac{\rho}{\rho_0} dR,$$

3) The air density inside the front of the shock wave is distributed in accordance with the interpolation formula which holds only for a strong shock wave:*

$$\rho(r) = \rho_f \left(\frac{r}{R_f}\right)^n, \tag{12.8}$$

r -- distance from the front of the shock wave, measured inside the shock wave.

The exponent n depends on the value of ρ_f and is determined by calculating the amount of air in the shock wave. Prior to occurrence of the shock wave the amount of air contained in the volume of radius R_f was $4\pi R^3_f \rho_0/3$. Thus

$$\frac{4}{3}\pi R^3_f \rho_0 = 4\pi \int_0^{R_f} \rho(r)\, r^2\, dr. \tag{12.8'}$$

Substituting into the integral the expression (12.8) instead of $\rho(r)$, we find that

$$4\pi \frac{\rho_f}{R_f{}^n} \frac{R_f{}^{n+3}}{n+3} = \frac{4}{3}\pi \rho_0 R_f{}^3.$$

Hence

$$n = 3\left(\frac{\rho_f}{\rho_0} - 1\right). \tag{12.9}$$

In calculating $P(t, R, E_{TT})$ it is possible to use either the exact solution of the problem of propagation of γ radiation of a point source in an infinite medium, in the form of the formulas (7.12) and the interpolation formulas for $B_r(\mu, R, \varepsilon)$ (see Appendix

*The dotted line in Figure 33 shows the distribution of the densities according to formula (12.8).

II, Table A22), or use the approximate interpolation formulas (7.14) and (12.1), which are sufficiently accurate in the region where they are valid, but which give an increasing error as the interval of distances where there are applicable is increased. In either case, the specific nature of the atomic explosion is taken into account by introducing into the formula for the dose power on the optical thickness, i.e., by replacing the expression μR by $\int_0^R \mu dR$ in the exponent and in the coefficient B_r of (7.12), and by replacing $\mu_{eff}R$ by $\int_0^R \mu_{eff} dR$ in the exponents of formulas (7.14) and (12.1).

The interpolation formulas (7.14) give rise to larger errors, but permit a more graphic presentation of the results, and consequently we shall use from now on the equations (7.14) and (12.1) as our basis.

Introducing into (12.1) the "optical thickness" instead of $\mu_{eff}R$, we obtain

$$P(t, R, E_{т.т.}) = \frac{5{,}12 \cdot 10^8 E_{т.т.}\, u(t)\, a}{R^2} e^{-\frac{\mu_{eff}}{\rho_0}\int_0^R \rho\, dR}. \qquad (12.10)$$

We shall consider the optical thickness for two cases:
1) the detector is contained inside the shock wave ($R < R_f$);
2) the detectors outside the shock wave ($R > R_f$).

In the first case ($R < R_f$)

$$-\mu_{eff}\int_0^R \frac{\rho}{\rho_0} dR = \mu_{eff}\left(-R + R - \frac{1}{\rho_0}\cdot\int_0^R \rho\, dR\right) =$$

$$= -\mu_{eff}R + \mu_{eff}\left(R - \int \frac{\rho}{\rho_0} dR\right) = -\mu_{eff}R + \mu_{eff} L_{eff}, \qquad (12.11)$$

where

$$L_{eff} = R - \int_0^R \frac{\rho}{\rho_0} dR. \qquad (12.12)$$

Replacing in (12.12) the value of ρ by expression (12.8) and carrying out the integration, we obtain

$$L_{eff} = R\left[1 - \frac{\rho_f/\rho_0}{\frac{3\rho_f}{\rho_0} - 2}\left(\frac{R}{R_f}\right)^{3\left(\frac{\rho_f}{\rho_0} - 1\right)}\right]. \qquad (12.13)$$

Substituting (12.11) in (12.10) we obtain

$$P(t,R,E_{..}) = \frac{5{,}12 \cdot 10^8 E_{T.T.}\, a\, u\,(t)\, e^{-\mu_{eff}R}\, \mu_{eff}\, L_{eff}}{R^2}, \text{ r/sec.} \qquad (12.14)$$

In the case of 2 (when $R > R_f$) we have

$$-\mu_{eff}\int_0^R \frac{\rho}{\rho_0}dR = -\mu_{eff}\int_0^{R_f} \frac{\rho}{\rho_0}dR - \mu_{eff}\int_{R_f}^R dR^* =$$

$$= \mu_{eff}\int_0^{R_f} \frac{\rho}{\rho_0}dR - \mu_{eff}\,[R - R_f] =$$

$$= -\mu_{eff}R + \mu_{eff}\left(R_f - \int_0^{R_f} \frac{\rho}{\rho_0}dR\right) =$$

$$= -\mu_{eff}\,R + \mu_{eff}\,L_{eff}, \qquad (12.15)$$

where

$$L_{eff} = R_f - \int_0^{R_f} \frac{\rho}{\rho_0}dR. \qquad (12.16)$$

Substituting in (12.16) the expression (12.8) and performing the integration we obtain

$$L_{eff} = R_f\,\frac{2\frac{\rho_f}{\rho_0} - 2}{3\frac{\rho_f}{\rho_0} - 2}. \qquad (12.17)$$

*When $R > R_f$ we have $\rho/\rho_0 = 1$.

Substituting (12.15) and (12.10) we obtain a formula identical with (12.14). Formula (12.14) covers both placements of the detector relative to the shock wave. The difference lies in the expressions for L_{eff}, namely (12.12) and (12.16), which differ from each other in that (12.12) contains R instead of R_f.

From a comparison of (12.14) with (12.1) we see that the distribution of the air density, produced by the shock wave, increases the dose power by a factor exp ($\mu_{eff} L_{eff}$). The factor by which the dose power is increased in the presence of a shock wave, relative to the dose power at the same instant of time but in the absence of a shock wave, is called the cavity factor of the dose power, K_p. In formula (12.14) the magnitude of the cavity factor of the dose power is approximated by the expression

$$K_p = e^{\mu_{eff} L_{eff}(t, E)}. \qquad (12.18)$$

Taking into account the statements made above concerning the influence of the shock wave, we introduce K_p into the initial formula (7.14)

$$P(R, t, E) = \frac{1{,}48 \cdot 10^{-5} G(t) \mu_e a e^{-\mu_{eff} R} K_p}{4\pi R^2} =$$

$$= \frac{1{,}48 \cdot 10^{-5} G(t) \mu_e a e^{-\mu_{eff} R} e^{\mu_{eff} L_{eff}}}{4\pi R^2}. \qquad (12.18')$$

In example (12.3), the cavity factor of the dose power is

$$K_p = e^{\mu_{eff} L_{eff}} = e^{L_{eff}/\lambda_{eff}} = e^{600/225} = 7.8. \qquad (12.18'')$$

The dependence of L_{eff} on t and E is expressed in terms of R_f and ρ_f/ρ_0, the values of which depend on the explosion energy and on the time elapsed after the explosion. In the case a very strong shock wave (i.e., when $\rho_f/\rho_0 \gg 1$) we obtain for L_{eff} the following limiting expressions:

In case 1

$$L_{eff} = R \qquad (12.19)$$

and consequently independent of the time.

In case 2 we get in accordance with (12.17)

$$L_{eff} = \frac{2}{3} R_f. \qquad (12.20)$$

The character of variation of ρ_f and R_f with time and explosion energy is as follows.

It is obvious that for a given explosion the radius of the front $R_f(t)$ will increase with time, and $\rho_f(t)/\rho_0$ will decrease. Comparing two explosions with energies E_1 and E_2 we can note that when R_f = const (i.e., $R_f = R_{f1} = R_{f2}$) the quantity ρ_f/ρ_0 increases with increasing explosion energy ($\rho_{f2} > \rho_{f1}$). When t = const, R_f increases with increasing explosion energy because of the increase in the speed of propagation of the shock wave, i.e., $R_{f2} > R_{f1}$. At the same time we have simultaneously $\rho_{f2} > \rho_{f1}$ (the character of variation of ρ_f and R_f with the energy follows from the law of similarity of shock waves).

If the values R_{f1} and ρ_f are known for an explosion of a bomb with energy E_1, then the same values ρ_f are obtained when a bomb of energy E_2 is exploded, but at a different time t_2 and at a different distance, namely:

at an instant of time

$$t_2 = t_1 \sqrt[3]{E_2/E_1}$$

and at a distance

$$R_{f2} = R_{f1} \sqrt[3]{E_2/E_1}.$$

The value of R_f and consequently also of L_{eff} depends also on the conditions of explosion. In the case of a surface explosion R_f is greater than in an aerial explosion with the same energy. This takes place because in a surface explosion the part of the explosion energy that should have gone into the lower half space, i.e., half the explosion energy, remains in the upper half space, where it produces an energy density which is twice as large compared with that of an aerial explosion. Therefore the parameters of the shock wave in the case of a surface explosion are of the same as would occur in an aerial explosion of twice the energy. In particular, in order to compare an aerial explosion with a surface explosion, it is necessary to use in the similarity equations twice the energy in the case of a surface explosion.

The changes in R_f and ρ_f determine the dependence of L_{eff} on the time and energy explosion. For a given explosion, L_{eff} increases with increasing time as a result of the increase in R_f. This increase takes place at an attenuated rate. With further increase in time after the explosion, L_{eff} decreases because of the increase in the air density in the cavity, due to the cooling and mixing with surrounding air. As $t \longrightarrow 0$, we get $L_{eff} \longrightarrow 0$ and $K_p \longrightarrow 1$. At constant t, the value of L_{eff} increases with the explosion energy as a result of the increase of R_f with increasing explosion energy.

This increase in L_{eff} causes the dose power at a given

instant of time to be nonlinear relative to the explosion energy and to increase faster than the energy (i.e., faster than the number of fragments).

Only at small values of t, when L_{eff} is small and consequently $K_p \approx 1$, is the dose power directly proportional to the number of fissions, i.e., to the explosion energy

$$P[t = O, R] = \frac{4{,}2 \cdot 10^8 E_{т.т.} \alpha e^{-R/\lambda_{eff}}}{R^2} =$$

$$= \frac{7{,}64 \cdot 10^8 E_{т.т.} e^{-R/230}}{R^2}, \text{ r/sec.} \qquad (12.21)$$

(we substituted values for u(0) from Table 1, and for α and λ_{eff} from Table 23).

The dose power of the fragment radiation, as a function of time, is determined by the product of two factors $u(t) \exp[\mu_{eff} L_{eff}(t)]$, of which one (the fragment activity) decreases and the other (a cavity factor of dose power) increases with increasing time. As a result of the competition between these two factors, the quantity P(t) has a maximum.

Figure 39 shows the P(t) dependence (the solid curve), calculated by B. V. Novozhilov* for the case of explosions with energy, 2, 20, 200, and 20,000 kilotons.

The unit dose power of the fragment radiation during the first instant of time after explosion.

Curve 3 characterizes the decrease in dose power due only to the radioactive decay of the fragments, and it yields the values of u(t) in Table 1.

The rise of the fragment cloud, which causes an increase in the distance from the sources to the detector, and the cooling of the incandescent air, decrease L_{eff} and should lead to a reduction in the maximum in the region of large values of time elapsed from the instant of explosion, and to a sharper decrease in P(t) than shown in Figure 39. The ratio of the ordinates of the curve 2 and 3 is equal to the cavity dose power factor K_p (12.18).

As can be seen from Figure 39, K_p can reach, in the case of strong explosions in the region of the maximum, several orders of magnitude. K_p decreases with increasing explosion energy. At the maximum, with an explosion energy of 2 kilotons, the value of K_p is 2, and it tends to 1 as $E_{TT} \rightarrow 0$. The instant of arrival of the maximum of dose power depends on the distance and on the explosion energy. At large distances, where the shock wave is strong, the maximum occurs earlier than at great distances, namely when the strong shock wave has passed beyond the place where the detector is located.

*This calculation was based on formula (7.12) and not (7.14).

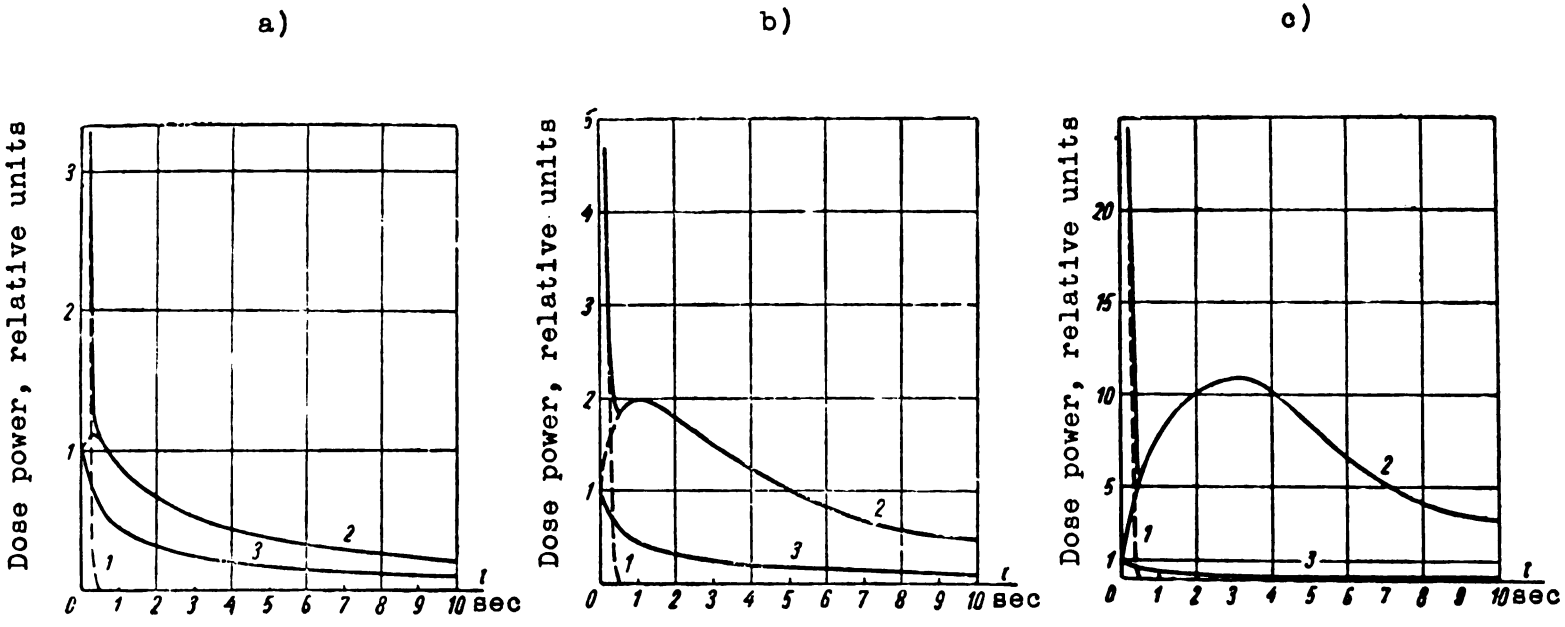

Figure 39. Dependence of the γ-radiation dose power on the time elapsed from the instant of explosion, for explosion energies E = 2 kilotons and R = 500 meters (a); E = 20 kilotons and R = 750 meters (b), and E = 200 kilotons and R = 1500 meters (c). 1 -- dose power of capture radiation; 2 -- dose power of fragment radiation. For comparison we give the change in activity of the fragments with time (curve 3). The solid curve shows the overall dose power. It is parallel to curve 3 only after a long time, after the cavity development has terminated.

At large distances the maximum may appear before the passage of the shock wave through the point under consideration. With increasing explosion energy, the maximum dose power will appear later (if we disregard short distances).

All the foregoing pertains to the dose power due to the fragment radiation. In addition, there exists a short-duration radiation due to capture of neutrons by nitrogen (Section 13). The effective values of the γ-radiation intensity and of the dose power are obtained by adding up both types of radiation, at which the characteristic features in the dose power occur.

13. INTENSITY OF SHORT-LIVED γ RADIATION. SUMMARY DOSE POWER.

From the aggregate of the short-lived radiation, we consider in the present section only the γ radiation due to the capture of neutron in the air, since this makes an appreciable contribution to the dose of the explosion γ rays (Section 1). The notion that short-lived γ radiation should appear during an atomic explosion, in accordance with the reaction $N^{14}(n, \gamma)N^{15}$, was first stated by P. A. Yampol'skii. The intensity of this radiation increases with time exponentially, since the number of events of capture per unit time is proportional to the concentration of the slow neutrons, and the concentration of neutrons decreases exponentially with a period which is called the lifetime of the neutrons τ. At 0°C and a pressure of 760 mm Hg

$$\tau = \frac{1}{n v \sigma_c} = \frac{1}{4{,}32 \cdot 10^{19} \cdot 1{,}7 \cdot 10^{-24} \cdot 2{,}2 \cdot 10^{3}} = \\ = 62 \cdot 10^{-3} \text{ sec.} \qquad (13.1)$$

Here n is the concentration of the nitrogen nuclei; $\sigma_c = 1.7 \times 10^{-24}$ is the summary cross section of the reactions $N^{14}(n, p)C^{14}$ and $N^{14}(n, \gamma)N^{15}$ with thermal neutrons, v = 2.2 cm/sec - rate of motion of thermal neutrons. The lifetime of the neutrons is inversely proportional to the air density.

Since the capture of the neutrons takes place during the time of passage of a strong shock wave, part of the neutrons is captured in the front of the wave, i.e., under conditions of increased air density and consequently, with shorter lifetime, giving rise to capture γ radiation with shorter period. The effective period of radiation is determined by the distribution of the neutrons in the cavity, in the front of the shock wave, and in unperturbed air, and the lifetime of the neutron in these places.

Let us consider γ radiation with a period 62×10^{-3} sec.

Since each neutron reacting with the nitrogen causes the emission of 0.64 Mev in γ radiation, the activity of the source of the short-lived radiation is

$$G_3(t) = q \frac{Q}{\tau} e^{-t/\tau} \cdot 0{,}64, \text{ Mev/sec}, \qquad (13.2)$$

where Q is the number of neutrons emitted to the air, i.e., not absorbed in the case of the bomb; q is the fraction of the neutrons captured in the air.

In the case of surface and low aerial explosion, some of the neutrons are captured by the earth,* so that the number of neutrons captured in the air amounts to a fraction of the total number of neutrons. In the case of an aerial explosion q = 1, and in the case of a surface explosion q = 0.5. Q is practically equal to the number of neutrons formed by fission, since we may assume that the neutrons are not absorbed in the shell because the lifetime of the shell ($\sim 10^{-5}$ sec) is less than the lifetime of the neutron in the shell ($\sim 10^{-4}$ sec) and the shell scatters without having time to capture the neutrons. However, the neutrons have time to slow down considerably in the shell and therefore their diffusion path in the air is short (the mean free path of the neutron in the air is strongly decreased with decreasing neutron energy). Thus, the greater part of the neutrons of the explosion are located near the center of the explosion, forming the so-called "neutron cloud".

Consequently, the greater part of the capture γ radiation is emitted in the region of the "neutron cloud" forming, a three-dimensional source of γ rays. At distances that are great compared with the dimensions of this source, it can be considered as a point source.

Thus, the dose power from the capture radiation can be estimated with the aid of formula (12.18') in which we replace G(t) by (13.2):

$$P_{capt} = \frac{1{,}48 \cdot 10^{-5} q \frac{Q}{\tau} e^{-t/\tau} \cdot 0{,}64\, \mu_e a e^{-R/\lambda_{eff}} e^{L/\lambda_{eff}}}{4\pi R^2}. \quad (13.3)$$

The number of Q neutrons released in an atomic explosion is determined by the explosion energy and by the type of the reaction. In fission bombs, two neutrons are emitted for each fission event (in the case of plutonium fission), or 1.5 neutrons in the case of U^{235} fission. In the case of a thermonuclear reaction, more neutrons are produced for the same reaction energy than in the case of fission. For example, in the reaction

$$_1H^2 + {}_1H^3 = {}_2He^4 + n + 17{,}6 \text{ Mev},$$

there are produced 10 neutrons for 180 Mev, while in uranium fission 1.5 neutrons are produced.

We shall carry out the estimate of P(R, t) for a plutonium

*In addition to the γ radiation from the region nearest to the center of explosion, there occurs γ radiation due to capture of neutrons used at large distances. An estimate shows that the radiation from the "neutron cloud" predominates at all distances.

bomb ($Q = 2 \times 1.45 \times 10^{23} E_{TT} = 2.9 \times 10^{23} E_{TT}$) in the case of an aerial explosion ($q = 1$).

The quantities μ_e, α, and λ_{eff} depend on the average quantum energy, which we assume to be equal to 6 Mev, although one must not exclude the possibility that it is less since the soft part of the spectrum was not investigated. Then $\mu_e = 1.9 \times 10^{-5}$ cm^{-1}, $\alpha = 1.2$ (for the distance interval from 400 to 1000 meters, Figure 15), $\lambda_{eff} = 410$ meters.

Substituting the values of the coefficients in (13.3), we get

$$P_{capt}[R, t] = \frac{8{,}1 \cdot 10^9 E_{T.T.} e^{-R/\lambda_{eff}} e^{L_{eff}/\lambda_{eff}} e^{-t/0.062}}{R^2}, \text{ r/sec} \quad (13.4)$$

(R is in meters and t in seconds).

The dose power diminishes exponentially with a period of 0.06 seconds. The main part of the capture radiation is emitted within 0.1 second. During this time L_{eff} does not have time to assume considerable dimensions and therefore exp $(L_{eff}/\lambda_{eff}) \approx 1$.

The shock wave exerts a much lesser influence on the intensity of the captured radiation than on the intensity of the fragment radiation. Therefore the intensity of the captured radiation, unlike the fragment radiation, is proportional to the explosion energy.

The dose power of the capture radiation, after a lapse of 0.05 second from the instant of explosion ($L_{eff} \approx 0$), amounts to

$$P[t = 0{,}05; R] = \frac{3{,}6 \cdot 10^9 E_{T.T.} e^{-R/\lambda_{eff}}}{R^2} \text{ r/sec.} \quad (13.5)$$

A. I. Khovanovich has shown, that if one takes into account the action of the cavity, then it is necessary to replace E_{TT} in formula (13.5) by $E_{TT}^{1.05}$. Table 26 lists the values of the dose power of the short-lived radiation during the instant of time 0.05 at a distance of 1300 meters from the center of the explosion.

The quantitative estimates (13.4), (13.5), and Table 26 pertain to a plutonium bomb. In the case of thermonuclear bombs, the number of neutrons per unit energy increases and the intensity of the short-lived radiation increases.

Table 26

Dose power of short-lived radiation 0.05 second after the explosion at the distance of 1300 meters

Plutonium bomb energy, kilotons	20	200	2000	20 000
Dose power, r/sec	$4{,}8 \cdot 10^3$	$5{,}4 \cdot 10^4$	$6 \cdot 10^5$	$6{,}8 \cdot 10^6$

The energy radiated during the capture of neutrons, 1 -- 1.28 Mev/fission (Section 3), is almost equal to the 1.8 Mev energy (Table 3) radiated by the fragments during the time that they are active in the explosion (i.e., after ~10 seconds). But since the time of radiation of the captured radiation is much shorter than that of the fragment radiation, the activity of the source of the capture radiation is much greater than the activity of the fragments.

At the initial instant of time after the explosion, the activity of the capture radiation of the plutonium bomb is

$$\frac{1.28 \text{ Mev/fission}}{0.062 \text{ sec}} = 20.6 \frac{\text{Mev}}{\text{sec-fission}}, \text{ i.e.,}$$

25 times greater than the activity of the fragments (0.82 Mev/sec-fission).

Let us compare the dose power of the capture and the fragment radiation at the initial instant of time, i.e., (13.4) and (12.21). We assume that R is equal to 1000 meters, and then

$$\frac{P_{capt}}{P_0} = \frac{8{,}1 \cdot 10^9 e^{-1000/410}}{7{,}64 \cdot 10^8 e^{-1000/230}} \approx 40.$$

The dose power of the capture radiation at the initial time is more than one order of magnitude greater than the dose power of the fragment radiation. With time the dose power of the fragment radiation increases, owing to the cavity action, and the short-lived radiation diminishes rapidly and monotonically. After several tenths of a second, the capture radiation can be neglect compared with fragment radiation.

Figure 39 shows graphically the dependence of the dose power of both types of radiation and of the summary dose power on the time elapsed from the instant of explosion.

The curve showing the dependence of the dose power has a characteristic shape. Having both a minimum and a maximum, the

behavior of this curve is determined by the competition between the action of the cavity and the reduction in the source activity with time. The character of the curve of Figure 39 varies with the explosion energy and with the distance from the center of explosion. The extrema of the curve are due to the action of the cavity on the fragment radiation, and therefore the smaller the explosion energy, i.e., the smaller the cavity, the less noticeable they are.

The capture radiation is harder than the fragment radiation, and therefore with increasing distance a filtration of the radiation in hardness takes place: the softer fragment radiation is absorbed earlier and the dose power is determined all the more by the capture radiation.

The relative placement of the extrema varies with the distance, with the size of the cavity (i.e., with the explosion energy), etc. The competition between the influence of u(t) and L(t, E, R) may distort the shape of the maximum on the curve of Figure 39. The extrema may turn into a point of inflection of the curve. At a great distance, the fragment radiation is absorbed and only the left branch of the curve of Figure 39, corresponding to the pure capture radiation, appears in practice.

14. DOSE OF GAMMA RADIATION. HARD COMPONENT.

Gamma radiation from an explosion consists of quanta of different energies. The greater part of the radiation energy is contained in two spectral intervals, the "centers of gravity" of which (Sections 2 and 3) are 2 Mev for the fragment radiation and 6 Mev for the capture short-lived radiation. We shall speak accordingly of the soft and hard components of the γ radiation of the atomic explosion. This distinction corresponds essentially to the different origin of the radiation, although the fragment radiation may contain a small fraction of quanta with energy greater than 2.2 Mev, and the capture radiation may contain softer radiation. We shall henceforth identify the hard components with the radiation due the capture of neutrons by the air.

The passage of the γ radiation through the air gives rise to a gradual preferred absorption of the softer components, so that at large distances only the hard component is received. The dose of the hard component can be determined by integrating expressions (13.3) or (13.4) with respect to the time

$$D_h[R, E] = \int_0^\infty P[t, R, E]\, dt =$$

$$= \frac{8{,}1 \cdot 10^9 E_{\text{т.т.}} e^{-R/\lambda_{\text{eff}}}}{R^2} \int_0^\infty e^{-t/0{,}062} dt, \text{ r}, \qquad (14.1)$$

$$D_h = \frac{5 \cdot 10^8 E_{\text{т.т.}} e^{-R/410}}{R^2}, \text{ r}. \qquad (14.2)$$

Here and henceforth the dose due to the γ rays of the atomic explosion is approximated by the expression

$$D = \frac{A}{R^2} e^{-R/\lambda_{eff}}, \text{ r.} \tag{14.3}$$

In the case of the hard component

$$A_h = 5 \cdot 10^8 E_{TT}, \text{ r} \cdot \text{m}^2. \tag{14.4}$$

The dose of the hard component is proportional to the number of neutrons formed in the explosion, and not to the number of fission events. Therefore when the number of neutrons per unit of released energy changes (for example, in the case of a thermonuclear bomb), the numerical coefficient of E_{TT} in expression (14.2) and (14.3) also changes. In the case of explosion of bombs with equal number of neutrons per unit energy, D_h is proportional to the energy. In strong explosions, the effect of the cavity may manifest itself in the dose of the hard component. It is always considerably less than the effect of the cavity on the dose of the fragment component, firstly because the hard component is radiated within a shorter time, when the cavity is small, and secondly because the harder the radiation, the greater the value of λ_{eff} and the smaller the influence of the cavity (13.3).

15. DOSE OF γ RADIATION. FRAGMENT COMPONENT. SUMMARY DOSE.

The dose of the fragment component can be estimated by integrating (12.14) with respect to time up to the instant of time t_{eff}, when radioactive decay of the fragments and the rising of the fragment cloud cause the intensity of the γ radiation to decrease to a value that can be neglected:

$$D(R, E) = 5{,}12 \cdot 10^8 E_{\text{т.т.}} \alpha e^{-R/\lambda_{eff}} \int_0^{t_{eff}} u(t)\, e^{\frac{L_{eff}(t,E)}{\lambda_{eff}}} dt, \text{ r.} \tag{15.1}$$

The integral contained in (15.1) can be represented in the form

$$\int_0^{t_{eff}} u(t)\, e^{\frac{L_{eff}(t,E)}{\lambda_{eff}}} dt =$$

$$= e \frac{\bar{L}_{eff}(E)}{\lambda_{eff}} \int_0^{t_{eff}} u(t)dt = e \frac{\bar{L}_{eff}(E)}{\lambda_{eff}} \bar{W}. \qquad (15.2)$$

Let us assume that t_{eff} = 10 seconds (Figure 34). Then

$$\bar{W} = \int_0^{10} u\,(t)\,dt = 1{,}8 \text{ Mev/fission}. \qquad (15.3)$$

We substitute in (15.1) the expressions (15.3), (15.2), α = 1.8 and λ_{eff} = 255 meters (Table 21).

$$D\,(R, E) = 1{,}66 \cdot 10^9 E_{т.т.} e^{-R/\lambda_{eff}} \frac{e^{\frac{\bar{L}_{eff}(E)}{255}}}{R^2}, \text{ r} \cdot \text{m}^2. \qquad (15.4)$$

In accordance with the notation (14.3)

$$A = 1{,}66 \cdot 10^9 E_{т.т.} e^{\frac{\bar{L}_{eff}(E)}{255}}, \text{r} \cdot \text{m}^2. \qquad (15.5)$$

The problem has reduced to a calculation $\bar{L}_{eff}(E)$ -- the average value of the radius of the cavity during the entire time of the emission of the quanta. It can be simplified by assuming that the cavity has been formed and that it has assumed its final dimensions rapidly compared with the time of emission of the greater part of radiation, i.e., that the greater part of the γ radiation is emitted at a constant value of L_{eff} close to the final dimension of the cavity. Let us calculate (15.1) on this assumption, assuming furthermore than $L_{eff}(E)$ is close to the final radius of the fire ball:

$$\bar{L}_{eff}(E) \approx L_{fb}. \qquad (15.6)$$

In this approximation the solution is the more accurate, the greater the time of formation of the final dimensions of the cavity compared with the time of emission of the γ rays, i.e., the more accurate, the greater the explosion energy.

The approximation $\bar{L} = L_{fb}$ is certainly incorrect for explosions with high energy, when the fire ball assumes its final dimensions relatively slowly, so that the greater part of the γ radiation is emitted prior to the time when the fire ball is

assumed its final dimensions, i.e.,

$$\bar{L}_{eff}(E) < L_{fb}. \tag{15.7}$$

The value of $\bar{L}_{fb}$, and consequently $\bar{L}_{eff}$, can be estimated from the energy contained in the fire ball. From the theory of a strong point explosion, given by L. I. Sedov [17], it follows that the energy of the incandescent air amounts to ~0.5 of the explosion energy. Then

$$\frac{4}{3}\pi L^3_{fb} a = 0.5\ E;\ L_{fb} = \sqrt[3]{\frac{0,5\,E}{\frac{4}{3}\pi a}}. \tag{15.8}$$

Here a is the energy per unit volume of fire ball. Since the energy of 1 gram of air is*

$$\frac{5R(T - T_1)}{28.8} = 0.35(T - T_1),\ \text{col/g}, \tag{15.9}$$

then, neglecting T_1 compared with T, we obtain

$$a = \rho \cdot 0,35\ T = \frac{\rho\, T_0}{P_0}\,\frac{P_1}{T}\,0.35\ T =$$

$$= 0.123\ P_1,\ \text{col/cm}^3 \tag{15.10}$$

(P_1, T_1 -- pressure and temperature of the air prior to the explosion;

ρ_0, P_0, T_0 -- respectively the normal density, pressure, and temperature of the air).

Substituting (15.10) and (15.8) and further in (15.4) and (15.5), we obtain

$$L_{fb} = 100 \sqrt[3]{\frac{E_{TT}}{P_1}} \tag{15.11}$$

*In this estimate we disregard the increase in specific heat with temperature and dissociation.

(P_1 is in atmospheres),

$$D = 1{,}66 \cdot 10^9 \cdot E_{т.т.}\, e^{-0{,}4\sqrt[3]{\frac{E_{т.т.}}{P_1}}} \frac{e^{-R/255}}{R^2}, \text{ r} \qquad (15.12)$$

$$A = 1{,}66 \cdot 10^9 E_{т.т.}\, e^{-0{,}4\sqrt[3]{\frac{E_{т.т.}}{P_1}}}, \text{ r} \cdot \text{m}^2. \qquad (15.13)$$

The expression (15.12) can be compared with the doses that prevailed in Hiroshima, i.e., with doses of the explosion of the so-called nominal bomb, E_{TT} = 20 kilotons.

The doses in Hiroshima at different distances of the epicenter are given in the article by Lewis [23]. The distances to the center of explosion were calculated under the assumption that the explosion took place at an altitude of 2000 feet.

Table 27

Radiation doses at different distances from the epicenter (according to the data of the Hiroshima explosion)

Distance from epicenter, meters	Distance from center, meters	Dose, r	Dose calculated from (15.12), r
750	950	2500	2600
1000	1170	800	720
1500	1620	90	64

If it is considered that (15.12) is an estimate no more accurate than 100 percent, then the agreement between (15.12) and the doses in Hiroshima can be regarded as good.

The dose of the fragment radiation increases not in proportion to the number of fragments, i.e., to the explosion energy, but faster than the explosion energy. This circumstance is explained (Section 12) by the reduction in the absorption of γ radiation in the cavity formed by the shock wave. The specific nature of the atomic explosion lies in the fact that the source of γ rays (explosion) changes the absorbing ability of the medium during the time of radiation.

The factor that shows by how many times the dose has been

increased by the shock wave is called the cavity dose factor K_D.

The coefficient A in formula (14.3) is thus made up of two factors: the factor proportional to the number of fragments and the cavity dose factor

$$K_D = e\,\frac{\overline{L}_{eff}(E)}{\lambda_{eff}}\,. \qquad (15.4)$$

In Table 28 are listed the values of the cavity dose factors for explosions, calculated from formula (15.19).

Table 28

Cavity dose factor for explosions of different energies

Explosion energy E_{TT}, kilotons	2	20	200	2000	20 000
Cavity dose factor K_D	1,3	2,5	6,8	29	112

In the particular case of formula (15.13), the cavity dose factor is

$$K_D = e^{0,4\sqrt[3]{E_{т.т.}/P_1}}\,.$$

Expression (15.12) pertains to points located outside the fire ball, i.e., outside the cavity.

Inside the cavity there is no absorption of γ rays (Section 12) and the dose changes as the inverse square of the distance

$$D \approx 1/R^2.$$

Figure 40 shows the dependence of the dose on the distance on a semi-logarithmic scale. The ordinate axis represents the logarithm of the product of the dose by the square of the distance ($\ln DR^2$): the abscissa represents the distances from the point of explosion.

The values of the coefficient A and λ_{eff} in formulas of the type (14.3), which are used in the calculation of doses can be obtained from Figure 40

$$\ln A = \ln (D R^2)_{R \to 0}, \tag{15.15}$$

$$\lambda_{ef} = -\frac{d R}{d (\ln D R^2)}. \tag{15.16}$$

The doses given by formula (14.3) and plotted in Figure 40 in form of straight lines 2 and 3 can be described approximately by a formula having different values λ' and accordingly A' (dotted). Let us equate the two descriptions at the middle of the interval $\bar{R}$ of interest to us:

$$\frac{A' e^{-\bar{R}/\lambda'_{eff}}}{\bar{R}^2} = \frac{A e^{-\bar{R}/\lambda'_{eff}}}{\bar{R}^2},$$

then

$$\ln A' = \ln A - \frac{\bar{R}}{\lambda_{eff}} \left(1 - \frac{\lambda_{eff}}{\lambda'_{eff}}\right). \tag{15.17}$$

The small error in the dose expressed by means of a straight line 2' instead of the straight line 2 amounts to

$$\frac{\Delta D}{D} = \frac{R - \bar{R}}{\lambda_{eff}} \left(1 - \frac{\lambda_{eff}}{\lambda'_{eff}}\right). \tag{15.18}$$

Figure 40 shows three characteristic reasons of the variation of the dose with the distance: region 1 -- inside the cavity, in which the dose varies as $\sim 1/R^2$; region 2 in which the action of fragment radiation predominates; region 3, in which the hard component is effective.

The distances $R_{1,2}$ and $R_{2,3}$ delineate these regions. When $R_{1,2} < R < R_{2,3}$, expression (15.12) and the more accurate expressions which are given later are correct. When $R > R_{2,3}$ expression (14.2) must be used.

Table 29 lists the values of $R_{1,2}$ and $R_{2,3}$ for different explosion energies.

The heaviest damage is produced by the γ rays in regions 1 and 2. The lethal radius, i.e., that value of R at which the dose is equal to 400 r and consequently in which the sickness leads to death in 50 percent of the cases, is located in region 2.

As already indicated, the use of the values of L_{fb} for the average cavity radius L in the calculation gives approximate results, which are good only for explosions of low-energy bombs.

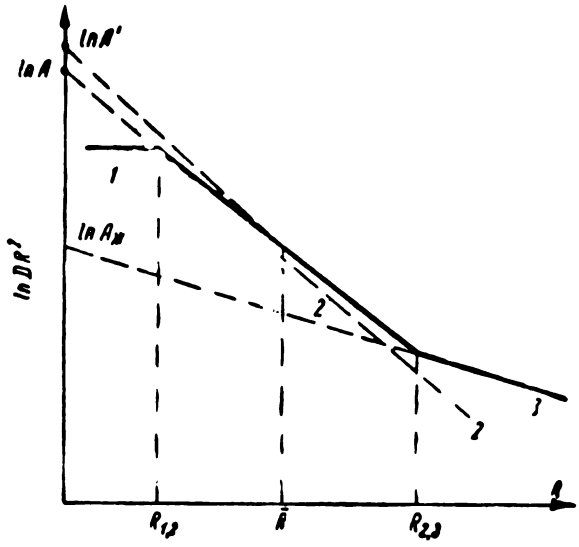

Figure 40. Dependence of the dose of γ radiation of an atomic explosion on the distance. 1, 2 -- regions where the dose is produced by the fragment radiation; 3 -- region of hard component. Curves 2 and 3 correspond to the interpolation formulas.

Table 29

Demarcation distances of the regions of action of the hard and fragment components, and also the region of exponential absorption of γ rays and "vacuum" region

Bomb energy, kiloton	2	20	200	2000	20 000
$R_{1,2}$, м	250	400	1180	2000	3500
$R_{2,3}$, м	1050	1400	2400	3500	5250

In the case of high explosion energy, one cannot expect satisfactory accuracy from the results of the calculations based on formulas (15.12) and (15.8), since L is known to be less than L_{fb}. In addition with increasing explosion energy, L should increase less rapidly than $\sim(E)^{1/3}$, (15.8). At powerful explosions the shock wave is strong during the time of emission of the majority of the γ

radiation. According to Sedov's theory, the radius of the front of the shock wave is the given instant of time $\sim(E)^{1/5}$, and one must therefore expect $\bar{L}$ to increase as $\sim(E)^{1/5}$ with increasing energy in the correct theory.

A detailed examination of the question of the dose leads to numerical value which can be described by various interpolation formulas. The following interpolation formula

$$D=6{,}6\cdot 10^{8}E_{т.т.}\,e^{0{,}925\sqrt[5]{E_{т.т.}}-6{,}25\cdot 10^{-5}E_{т.т.}}\times \times\frac{e^{-R\rho/300}}{R^{2}},\ \text{r} \tag{15.19}$$

is written in the form corresponding to the physical notions regarding the action of the shock wave.

One can use also another formula:*

$$D=1{,}4\cdot 10^{9}E_{т.т.}\,(1+0{,}2\,E_{т.т.}^{0{,}65})\,\frac{e^{-R\rho/300}}{R^{2}} \tag{15.20}$$

These formulas are valid when $R_{1,\,2}<R<R_{2,\,3}$

$$\frac{1}{\mu_{eff}}=\lambda_{eff}=\frac{300}{\rho}\ \text{m}. \tag{15.21}$$

(ρ is an mg/cm^3).

Formulas (15.19) and (15.20) correspond to the following values of A and K_D:

$$\left.\begin{aligned}A&=6{,}6\cdot 10^{8}E_{т.т.}\,e^{0{,}925\,E_{т.т.}^{1/5}}-6{,}25\cdot 10^{-5}E_{т.т.}\\ K_D&=0{,}47\,e^{0{,}925\,E_{т.т.}^{1/5}}-6{,}25\cdot 10^{-5}E_{т.т.}\end{aligned}\right\}, \tag{15.19'}$$

$$\left.\begin{aligned}A&=1{,}4\cdot 10^{9}E_{т.т.}\,(1+0{,}2\,E_{т.т.}^{0{,}65}),\\ K_D&=1+0{,}2\,E_{т.т.}^{0{,}65}.\end{aligned}\right\} \tag{15.20'}$$

In the case of a surface explosion, the radius of the cavity

*Formula (15.20) was proposed by I. A. Solodukhin and P. A. Yampol'skii.

is greater and corresponds to the radius of a cavity produced an aerial explosion with twice the energy (Section 12). Therefore the dose is greater in a surface explosion than in an aerial explosion of a bomb of the same energy. The doubling of the volume of the cavity in the case of a surface explosion, compared with an aerial explosion, remains valid only for part of the time of the radiation of the γ rays, since the semi-spherical region of the incandescent air breaks away with time from the earth and becomes spherical.

It is possible, however, to calculate the dose with sufficient approximation in the case of a surface explosion by replacing L_{TT} by $2E_{TT}$ in the exponential of (15.19) and in the term $E_{TT}^{0.65}$ in (15.20), as if the cavity were semi-spherical all the time.

Figures 41 and 42 show nomograms* for the calculations of the dose from γ rays in region 2 of Figure 40, i.e., in the cases of greatest practical importance.

Figures 41 and 42 pertain to aerial and surface explosions, respectively.

The values of the dose are marked on the left side of the middle vertical scale, and are read at the places where it intersects the straight line joining the values of E_{TT} on the right vertical scale and R, km on the left vertical scale.

On the right side of the middle vertical scale is marked the thickness of the shielding necessary to reduce the determined dose to 1 r. The thickness of the shield is given in effective ranges of the quanta in the shield material, λ_{eff} (Section 17).

The curve located on the nomogram yields the values of $R_{1,2}$ and $R_{2,3}$, which shows under what distances the nomogram can be used:

$$R_{1,2} < R < R_{2,3}.$$

The doses given in the nomogram are calculated for the standard air density at 25°C, $\rho = 1.17$ mg/cm^3, and for $\lambda_{eff} = 300/\rho = 255$ meters. At any other air density one must introduce a correction in the value of the dose obtained by means of the nomogram.

As the air density changes, a change takes place in the values of λ_{eff} and A in equation (14.3). λ_{eff} changes in inverse portion to the density, so that the change can be taken readily into account. The parameters of the shock wave, and consequently the cavity factor which is included in A, depend on the density of the air in a different manner than λ.

*These nomograms were prepared by V. V. Novozhilov in accordance with formula (15.19).

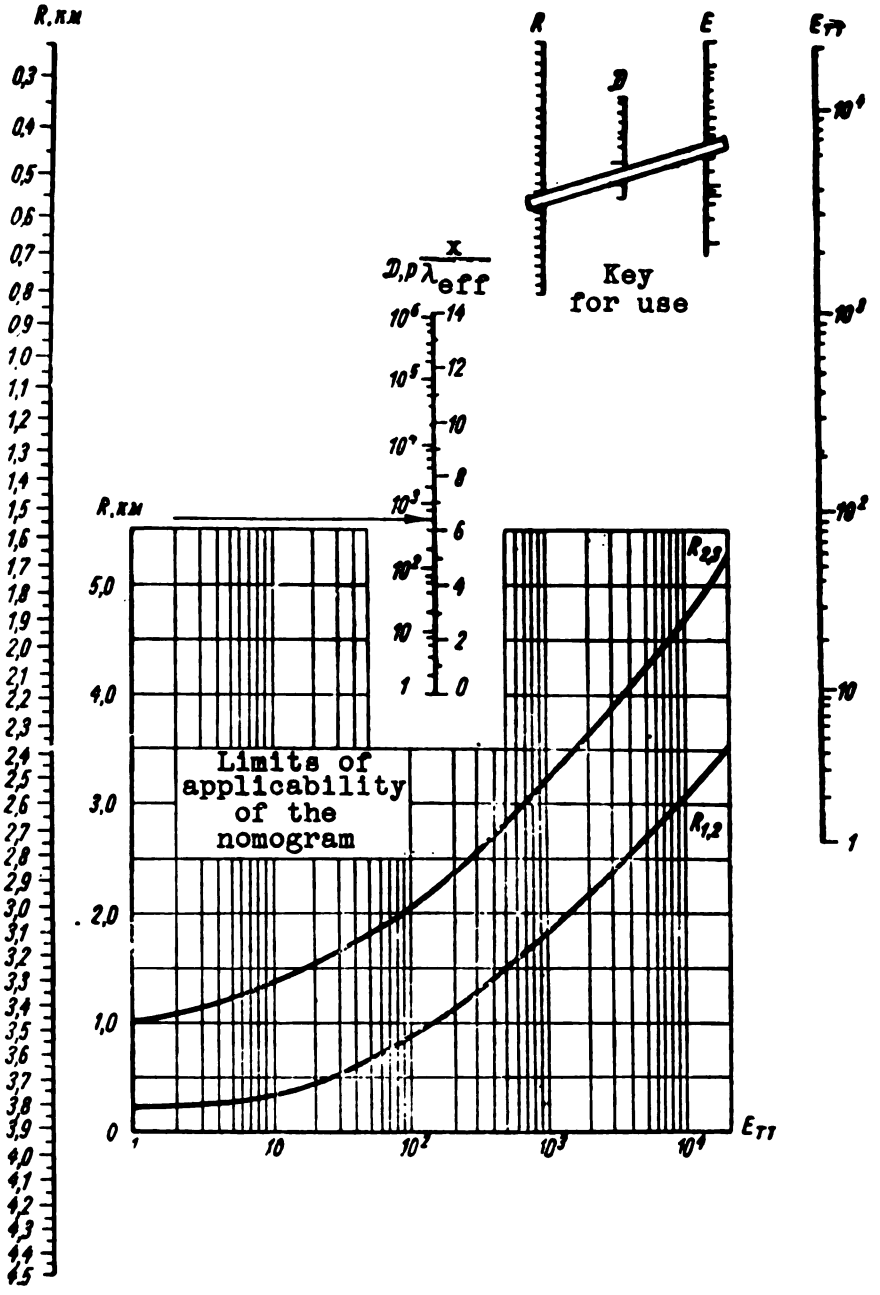

Figure 41. Nomogram for the calculation of the dose of γ radiation in the case of an aerial atomic explosion (the arrow indicates the lethal dose).

An exact calculation of the correction of the nomogram for the change in density would be too cumbersome. We give here two approximations. One is based on the assumption that in formula (15.19) and (15.19') the value of A is independent of the density of the air. Then, differentiating (14.3) or (15.19) with respect to λ with allowance for (15.21), and assuming that $\Delta D/D \ll 1$, we obtain

$$\frac{\Delta D}{D} = -\frac{R}{255}\frac{\Delta \rho}{\rho}. \qquad (15.22)$$

The second approximation is obtained by considering that the cavity factor contains also $\lambda_{eff}(\rho)$ (15.14), but assuming that $\bar{L}_{eff}$ is independent of the density. Then

$$\frac{\Delta D}{D} = -\frac{R - \bar{L}_{eff}}{255}\frac{\Delta \rho}{\rho}. \qquad (15.23)$$

Since in fact the radius of the cavity decreases somewhat with increasing air density, the ratio $\bar{L}_{eff}/\lambda_{eff}$, which according to (15.14) and (15.15) determines the value of A, changes less with ρ than when $\bar{L}_{eff}$ is independent of the density. Therefore approximately (15.23) should give values $\Delta D/D$ which are too high, i.e.,

$$(15.22) < \frac{\Delta D}{D} < (15.23).$$

Inasmuch as we deal with a small correction $\Delta D/D$, we can confine ourselves in its calculation to the simpler expression namely (15.22).

The damaging action of the γ radiation can be characterized by the magnitude of the lethal radius R_l, i.e., the value of R after which the dose becomes equal to 400 r, and consequently, radiation sickness leads to death in 50 percent of the cases.* The lethal radius is in region 2 of Figure 40, i.e., in the region of action of the fragment radiation, when the dose is given by formulas (15.19), (15.20), and (15.12).

Table 30 gives the values of the lethal radius of the γ radiation for explosions of atomic bombs in different energy.

In explosions whose energy does not exceed 200 kilotons, R can be expressed by an interpolation formula proposed by V. V. Zvonov:

$$R_l = 622 \cdot E_{TT}^{0.238}, \text{ m}.$$

*In addition to the γ radiation, the radiation dose is produced also by neutrons. In most cases, however, the dose due to the neutrons is less than the dose due to the γ radiation, so that the biological effects in the region of the explosion are determined by the γ radiation.

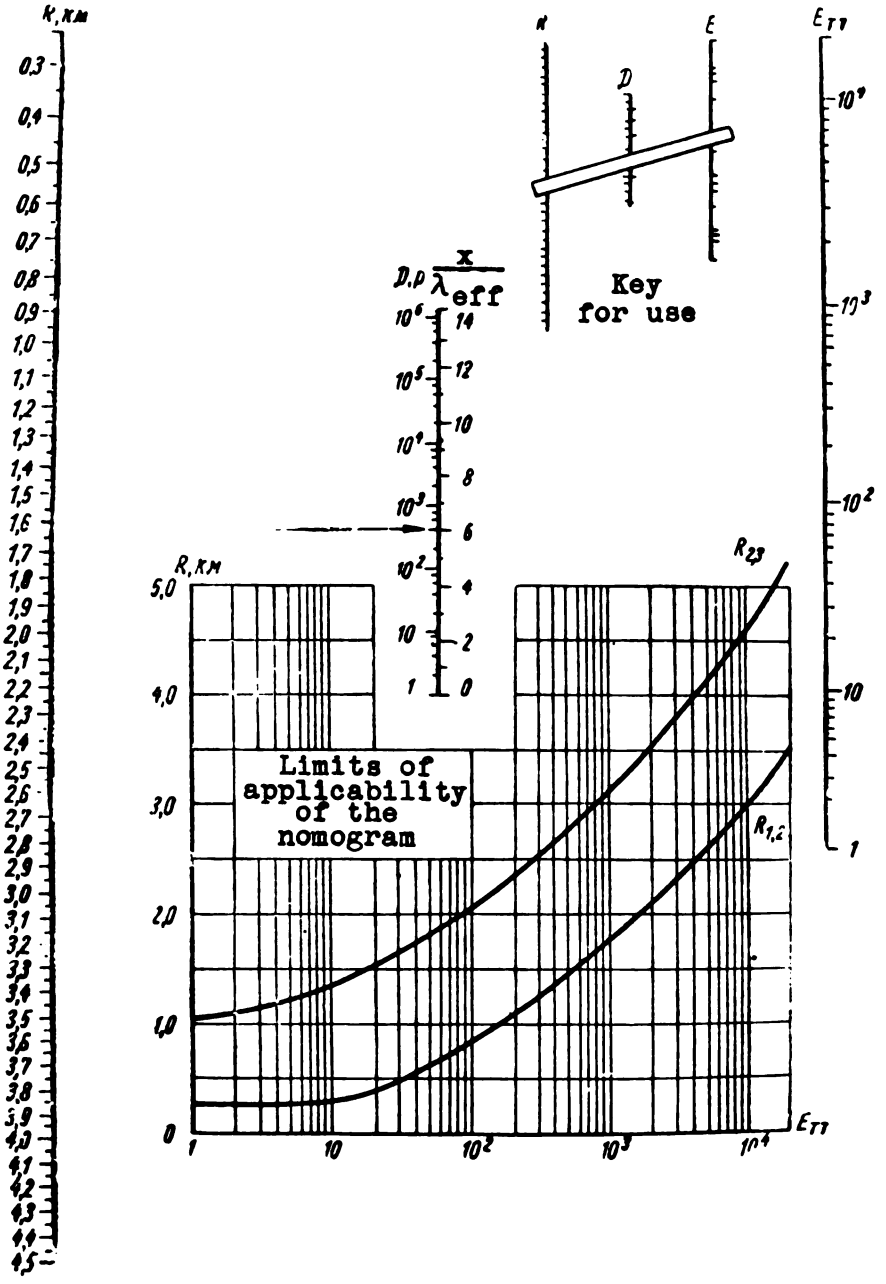

Figure 42. Nomogram for the calculation of the γ-ray dose in the case of a surface atomic explosion (the arrow indicates the lethal dose).

Expressions (15.19) and (15.20) for the γ ray doses of the fragment component apply to fission bombs. In the case of pure hydrogen bombs the relation between the number of quanta and the explosion energy is different than in fission bombs, and therefore these formulas must be changed.

Table 30

Lethal radius of γ radiation has a function of the energy of the atomic explosion

Explosion energy, kiloton	2	20	200	2000	20 000
Lethal radius, meters	720	1220	1850	2650	3480

In formulas (15.12), (15.19), and (15.20) the expression for the explosion energy E_{TT} is contained, firstly, in form of a factor in the first power in the numerical coefficient, and secondly in the form of an exponent in (15.12) and (15.19) or in the bracket in formula (15.20).

The expressions for E_{TT} have different physical meanings. The doses are in any case proportional to the number of fragments, so that the first power of the factor E_{TT} represents the number of fissions, as can also be seen from the derivation of formula (15.12). The quantity E_{TT} contained in the exponent in (15.12) and (15.19) and in the bracket of (15.20) characterizes the action of the cavity and describes the dimension of the cavity, i.e., the explosion energy. The number of fragments (i.e., the amount of γ radiation) in the case of fission bombs is determined by the explosion energy, just as is the dimension of the cavity.

In the case of hydrogen bombs the number of fragments is determined not by the entire explosion, but only by that part of the energy which is connected with the fission reaction, but the dimension of the cavity is determined by the entire explosion energy. Therefore in the case of a hydrogen explosion the expression for the explosion energy should be contained only in that term of the formula, which characterizes the action of the cavity, while the coefficient E_{TT} in the first power should represent only part of the total energy, corresponding to the energy connected with the fission reaction.

16. TIME OF ACCUMULATION OF γ-RADIATION DOSE. RATIO OF THE DOSES FROM THE FRAGMENT AND FROM THE HARD COMPONENT.

The dose of γ radiation is made of the dose due to the capture radiation and the dose due to the fragment radiation. The capture radiation terminates within practically 0.3 seconds while the fragment radiation lasts several seconds. This ratio indeed determines the time of accumulation of the dose. The time of

accumulation depends on the distance to the place of explosion and on the energy of explosion. At the distances where the dose is determined by the capture radiation (i.e., in region 3 of Figure 40; $R > R_{2,3}$, Table 29) the main part of the dose is accumulated within 0.2 seconds. At shorter distances -- in region 2 of Figure 40 -- the dose accumulated within several seconds. The greater the explosion energy the longer the dose accumulates, since the longer is the time of growth of the cavity produced by the shock wave. The greater the distance, the more rapidly the dose accumulates since the role of the capture radiation becomes greater here.

The time of accumulation of the dose can be of practical interest. The point is that the magnitude of the dose is critical within certain limits as far as the lethal result of radiation sicknesses is concerned. For example, in the case of 400 r, death is inevitable in 50 percent of the cases, and when the dose is half the size, there are practically no deaths. If the dose accumulates within several seconds, then the primitive protection measures become possible (within 1 -- 2 seconds one can lie down on the bottom of a trench, etc.), which even in a case of a comparatively small reduction in the dose may lead to a favorable outcome of radiation sickness.

The plot of Figure 43, based on the calculations of B. V. Novozhilov* shows the speed of accumulation of the dose and explosions of atomic bombs of large and small energy.

In Figure 43a (E = 2 kilotons) it is shown that the dose accumulates much more rapidly at a large distance (1500 meters) in the action region of the hard component than at a short distance (500 meters).

Figures 43b and c show the long duration of accumulation of the dose in the case of high-energy explosions.

Table 31 lists the time necessary for the accumulation of 50 percent of the dose and that fraction of the dose, which is accumulated after 2 seconds (i.e., after the minimum time necessary to take shelter against γ radiation) at the distance indicated in the second row. These distances are close to R (Table 31).

*The rise of the fragment cloud and the cooling of the air in the cavity have been disregarded, and therefore the time of accumulation of the dose at high energy of explosion is exaggerated.

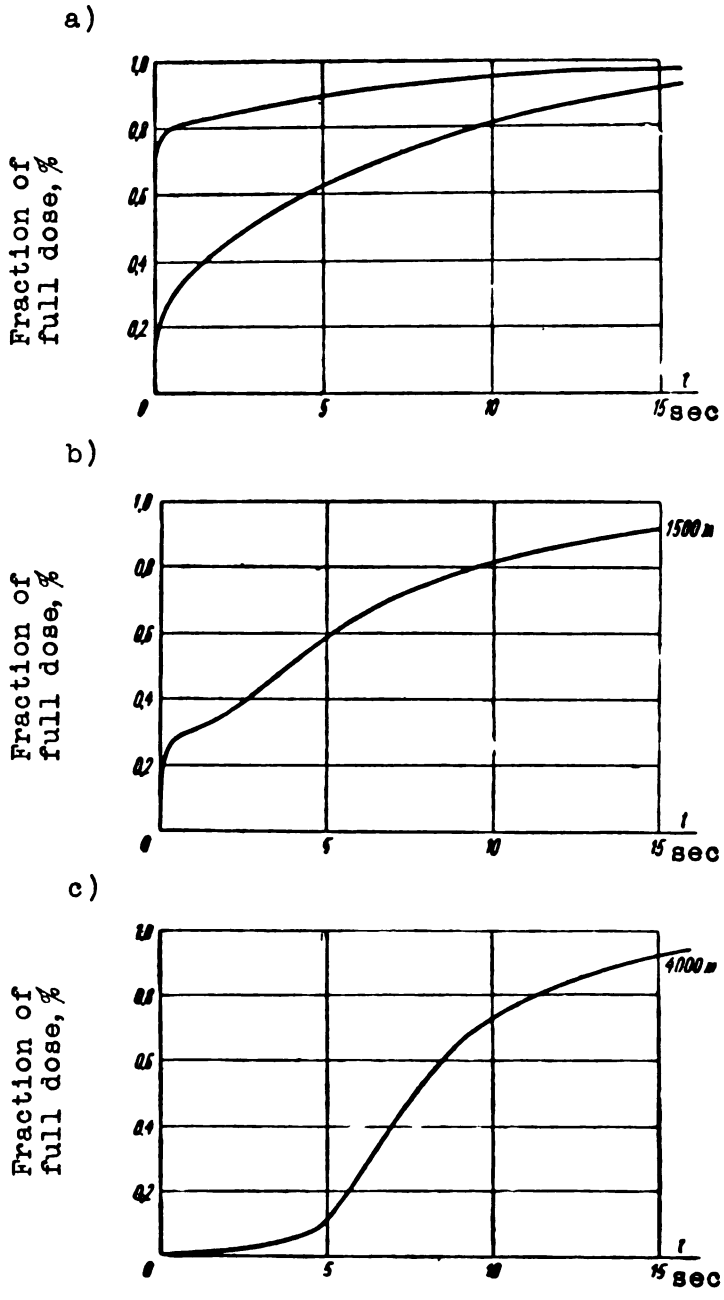

Figure 43. Speed of accumulation of dose of γ radiation in explosions of atomic bomb with energy 2 megatons (a); the upper curve is for a distance of 1500 meters from the center of the explosion, while the lower one is for 500 meters; 200 kilotons (b); 20,000 kilotons (c). At the end each curve on Figures 43b and c is marked the distance from the center of explosion.

Table 31

Type of accumulation of dose in explosions of atomic bombs with different energies

Explosion energy, kilotons	2	20	200	2000	20 000
Distance, meters.....	500	1000	1500	2500	4000
Time of accumulation of 50% dose, seconds.....	2,5	2,5	4	7	8
Fraction of dose accumulated after 2 seconds, %.....	45	45	35	10	2
Dose due to capture radiation, %.....	20	30	27	7	0,15

The table is based on the data of Figure 43.

Figures 40, 43 and Table 31, as well as a comparison of formulas (14.2) and (15.19), show that the greater part of the dose in region 2 is produced by γ radiation of the fragments.

The predominance of the fragment γ radiation in the production of the dose, which manifests itself particularly strongly in the case of explosion of high-energy bombs, calls for certain explanation, since the energy of the γ rays, released upon decay of the fragments during the time that they stay in the explosion region is by far not the predominate one, compared with the energy of other sources of γ rays.

In a case of a strong explosion the γ-radiation dose builds up within a time close to 10 seconds. Within this time the fragments release 1.8 Mev/fission. Each fission gives rise to two neutrons, which in the case of an aerial explosion are captured by nitrogen and yield 2 x 0.65 = 1.3 Mev/fission.

In the case of a surface explosion, one half of the total number of neutrons is captured by the air and one half is captured in the earth. Consequently, in the case of a surface explosion there is released by capture radiation* 1 x 0.65 + 1 x 8 = 8.65 Mev/fission.

Thus, in the case of an aerial explosion the γ radiation of the fragments amounts to 1.8 : (1.8 + 1.3) = 0.58, while in the case of a surface explosion it amounts to only 1.8 : (1.8 + 8.6) = = 0.17 of the total energy of γ radiation released within a few seconds after the explosion. Nevertheless, the fragment radiation predominates in the production of the dose. This is due to the action of the cavity, which makes the passage of the γ rays from the fragment through the air easier than the passage of the γ rays due to neutron capture.

*We disregard the fact that part of the neutrons is absorbed by the hydrogen in the earth, releasing thereby not 8 but only 2.2 Mev.

The cavity develops within a time which is long compared with the time of emission of the capture radiation, and is comparable with the time of emission of the fragment radiation (and the greater the bomb energy, the stronger this ratio of the time interval manifests itself). Therefore the action of the cavity always produces more favorable conditions for prolonged radiation than the short-lived radiation, and the greater the bomb energy, the stronger this predominance of prolonged (fragment) radiation over the short-lived one manifests itself, since the cavity radius is greater. In addition, the action of the cavity always produces a relative preference for the softer fragment radiation compared with the harder capture radiation. The action of the fragment radiation is strengthened by the cavity. The amplification coefficients are listed in Table 28 and amount to several orders of magnitude. It turns out therefore that fragment radiation contributes more to the production of the dose than a nearly equal amount of capture radiation.

The capture γ radiation which travels from the earth is in a less favorable situation from the geometrical point of view than the radiation from the fragments, since it is attenuated by the absorption in the surface layer of the earth, because the capture of neutrons in the earth takes place in a surface layer 30 centimeters thick.

If we speak of points located on the surface of the earth and high up in the air, then the capture radiation from the earth cannot act directly on these points, and only scattered radiation should be effective.

In the case of explosion of a low-energy bomb, the effect of the cavity is less pronounced because of its small dimensions, and therefore the capture γ radiation assumes an important role in the dose.

The share of the fragment radiation in the overall dose is determined not only by the energy of the bomb but also by the distance of the center of explosion. The capture γ radiation is harder than the fragment radiation, and because when a bomb of given energy is exploded the fraction of the capture radiation increases with increasing distance from the center of explosion, and at sufficiently large distances the dose of γ rays is determined only by the capture radiation (region 3, Figure 40).

17. REMARKS ON THE CALCULATION OF THE DOSE OF γ RADIATION IN SHELTERS.

The large magnitude of the γ-radiation doses in open spaces makes it necessary to require a sufficient attenuation of the γ radiation by means of shelters that shield against the shock wave and the heat. The doses in shelters must be calculated to account for the construction of the buildings, and therefore such a calculation is an engineering problem.

In the present work, which is devoted to the physical aspect of the action of the radiation, there is no need for entering into the numerous details of problems of this kind. We shall confine ourselves only to a few remarks concerning the approach to the calculation of dose in shelters under the specific conditions of an atomic explosion.

Scattered radiation. In the case of an atomic explosion the dose is produced not only (and not so much) by the direct radiation, but also by the scattered radiation, as follows from the theory of multiple scattering of γ quanta (Chapter II). Good protection only on the explosion side, i.e., from the direct ray, protects a little from γ radiation. The shelter may also have a weak spot, i.e., a thin portion in the shielding layer or an opening (entrance, ventilation, opening of trench). Even if this opening is so constructed that the direct ray cannot pass through inside the building, it may be a principal and dangerous source of radiation inside the shelter, since scattered radiation may enter through it.

To estimate the dose produced by the scattered radiation, use can be made of formula (7.20). The value of $\delta(\theta)$ entering into (7.20) can be obtained from Eq. (7.24). However, the scarcity of information on the value of $\delta(\theta)$, the possibility of using formula (7.24) in a greater interval of R/λ than the interval for which it was derived, the spreading of the angles θ as be the γ-radiation source is not a point, etc., makes it necessary to have a certain "safety factor" in the expression for $\delta(\theta)$. This can be obtained by increasing the results obtained by formula (7.24) by a factor of several times.

In the region of action of the hard component, the angular distribution of the scattered radiation should be more anisotropic than given by (7.24). Consequently the application of (7.24) to this region gives excessive values of $D(\theta)$, i.e., the danger due to the scattering radiation will in any case not be underestimated.

The dose due to the radiation entering into the shelter through a "weak spot" and scattered from the walls can be estimated with the aid of the values of the albedo, given in Section 11.

Absorption in shielding layers. In practice it may be necessary to use a variety of placements of shielding layers relative to the center of explosion and exact calculations of such layers may be very difficult because of the complicated spectral composition and angular distributions of the γ radiation incident on the shield. If exact calculation is not always possible, it is always possible to make a limiting calculation, in which the shielding layers and the doses behind the shield will not be underestimated. Such a limiting calculation is obtained from the condition that the shielding layer is located perpendicular to the direct ray and that the dose is produced by a parallel flux of quanta, the energy of which is equal to the average energy of the quanta radiation (i.e., 2 Mev) or the capture radiation (6 Mev), depending on whether the shield is region 2 or in region 3 (Figure 40). Such a case was analyzed in Section 10.

The dose behind the shield can be expressed by means of an interpolation formula of the type (7.13) or (10.1)

$$D = D_0 K_r = D_0 \alpha e^{-x/\lambda_{eff}}. \qquad (17.1)$$

The values of the coefficients of α and λ_{eff} can be obtained from Figure 26. The values of λ_{eff} for concrete, earth, brick, and wood can be obtained from the density ratios.

The values of the coefficients α and λ_{eff} of formula (17.1)

for concrete and steel in the case of fragment radiation, are as follows:

	Concrete	Steel
α	1.5	1.5
λ_{eff}, cm	13.5	4.0

The thickness of the shielding in units of λ_{eff} (i.e., x/λ_{eff}) is given in the nomographs of Figures 36 and 37, on the right side of the middle vertical scale.

In the region of action of the hard component, λ_{eff} for concrete is 22 centimeters.

BIBLIOGRAPHY

1. Malafeev, A. I., Sakharov, V. N. Atomnaya energiya (Atomic Energy), Vol. III, 10, (1957).
2. Yadernye reaktory (Nuclear Reactors), Collection, Part 1. Physics of nuclear reactors, IL, Moscow, 1956, p. 285.
3. Lundby, A., Winter, B., Andersen, E., Enger, H. (Paper No. 891 at the International Conference on Peaceful Uses of Atomic Energy, Geneva, 1955).
4. Leipunskii, O. I., Sakharov, V. N., Tereshchenko, V. I. Atomnaya energiya, Vol. II, 3 (1957).
5. Kinsey, B. B., Bartholomew, G. A., Walker, W. H. Phys. Rev. 77, 723 (1950).
6. Hughes, Neutron Pile Research, Foreign Literature Press, 1954, p. 442.
7. Davisson, C. M., Evans, R. D. Rev. Mod. Phys. 24, No 2, 79 (1952).
8. Fano, U. Nucleonics, Vol. 11, No 8, p. 8 (1953).
9. Spenser, L. V., Fano, U. J. Research, N. B. S., 46, 446 (1951). Spenser, L. V., Fano, U. Phys. Rev., 81, 464, 1951. Fano, U. Nucleonics, 11, No 9, p. 55 (1953).
10. Goldstein, Wilkins. Fina Report. U. S. Atomic Energy Commis, No. 40, 3075 (1955).
11. White, G. R. Phys. Rev., 80, 154 (1950).
12. Soole, B. W. Proc. Roy. Soc., 230, No 1182, 342 (1955).
13. Hirshfelder, J., Magee, J., Hull, H. Phys. Rev., 73, 852 (1948). Hirshfelder, J., Adams, E. Phys. Rev. 73, 862 (1948).
14. Wyckoff. Radiology, 63, 94 (1954).
15. Perkins, J. E. J. Appl. Phys., 26, No 6, 655 (1955).
16. Evans, Hayward, John, Hubble. Phys. Rev., 93, 1. 955 (1954).
17. Sedov, L. I. Metody podobiya i razmernosti v mekhanike (Similarity and Dimensionality Methods in Mechanics), GITTL, 1954.
18. Bulatov, B. P., Garusov, E. I. Atomnaya energiya, Vol. 5, 631 (1958).
19. Heitler, W. The Quantum Theory of Radiation (Russ. Transl.) I.L. Moscow, 1956, p. 252, Figure 10.
20. Segre, E. (Editor), Experimental Nuclear Physics). (Russ. Transl.), I.L. Moscow, 1955, Vol. I, p. 269.
21. Sakharov, V. N. Atomnaya energiya, Vol. III, 57 (1957).
22. Roys, P. A., Shure, K., Taylor, J. J., Phys. Rev. 95, 911 (1954).
23. Lewis, E. B. Science., 125, 965 (1957).
24. Rockwell, T., III (Editor), Reactor Shielding. Design Manual. McGraw Hill B. C., 1956, p. 447.
25. Siegbahn, Kai, Beta and γ-ray spectroscopy North-Golland Publishing Company, Amsterdam, 1955, p. 35.

26. The effects of nuclear weapons, Somuel Glasston (Editor) United States Atomic Energy Commission, p. 351 (1957).
27. Aglintsev, K. K. Dozimetriya ioniziruyushchikh izlucheniy (Dosimetry of Ionizing Radiation), Gostekhizdat, 1950, p. 217.

APPENDIX I

INFORMATION ON γ RADIATION OF FISSION FRAGMENTS*

(compiled by M. Ya. Gen, M. S. Ziskin, and E. I. Intezarova)

*This appendix was based on the following works: a) Hunter and Ballow, Nucleonics, 9, No. 5, 1955, b) Corvell and Sugarman, Radiochemical Studies: the Fission Products. Book 2, c) Seaborg. Rev. Mod. Phys., 25. No. 2, 469, 1953, d) Nesmeyanov A. N., Lapitskii A. V., and Rudenko N. P., Poluchenie radioktivnykh izotopov (Production of Radioactive Isotopes), Goskhimizdat, 1954.

Table A1

γ Radiation of Fragments 1 Hour after Fission

$u(1\ hr) = 4.18 \times 10^{-1}$ Mev/sec $\times 10^4$ fissions*

Contribution of radiation of individual isotopes to u(1 hr), %

Xe^{38}, Cs^{138}	30,6	Y^{94}	16,3
$Te^{133\,m}$ Te^{133}	18,0	Ce^{146}, Pr^{146}	14,8

Isotopes	Half life	Fraction of decays of the isotope in the total number of decays of all the fragments, percent	Absolute number of decays per second per 10^4 fissions (x 10^2)	Energy of γ quanta from fragments, Mev	Yield of γ quanta with energy $E\gamma$ percent of number of decays	Intensity of radiation of the energy of the corresponding γ quantum, Mev/sec per 10^4 fissions x 10^2	Overall intensity of radiation of energy by the given isotope Mev/sec per 10^4 fissions (x 10^2)	Maximum energy of β particles**, Mev
Nd^{149}	1,8hrs	1,03	1,05	0,266	unknown	—	0,12	1,5
				0,422	.	—		
				0,538	.	—		
				0,65	.	—		
				0,03	.	—		
				0,097	.	—		
				0,112	.	—		
				0,114	100	0,12		
				0,124	unknown	—		
				0,188	.	—		
				0,198	.	—		
				0,211	.	—		
				0,226	.	—		
				0,24	.	—		
Y^{94}	10hrs	1,06	1,08	0,7	100	0,76	0,76	3,1
Mo^{102}	11 min	1,15	1,19	unknown				unknown
Tc^{104}	25 sec	1,2	1,24					
I^{135}	6,6 hrs	1,46	1,5	2,4	1,1	0,04	0,04	0,9

*u(t) -- summary intensity of radiation of energy from all the fission products at the instant after fission.

**In the case of a branched decay scheme, the weighted average is given for the maximum value of the β-particle energy.

Table A1 (continued)

Isotopes	Half life	Fraction of decays of the isotope in the total number of decays of all the fragments, percent	Absolute number of decays per second per 10^4 fissions ($\times 10^2$)	Energy of γ quanta from fragments, Mev	Yield of γ quanta with energy E_γ percent of number of decays	Intensity of radiation of the energy of the corresponding γ quantum, Mev/sec per 10^4 fissions $\times 10^2$	Overall intensity of radiation of energy by the given isotope Mev/sec per 10^4 fissions ($\times 10^2$)	Maximum energy of β particles**, Mev
Ce^{146}	13,9 min	1,6	1,65	0,11	unknown	—		0,9
				0,142	.	—		
				0,27	.	—		
				0,22	.	—		
				0,32	.	—		
Rb^{88}	17.8 min	1,7	1,8	1,85	20	0,67	0,89	4,8
				2,8	2	0,1		
				0,95	7	0,12		
Kr^{88}	2,8 hrs	1,7	1,8	0,028	68	0,034	0,034	1,0
Mo^{101}	14.6 min	2,2	2,26	0,19	100	0,43	1,95	1,5
				0,960	70	1,52		
Kr^{87}	78 min	2,35	2,43	2,3	12,5	0,7	1,4	2,7
				1,89	12,5	0,58		
				0,405	12,5	0,12		
$Te^{131\,m}$	30 hrs	2,4	2,48	0,177	100	0,44	1,55	
Te^{131}	25 min	2,4	2,48	0,16	100	0,39		1,7
				0,64	45	0,72		
La^{141}	3,7 hrs	2,4	2,48	1,5	5	0,19	0,19	2,4
Rb^{89}	15.4 min	2,65	2,73	unknown				3,8
Sr^{92}	2,7 hrs	3,1	3,2	.	—			unknown
Xe^{138}	17 min	3,4	3,5	.	—			.
La^{143}	19 .	3,5	3,61	.	—			.
Ba^{141}	18 .	4	4,13	.	—			2,8
Te^{133m}	62 .	4,3	4,44	0,4	100	1,8	7,5	—
Te^{133}	2 .	4,3	4,44	0,6	100	2,7		1,6
				1,0	70	3,0		
Te^{134}	44 .	4,3	4,44	unknown				unknown
J^{134}	52,5 .	4,7	4,85	0,86	30	1,25	1,25	2,0
				1,1	—	—		
				1,78	—	—		

Table A1 (continued)

Isotopes	Half life	Fraction of decays of the isotope in the total number of decays of all the fragments, percent	Absolute number of decays per second per 10^4 fissions ($\times 10^2$)	Energy of γ quanta from fragments, Mev	Yield of γ quanta with energy E_γ percent of number of decays	Intensity of radiation of the energy of the corresponding γ quantum, Mev/sec per 10^4 fissions $\times 10^2$	Overall intensity of radiation of energy by the given isotope Mev/sec per 10^4 fissions ($\times 10^2$)	Maximum energy of β particles**, Mev
Y^{94}	16,5min	4,7	4,85	1,4	100	6,8	6,8	5,4
La^{142}	74 .	5,2	5,35	0,25	unknown	--	--	unknown
				0,63	.	--		
				0,87	.	--		
Pr^{146}	25 .	5,4	5,56	0,455	100	2,53	6,21	3,1
				0,750	22	0,94		
				1,49	33	2,74		
Ba^{139}	85 .	5,6	5,8	0,163	26	0,25	0,29	2,3
				1,05	0,6	0,04		
Y^{95}	10,5 .	5,6	5,8	unknown	--	--	--	unknown
Cs^{138}	33 .	8,6	8,9	1,44	100	12,8	12,8	2,7
				0,463	unknown	-		
				0,98	.	—		
Ce^{145}	1,8hrs	3,4	3,5	unknown	--	--	--	2,0

Table A2

γ Radiation of Fragments 3 Hours after Fission

u(3 hrs) = 1.00 x 10^{-1} Mev/sec x 10^4 fissions

Contribution of radiation of individual isotopes in u(3 hrs), %

Te^{133m}, Te^{133}, J^{133}	20,8	Sr^{91}, Y^{91m}	9,6
Cs^{138}	14,7	Y^{93}	7,1
Zr^{97}, Cb^{97m}, Cb^{97}	8,3	Kr^{88}, Rb^{88}	6,8
Sr^{92}, Y^{92}	8,3	Te^{134}, J^{134}	5,8

Isotopes	Half life	Fraction of decays of the isotope in the total number of decays of all the fragments, percent	Absolute number of decays per second per 10^4 fissions (x 10^3)	Energy of γ quanta from fragments, Mev	Yield of γ quanta with energy E_γ percent of number of decays	Intensity of radiation of the energy of the corresponding γ quantum, Mev/sec per 10^4 fissions x 10^3	Overall intensity of radiation of energy by the given isotope Mev/sec per 10^4 fissions (x 10^3)	Maximum energy of β particles, Mev
Kr^{85m}	4,36 hrs	1	3,1	0,15 0,305	77 23	0,36 0,22	0,58	0,7
Ru^{105}	4,5 hrs	1,03	3,2	0,726 0,130	100 100	2,3 0,42	2,72	1,1
Ce^{143}	33 hrs	1,03	3,2	0,290 0,360 0,660 0,720	51 16 11 11	0,48 0,18 0,23 0,26	1,15	1,1
Pr^{146}	25 min	1,1	3,3	0,455 0,750 1,49	100 22 33	1,50 0,54 1,62	3,66	3,1
Xe^{135m}	15,3 .	1,2	3,7	0,52	80	1,54	2,28	—
Xe^{135}	9,2 hrs	1	3,1	0,25	95	0,74		0,9
Y^{91m}	51 min	1,2	3,7	0,551	91	1,86	1,86	—
J^{133}	22,4 hrs	1,25	3,87	0,53 0,85 1,4	94 5 1	1,92 0,16 0,06	2,14	1,2

Table A2 (continued)

Isotopes	Half life	Fraction of decays of the isotope in the total number of decays of all the fragments, percent	Absolute number of decays per second per 10^4 fissions (x 10^3)	Energy of γ quanta from fragments, Mev	Yield of γ quanta with energy Eγ percent of number of decays	Intensity of radiation of the energy of the corresponding γ quantum, Mev/sec per 10^4 fissions x 10^3	Overall intensity of radiation of energy by the given isotope Mev/sec per 10^4 fissions (x 10^3)	Maximum energy of β particles, Mev
Nd^{149}	1,8hrs	1,6	4,96	0,538	unknown		0,57	1,5
				0,65				
				0,03				
				0,097				
				0,112				
				0,114	100	0,57		
				0,124	unknown			
				0,188				
				0,211				
				0,198				
				0,226				
				0,240				
				0,266				
				0,422				
Y^{96}	10,5 min	1,8	5,59	unknown				unknown
Cb^{97m}	60 sec	2,0	6,21	0,75	99	4,61	8,36	
Cb^{97}	74 min	1,8	5,59	0,67	100	3,75		1,3
Zr^{97}	17hrs	2,0	6,21	no γ-radiation				1,9
Te^{134}	44 min	2,3	7,23	unknown				unknown
Kr^{87}	76 .	2,7	8,39	2,3	12,5	2,4	4,81	3,0
				1,89	12,5	1,98		
				0,41	12,5	0,43		
Sr^{91}	9,7hrs	3	9,3	1,4	7	0,91	7,79	1,6
				1,03	3,3	3,17		
				0,640	30	1,8		
				0,750	7	0,49		
				0,66	23	1,42		
Cs^{138}	33 min	3,3	10,2	0,468	unknown		14,7	2,6
				0,98				
				1,44	100	14,7		
Y^{93}	10 hrs	3,3	10,2	0,7	100	7,1	7,1	3,1
Te^{133m}	62 min	3,55	11,0	0,4	100	4,4	18,7	
Te^{133}	2 .	3,55	11,0	1,0	70	7,7		1,6
				0,6	100	6,6		

Table A2 (continued)

Isotopes	Half life	Fraction of decays of the isotope in the total number of decays of all the fragments, percent	Absolute number of decays per second per 10^4 fissions (x 10^3)	Energy of γ quanta from fragments, Mev	Yield of γ quanta with energy Eγ percent of number of decays	Intensity of radiation of the energy of the corresponding γ quantum, Mev/sec per 10^4 fissions x 10^3	Overall intensity of radiation of energy by the given isotope Mev/sec per 10^4 fissions (x 10^3)	Maximum energy of β particles, Mev
Pr^{146}	4,5 hrs	3,88	11,9	no γ - radiation	—	—	—	1,7
Kr^{88}	2,8 .	3,9	12,3	0,028	68	0,23	0,23	1,2
J^{136}	6,68 .	4,2	13,0	1,3	unknown	-	0,35	0,9
				2,4	1,1	0,35		
				1,8	unknown	—		
Rb^{86}	17,8 min	4,3	13,3	1,85	20	4,95	6,59	4,8
				2,8	2	0,75		
				0,95	7	0,89		
Y^{92}	3,5 hrs	4,5	13,9	0,6	100	8,35	8,35	3,5
Ce^{145}	1,8 .	5,6	17,3	unknown	—	—	—	2,0
La^{142}	74 min	6	18,6	0,25	unknown	—	—	unknown
				0,63	.	-		
				0,87	.	-		
La^{141}	3,7 hrs	6,6	20,9	1,5	5	1,57	1,57	2,4
Sr^{92}	2,7 .	6,6	20,9	unknown	—	—	—	unknown
J^{134}	52 min	7,2	22,3	0,86	30	5,77	5,77	2,0
				1,1	—			
				1,78	-			
Ba^{139}	85 min	7,5	23,2	0,163	26	0,98	1,13	2,3
				1,05	0,6	0,15		

Table A3

γ Radiation of Fragments 20 Hours after Fission

$u(20\ hrs) = 1.57 \times 10^{-2}$ Mev/sec $\times 10^4$ fissions

Contribution of radiation of individual isotopes to u(20 hrs), %

Zr^{97}, Cb^{97m}, Cb^{97}	28,3	J^{133}	8,3
Sr^{91}, Y^{91m}	17,1	Y^{92}	8,2
Y^{93}	12,8	Te^{132}, J^{132}	7,1
J^{135}, Xe^{135m}, Xe^{135}	8,8		

Isotopes	Half life	Fraction of decays of the isotope in the total number of decays of all the fragments, percent	Absolute number of decays per second per 10^4 fissions ($\times 10^4$)	Energy of γ quanta from fragments, Mev	Yield of γ quanta with energy $E\gamma$ percent of number of decays	Intensity of radiation of the energy of the corresponding γ quantum, Mev/sec per 10^4 fissions $\times 10^4$	Overall intensity of radiation of energy by the given isotope Mev/sec per 10^4 fissions ($\times 10^4$)	Maximum energy of β particles, Mev
Ba^{140}	12,8 days	1	3,58	0,54 0,51 0,03 0,16	30 10 100 70	0,58 0,11 0,11 0,4	1,2	0,8
Rh^{105}	36,5 hrs	1,1	3,94	0,32	5	0,06	0,06	0,6
Pm^{149}	47 .	1,2	4,3	0,285	100	1,22	1,22	1,1
Te^{132}	77 .	2,15	7,7	0,22 0,13	40 30	0,68 0,3	0,98	0,2
J^{132}	2,4 .	2,2	7,89	0,6 1,4	100 50	4,73 5,52	10,25	1,5
La^{141}	3,7 .	2,25	8,05	1,5	5	0,6	0,6	2,4
Y^{91m}	51 min	3,05	10,95	0,551	91	5,50	5,50	
Mo^{99}	67 hrs	3,8	13,6	0,181 0,741 0,780	97,5 17,5 2,5	2,1 1,77 0,24	4,4	1,1
Pr^{145}	4,5 .	4,4	15,8	no γ-radiation	–	—	—	1,7
J^{135}	6,68 .	5,4	19,7	2,4 1,3 1,8	1,1 unknown .	0,52 — --	0,52	0,9

Table A3 (continued)

Isotopes	Half life	Fraction of decays of the isotope in the total number of decays of all the fragments, percent	Absolute number of decays per second per 10^4 fissions (x 10^4)	Energy of γ quanta from fragments, Mev	Yield of γ quanta with energy $E\gamma$ percent of number of decays	Intensity of radiation of the energy of the corresponding γ quantum, Mev/sec per 10^4 fissions x 10^4	Overall intensity of radiation of energy by the given isotope Mev/sec per 10^4 fissions (x 10^4)	Maximum energy of β particles, Mev
Ce^{143}	33 hrs	5,8	20,6	0,290 0,360 0,660 0,720	51 16 11 11	3,05 1,13 1,5 1,64	7,4	1,1
Y^{92}	3,5 .	6	21,5	0,6	100	12,9	12,9	3,5
J^{139}	22,4 .	6,6	23,7	0,53 0,85 1,4	94 5 1	11,8 1,0 0,33	13,1	1,2
Sr^{91}	9,7 .	7	25,5	1,4 1,03 0,640 0,750 0,66	7 33 30 7 2,3	2,5 8,7 4,9 1,33 3,88	21,3	1,6
Y^{93}	10 .	8	28,7	0,7	100	20,0	20,0	3,1
Zr^{97}	17 .	8,5	30,8	no γ-radiation	—	—	--	1,9
Cb^{97m}	60 sec	8,5	30,8	0,75	99	22,8	44,4	--
Cb^{97}	74 min	9,0	32,3	0,67	100	21,6		1,3
Xe^{135m}	15,3 .	1,62	5,9	0,52	84	2,58	13,38	—
Xe^{135}	9,2 hrs	12,5	44,8	0,25	96	10,8		0,9

Table A4

γ Radiation of Fragments 2 Days after Fission

u(2 days) = 5.35 x 10^{-3} Mev/sec x 10^4 fissions

Contribution of radiation of individual isotopes in u(2 days), %

Zr^{97}, Cb^{97m}, Cb^{97}	27,2	Ce^{143}	8,0
Te^{132}, J^{132}	17,0	Sr^{91}, Y^{91m}	7,0
J^{133}, Xe^{133}	11,2	Mo^{99}	6,6
Ba^{140}, La^{140}	8,4	Y^{93}	5,6

Isotopes	Half life	Fraction of decays of the isotope in the total number of decays of all the fragments, percent	Absolute number of decays per second per 10^4 fissions (x 10^4)	Energy of γ quanta from fragments, Mev	Yield of γ quanta with energy Eγ percent of number of decays	Intensity of radiation of the energy of the corresponding γ quantum, Mev/sec per 10^4 fissions x 10^5	Overall intensity of radiation of energy by the given isotope Mev/sec per 10^4 fissions (x 10^5)	Maximum energy of β particles, Mev
J^{135}	6,68 hrs	1	1,19	2,4 1,3 1,8	1,1 unknown .	0,32	0,32	0,9
Y^{91m}	51 min	1,33	1,64	0,551	91	8,22	8,22	—
Ce^{141}	30 days	1,38	1,64	0,145	67	1,6	1,6	0,5
Nd^{147}	11,3 .	1,4	1,66	0,092 0,318 0,532	60 15 25	0,92 0,79 2,21	3,92	0,7
Pr^{143}	13,7 .	1,65	1,93	no γ-radiation	—	—	—	0,9
La^{140}	40 hrs	1,7	2,02	0,093 0,335 0,49 0,82 1,62 2,55	1,3 4 30 22 75 4	3,03 0,27 2,98 3,65 24,6 2,07	33,53	1,3
Rh^{105}	36,5 .	2,1	2,49	0,32	5	0,40	0,40	0,6

Table A4 (continued)

Isotopes	Half life	Fraction of decays of the isotope in the total number of decays of all the fragments, percent	Absolute number of decays per second per 10^4 fissions ($\times 10^4$)	Energy of γ quanta from fragments, Mev	Yield of γ quanta with energy $E\gamma$ percent of number of decays	Intensity of radiation of the energy of the corresponding γ quantum, Mev/sec per 10^4 fissions $\times 10^5$	Overall intensity of radiation of energy by the given isotope Mev/sec per 10^4 fissions ($\times 10^5$)	Maximum energy of β particles, Mev
J^{131}	8 days	2,35	2,79	0,722	2,8	0,59	11,16	0,6
				0,637	9,3	1.65		
				0,163	0,7	0,03		
				0,365	80,9	8,25		
				0,284	6,3	0,50		
				0,08	6,3	0,14		
Pm^{149}	47 hrs	2,5	2,96	0,285	100	8,4	8,4	1,1
Ba^{140}	12,8 days	2,95	3,5	0,54	30	5,7	11,8	0,8
				0,31	10	1,1		
				0,03	100	1,1		
				0,16	70	3,9		
Sr^{91}	9,7 hrs	3	3,65	1,4	7	3,5	29,7	1,6
				1,03	33	12,1		
				0,640	30	6,8		
				0,750	7	1,87		
				0,66	23	5,4		
Y^{93}	10 .	3,6	4,27	0,7	100	29,8	29,8	3,1
Xe^{133}	5,3 days	4,2	4,98	0,081	35	1,43	1,43	0,3
Te^{132}	77 hrs	5,2	6,16	0,22	40	5,4	7,8	0,2
				0,13	30	2,4		
J^{132}	2,4 .	5,4	6,41	0,6	100	38,5	83,4	1,5
				1,4	50	44,9		
Xe^{135}	9,2 .	7,8	9,25	0,25	96	22,2	22,2	0,8
Zr^{97}	17 .	8,4	9,96	no γ-radiation	—	—	—	1,9
J^{133}	22,4 .	8,5	10,5	0,53	94	52,5	58,4	1,2
				0,85	5	4,47		
				1,4	1	1,47		

Table A4 (continued)

Isotopes	Half life	Fraction of decays of the isotope in the total number of decays of all the fragments, percent	Absolute number of decays per second per 10^4 fissions ($\times 10^4$)	Energy of γ quanta from fragments, Mev	Yield of γ quanta with energy $E\gamma$ percent of number of decays	Intensity of radiation of the energy of the corresponding γ quantum, Mev/sec per 10^4 fissions $\times 10^5$	Overall intensity of radiation of energy by the given isotope Mev/sec per 10^4 fissions ($\times 10^5$)	Maximum energy of β particles, Mev
Mo^{99}	67 hrs	9	10,7	0,181	97,5	19,0	35,1	1,1
				0,741	17,5	14,0		
				0,780	2,5	2,1		
Ce^{143}	33 .	10	11,9	0,290	51	17,6	42,6	1,1
				0,360	16	6,9		
				0,660	11	8,7		
				0,720	11	9,4		
Cb^{97m}	60 sec	8,4	9,96	0,75	99	74	146,0	
Cb^{97}	74 min	9	10,7	0,67	100	72		1,3

Table A5

γ Radiation of Fragments 3 Days after Fission
u(3 days) = 3.21 x 10^{-3} Mev/sec x 10^4 fissions
Contribution of radiation of individual isotopes to u(3 days), %

Te^{132}, J^{132}	23,6	J^{133}, Xe^{133}	8'8
Zr^{97}, Cb^{97m} Cb^{97}	18,2	Mo^{99}, Tc^{99}	9,1
Ba^{140}, La^{140}	17,3	Ce^{143}	8,3

Isotopes	Half life	Fraction of decays of the isotope in the total number of decays of all the fragments, percent	Absolute number of decays per second per 10^4 fissions (x 10^4)	Energy of γ quanta from fragments, Mev	Yield of γ quanta with energy E_γ percent of number of decays	Intensity of radiation of the energy of the corresponding γ quantum, Mev/sec per 10^4 fissions x 105	Overall intensity of radiation of energy by the given isotope Mev/sec per 10^4 fissions (x 105)	Maximum energy of β particles, Mev
Sr^{91}	9,7 hrs	1,01	0,75	1,4 1,03 0,640 0,750 0,66	7 33 30 7 23	0,73 2,55 1,44 0,35 1,14	6,2	1,6
Y^{91m}	51 min	0,4	0,3	0.551	91	1,5	1,51	—
Y^{91}	57 days	1,01	0,75	1,2 0,2	0,1 0,1	0,009 0,002		1,5
Zr^{95}	66 .	1,08	0,8	0,721	99	5,7	5,7	0,4
Y^{93}	10 hrs	1,25	0,93	0,7	100	6,5	6,5	3,1
Tc^{99}	5,9 .	1,25	0,93	0,02 0,142 0,140	% low 1 90	— 1,01 1,17	1,18	—
Rh^{105}	36,5 .	2,19	1,62	0,32	5	0,26	0,26	0,6
Ce^{141}	30 days	2,2	1,63	0,145	67	1,58	1,58	0,5
Nd^{147}	11 .	2,2	1,63	0,092 0,318 0,532	60 15 25	0,9 0,78 2,17	3,82	0,7
Pm^{149}	47 hrs	2,9	2,14	0,285	100	6,05	6,05	1,1
Xe^{135}	9,2 .	3,15	2,32	0,25	96	5,6	5,6	0,8

Table A5 (continued)

Isotopes	Half life	Fraction of decays of the isotope in the total number of decays of all the fragments, percent	Absolute number of decays per second per 10^4 fissions (x 10^4)	Energy of γ quanta from fragments, Mev	Yield of γ quanta with energy $E\gamma$ percent of number of decays	Intensity of radiation of the energy of the corresponding γ quantum, Mev/sec per 10^4 fissions x 10^5	Overall intensity of radiation of energy by the given isotope Mev/sec per 10^4 fissions (x 10^5)	Maximum energy of β particles, Mev
Pr^{143}	13,7 days	3,2	2,36	no γ-radiation	—	—	—	0,9
La^{140}	40 hrs	3,6	2,66	0,093	1,3	0,03	44,2	1,3
				0,335	4	0,36		
				0,49	30	3,9		
				0,82	22	4,8		
				1,62	75	32,4		
				2,55	4	2,71		
J^{131}	8 days	3,6	2,66	0,722	2,8	0,54	10,6	0,6
				0,627	9,3	1,57		
				0,163	0,7	0,03		
				0,365	80,9	7,8		
				0,284	6,3	0,48		
				0,08	6,3	0,13		
Zr^{97}	17 hrs	5,4	4	no γ-radiatin	—	—	—	1,9
Cb^{97m}	60 sec	5,4	4	0,75	99	29,7	58,5	—
Cb^{97}	47 min	5,8	4,3	0,67	100	28,8		1,3
J^{133}	22 5 hrs	6,5	4,8	0,53	94	23,9	26,6	1,2
				0,85	5	2,03		
				1,4	1	0,67		
Ba^{140}	22,8 days	4,6	3,4	0,54	30	5,5	11,4	0,8
				0,31	10	1,05		
				0,03	100	1,02		
				0,16	70	3,81		
Te^{132}	77 hrs	7	5,2	0,22	40	4,58	6,6	0,2
				0,13	30	2,03		
J^{132}	2,4 .	7,2	5,31	0,6	100	31,9	69,1	1,5
				1,4	50	37,2		

Table A5 (continued)

Isotopes	Half life	Fraction of decays of the isotope in the total number of decays of all the fragments, percent	Absolute number of decays per second per 10^4 fissions ($\times 10^4$)	Energy of γ quanta from fragments, Mev	Yield of γ quanta with energy E_γ percent of number of decays	Intensity of radiation of the energy of the corresponding γ quantum, Mev/sec per 10^4 fissions $\times 10^5$	Overall intensity of radiation of energy by the given isotope Mev/sec per 10^4 fissions ($\times 10^5$)	Maximum energy of β particles, Mev
Xe^{133}	5,3 days	7,2	5,31	0,081	36	1,55	1,55	0,3
Ce^{143}	33 hrs	10	7,4	0,290	51	11,0	26,5	1,1
				0,360	16	4,25		
				0,660	11	5,4		
				0,720	11	5,85		
Mo^{99}	67 .	11,5	8,5	0,181	97,5	15,0	27,7	1,1
				0,741	17,5	11,0		
				0,780	2,5	1,66		

Table A6

γ Radiation of Fragments 10 Days after Fission

u(10 days) = 9.5 x 10^{-4} Mev/sec x 10^4 fissions

Contribution of radiation of individual isotopes to u(10 days), %

Ba^{140}, La^{140}	51,5	Zr^{95}	5,6
Te^{132}, J^{132}	17,6	J^{131}	6,4
Mo^{99}	8,9		

Isotopes	Half life	Fraction of decays of the isotope in the total number of decays of all the fragments, percent	Absolute number of decays per second per 10^4 fissions (x 10^4)	Energy of γ quanta from fragments, Mev	Yield of γ quanta with energy E_γ percent of number of decays	Intensity of radiation of the energy of the corresponding γ quantum, Mev/sec per 10^4 fissions x 105	Overall intensity of radiation of energy by the given isotope Mev/sec per 10^4 fissions (x 105)	Maximum energy of β particles, Mev
Ru^{103}	42 days	2,6	0,58	0,498 0,005	96 unknown	2,78 —	2,78	0,25
Rh^{103}	57 min	2,55	0,57	0,04	100	0,22	0,22	—
Sr^{89}	53 days	2,8	0,62	no γ-radiation		—	—	1,5
Y^{91}	57 .	3,2	0,71	1,2 0,2	0,1 0,1	0,009 0,001	0,01	1,5
Zr^{95}	65 .	3,3	0,74	0,721 0,231	99 1	5,3 0,02	5,32	0,4
Nd^{147}	11 .	4,8	1,06	0,092 0,318 0,532	60 15 25	0,59 0,51 1,41	2,51	0,7
Te^{132}	77 hrs	5,1	1,16	0,22 0,13	40 30	1,02 0,45	1,47	0,2
J^{133}	2,4 .	5,3	1,17	0,6 1,4	100 50	7,02 8,20	15,22	1,5
Ce^{141}	30 days	6,3	1,34	0,145	67	1,3	1,3	0,5

Table A6 (continued)

Isotopes	Half life	Fraction of decays of the isotope in the total number of decays of all the fragments, percent	Absolute number of decays per second per 10^4 fissions (x 10^4)	Energy of γ quanta from fragments, Mev	Yield of γ quanta with energy $E\gamma$ percent of number of decays	Intensity of radiation of the energy of the corresponding γ quantum, Mev/sec per 10^4 fissions x 10^5	Overall intensity of radiation of energy by the given isotope Mev/sec per 10^4 fissions (x 10^5)	Maximum energy of β particles, Mev
J^{131}	8 days	6,8	1,51	0,722	2,8	0,31	6,06	0,6
				0,637	9,3	0,90		
				0,163	0,7	0,017		
				0,365	80,9	4,48		
				0,284	6,3	0,27		
				0,08	6,3	0,08		
Mo^{99}	67 hrs	6,8	1,51	0,181	97,5	2,67	7,58	1,1
				0,741	17,5	1,96		
				0,780	2,5	2,95		
Pr^{143}	13,7 days	10	2,21	no γ-radiation	—	—	—	0,9
Ba^{140}	12,8 days	10,5	2,32	0,54	30	3,75	7,77	0,8
				0,31	10	0,72		
				0,03	100	0,70		
				0,16	70	2,6		
La^{140}	40 hrs	11,8	2,64	0,093	1,3	0,03	44,0	1,3
				0,335	4	0,36		
				0,49	30	3,9		
				0,82	22	4,76		
				1,62	75	32,2		
				2,55	4	2,7		
Xe^{133}	5,3 days	11,5	2,54	0,081	36	0,74	0,74	0,3

Table A7

γ Radiation of Fragments 30 Days after Fission
u(30 days) = 2.97 x 10^{-4} Mev/sec x 10^4 fissions
Contribution of radiation of individual isotopes to u(30 days), %

Ba^{140}, La^{140} . . . . . 61,2 Ru^{103}, Rh^{103m} 7,3
Zr^{95}, Cb^{95} 22,2

Isotopes	Half life	Fraction of decays of the isotope in the total number of decays of all the fragments, percent	Absolute number of decays per second per 10^4 fissions (x 10^3)	Energy of γ quanta from fragments, Mev	Yield of γ quanta with energy Eγ percent of number of decays	Intensity of radiation of the energy of the corresponding γ quantum, Mev/sec per 10^4 fissions x 10^6	Overall intensity of radiation of energy by the given isotope Mev/sec per 10^4 fissions (x 10^6)	Maximum energy of β particles, Mev
Ce^{144}	275 days	2	1,49	0,134	30	0,6	0,6	0,3
Pr^{144}	17,5 min	2	1,49	0,696	1	0,10	0,52	2,9
				2,18	1	0,33		
				1,48	0,4	0,9		
Xe^{133}	5,3 days	2,5	1,87	0,081	36	0,55	0,55	0,3
J^{131}	8 .	3,6	2,69	0,722	2,8	0,55	10,8	0,6
				0,637	9,3	1,6		
				0,163	0,7	0,03		
				0,365	80,9	8,0		
				0,284	6,3	0,48		
				0,08	6,3	0,14		
Nd^{147}	11 .	4,1	3,07	0,092	60	1,69	7,25	0,7
				0,318	15	1,46		
				0,532	25	4,1		
Cb^{95}	35 .	4,1	3,07	0,745	100	22,8	22,8	0,2
Rh^{103m}	57 min	5,5	4,12	0,04	100	1,64	1,64	
Ru^{103}	42 days	5,6	4,19	0,498	96	20,0	20,0	0,25
				0,005	unknown	—		
Sr^{89}	53 .	6,7	5,02	no γ-radiation	—	—		1,5
Y^{91}	57 .	7,5	5,62	1,2	0,1	0,07	0,08	1,5
				0,2	0,1	0,01		
Zr^{95}	65 .	8,1	6,06	0,721	99	43,0	43,1	0,4
				0,231	1	0,1		
Ba^{140}	12,8 .	10,8	8,08	0,54	30	13,1	27,1	0,8
				0,31	10	2,5		
				0,03	100	2,42		
				0,16	70	9,05		
Pr^{143}	13,7 .	11,2	8,37	no γ-radiation	—	—	—	0,9

Table A7 (continued)

Isotopes	Half life	Fraction of decays of the isotope in the total number of decays of all the fragments, percent	Absolute number of decays per second per 10^4 fissions ($\times 10^5$)	Energy of γ quanta from fragments, Mev	Yield of γ quanta with energy E_γ percent of number of decays	Intensity of radiation of the energy of the corresponding γ quantum, Mev/sec per 10^4 fissions $\times 10^6$	Overall intensity of radiation of energy by the given isotope Mev/sec per 10^4 fissions ($\times 10^6$)	Maximum energy of β particles, Mev
La^{140}	40 hrs	12,5	9,35	0,093	1,3	0,11	154,4	1,3
				0,335	4	1,26		
				0,49	30	13,5		
				0,82	22	16,9		
				1,62	75	113,0		
				2,55	4	9,6		
Ce^{141}	30 days	11,2	8,37	0,145	67	8,1	8,1	0,5

Table A8

γ Radiation of Fragments 200 Days after Fission

u(200 days) = 2.33 x 10^{-5} Mev/sec x 10^4 fissions

Contribution of radiation of individual isotopes to u(200 days), %

Zr^{95}, Cb^{95} . . . . . 99.6 Ru^{106}, Rh^{106m} 5,7

Isotopes	Half life	Fraction of decays of the isotope in the total number of decays of all the fragments, percent	Absolute number of decays per second per 10^4 fissions (x 10^6)	Energy of γ quanta from fragments, Mev	Yield of γ quanta with energy $E\gamma$ percent of number of decays	Intensity of radiation of the energy of the corresponding γ quantum, Mev/sec per 10^4 fissions x 10^7	Overall intensity of radiation of energy by the given isotope Mev/sec per 10^4 fissions (x 10^7)	Maximum energy of β particles, Mev
Ru^{106}	1 year	1,1	0,79	no γ-radiation	—	—	—	0,04
Rh^{106}	30 sec	1,1	0,79	0,516 0,619 0,88 1,045 1,11 1,54	20,3 13,4 0,3 1,7 0,4 0,2	0,83 0,51 0,02 0,14 0,04 0,02	1,56	3,0
Ce^{141}	30 days	1,9	1,37	0,145	67	1,36	1,36	0,5
Pm^{147}	2,6 years	2,2	1,59	no γ-radiation	—	—	—	0,3
Rh^{103m}	57 min	3,5	2,52	0,04	100	1,01	1,01	—
Ru^{103}	42 days	3,6	2,6	0,498 0,002	96 unknown	12,4 -	12,4	0,25
Sr^{89}	53 .	7,9	5,7	no γ-radiation	—	—	—	1,5
Y^{91}	57 .	10,4	7,9	1,2 0,2	0,1 0,1	0,10 0,02	0,12	1,5
Ce^{144}	275 .	13	9,4	0,134	30	3,78	3,78	0,3
Pr^{144}	17,5 min	13	9,4	0,696 2,18 1,48	1 1 0,4	0,66 2,05 0,55	3,26	2,9

Table A8 (continued)

Isotopes	Half life	Fraction of decays of the isotope in the total number of decays of all the fragments, percent	Absolute number of decays per second per 10^4 fissions (x 10^6)	Energy of γ quanta from fragments, Mev	Yield of γ quanta with energy $E\gamma$ percent of number of decays	Intensity of radiation of the energy of the corresponding γ quantum, Mev/sec per 10^4 fissions x 10^7	Overall intensity of radiation of energy by the given isotope Mev/sec per 10^4 fissions (x 10^7)	Maximum energy of β particles, Mev
Zr^{95}	66 days	14,4	10,4	0,721 0,231	99 1	71,0 0,24	74,2	0,4
Cb^{95}	35 .	25	18	0,745	100	135	135	0,2

Table A9

γ Radiation of Fragments 1 Year after Fission

u(1 year) = 4.57×10^{-6} Mev/sec x 10^4 fissions

Contribution of radiation of individual isotopes to u(1 year), %

Zr^{95}, Cb^{95} . . . . . 82,7 Ce^{144}, Pr^{144} 10,2

Isotopes	Half life	Fraction of decays of the isotope in the total number of decays of all the fragments, percent	Absolute number of decays per second per 10^4 fissions (x 10^6)	Energy of γ quanta from fragments, Mev	Yield of γ quanta with energy Eγ percent of number of decays	Intensity of radiation of the energy of the corresponding γ quantum, Mev/sec per 10^4 fissions x 10^7	Overall intensity of radiation of energy by the given isotope Mev/sec per 10^4 fissions (x 10^7)	Maximum energy of β particles, Mev
Cs^{137}	33 years	1,46	0,342	no γ-radiation	—	—	—	0,6
Ba^{137}	2,6 min	1,36	0,315	0,661	100	2,08	2,08	—
Sr^{90}	19,9 years	1,85	0,437	no γ-radiation	—	—	—	0,5
Y^{90}	61 hrs	1,85	0,437	no γ-radiation	—	—	—	2,2
Ru^{106}	1 year	2,45	0,572	no γ-radiation	—	—	—	0,04
Rh^{106}	30 sec	2,45	0,572	0,516	20,5	0,61	1,15	3,0
				0,619	10,4	0,37		
				0,88	0,3	0,02		
				1,045	1,7	0,10		
				1,14	0,4	0,03		
				1,54	0,2	0,02		
Sr^{89}	53 days	2,65	0,621	no γ-radiation	—	—	—	1,5
Y^{91}	57 .	3,8	0,89	1,2	0,1	0,001	0,003	1,5
				0,2	0,1	0,002		
Pm^{147}	2,6 years	5,7	1,33	no γ-radiation	—	—	—	0,2
Zr^{95}	66 days	7,1	1,66	0,721	99	12,0	12,04	0,4
				0,231	1	0,04		

Table A9 (continued)

Isotopes	Half life	Fraction of decays of the isotope in the total number of decays of all the fragments, percent	Absolute number of decays per second per 10^4 fissions (x 10^6)	Energy of γ quanta from fragments, Mev	Yield of γ quanta with energy $E\gamma$ percent of number of decays	Intensity of radiation of the energy of the corresponding γ quantum, Mev/sec per 10^4 fissions x 10^7	Overall intensity of radiation of energy by the given isotope Mev/sec per 10^4 fissions (x 10^7)	Maximum energy of β particles, Mev
Cb^{95}	35 days	14,9	3,48	0,745	100	25,8	25,8	0,2
Ce^{144}	275 .	26,5	6,2	0,134	30	2,5	2,5	0,3
Pr^{144}	17,5 min	26,5	6,2	0,696 2,18 1,48	1 1 0,4	0,43 1,35 0,37	2,15	2,9

Table A10

γ Radiation of Fragments 3 Years after Fission

u(3 years) = 3.82 x 10^{-7} Mev/sec x 10^4 fissions

Contribution of radiation of individual isotopes to u(3 years), %

Cs^{137}, Ba^{137} . . . . . 67,6 Ru^{106}, Rh^{106} 8,7

Ce^{144}, Pr^{144} 23.7

Isotopes	Half life	Fraction of decays of the isotope in the total number of decays of all the fragments, percent	Absolute number of decays per second per 10^4 fissions (x 10^7)	Energy of γ quanta from fragments, Mev	Yield of γ quanta with energy Eγ percent of number of decays	Intensity of radiation of the energy of the corresponding γ quantum, Mev/sec per 10^4 fissions x 10^8	Overall intensity of radiation of energy by the given isotope Mev/sec per 10^4 fissions (x 10^8)	Maximum energy of β particles, Mev
Ru^{106}	1 year	2,95	1,67	no γ-radiation	—	—	—	0,04
Rh^{106}	30 sec	2,95	1,67	0,516	20,5	1,75	3,3	3,0
				0,619	10,4	1,08		
				0,88	0,3	0,05		
				1,045	1,7	0,30		
				1,14	0,4	0,08		
				1,54	0,2	0,05		
Cs^{137}	33 years	6,8	3,9	no γ-radiation	—	—	—	0,6
Ba^{137}	2,6 min	6,8	3,9	0,661	100	25,8	25,8	—
Sr^{90}	19,9 yrs	8,7	5,0	no γ-radiation	—	—	—	0,5
Y^{90}	61 hrs	8,7	5,0	no γ-radiation	—	—	—	2,2
Ce^{144}	275 days	20,8	12	0,134	30	4,85	4,85	0,3
Pr^{144}	17,5 min	20,8	12	0,693	1	0,83	4,2	2,9
				2,18	1	2,63		
				1,48	0,4	0,71		
Pm^{147}	2,6 years	19	11	no γ-radiation	—	—	—	0,2

Table All

γ Radiation of Fission Fragments 4 Years after Fission

u(4 years) = 3.11 x 10^{-7} Mev/sec 10^4 fission

Contribution of radiation of individual isotopes to u(4 years), %

Cs^{137}, Ba^{137} . . . . . 80,8 Ru^{106}, Rh^{106} 6,0
Ce^{144}, Pr^{144} 13,1

Isotopes	Half life	Fraction of decays of the isotope in the total number of decays of all the fragments, percent	Absolute number of decays per second per 10^4 fissions (x 10^7)	Energy of γ quanta from fragments, Mev	Yield of γ quanta with energy Eγ percent of number of decays	Intensity of radiation of the energy of the corresponding γ quantum, Mev/sec per 10^4 fissions x 10^8	Overall intensity of radiation of energy by the given isotope Mev/sec per 10^4 fissions (x 10^8)	Maximum energy of β particles, Mev
Kr^{85}	9,4 years	1,22	0,49	0,54	0,65	0,02	0,02	0,7
Ru^{106}	1 ,	2,35	0,95	no γ-radiation	—	—	—	0,04
Rh^{106}	30 sec	2,35	0,95	0,516 0,619 0,88 1,045 1,14 1,54	20,5 10,4 0,3 1,7 0,4 0,2	1,01 0,62 0,03 0,17 0,04 0,03	1,9	3,0
Cs^{137}	33 years	9,4	3,8	no γ-radiation	—	—	—	0,6
Ba^{137}	2,6 min	9,4	3,8	0,661	100	25,1	25,1	—
Sr^{90}	19,9 yrs	12,0	4,8	no γ-radiation	—	—	—	0,5
Y^{90}	61 hrs	12,0	4,8	no γ-radiation	—	—	—	2,2
Ce^{144}	275 days	13,5	5,45	0,134	30	2,18	2,18	0,3
Pr^{144}	17,5 min	13,5	5,45	0,693 2,18 1,48	1 1 0,4	0,38 1,19 0,32	1,89	2,9
Pm^{147}	2,6 years	21,5	8,7	no γ-radiation	—	—	—	0,2

Table A12

γ Radiation of Fragments 10 Years after Fission

$u(10\ \text{years}) = 2.21 \times 10^{-7}$ Mev/sec $\times 10^4$ fissions

Contribution of radiation of individual isotopes to u(10 years), %

Cs^{137} и Ba^{137} 100

Isotopes	Half life	Fraction of decays of the isotope in the total number of decays of all the fragments, percent	Absolute number of decays per second per 10^4 fissions ($\times 10^8$)	Energy of γ quanta from fragments, Mev	Yield of γ quanta with energy Eγ percent of number of decays	Intensity of radiation of the energy of the corresponding γ quantum, Mev/sec per 10^4 fissions $\times 10^8$	Overall intensity of radiation of energy by the given isotope Mev/sec per 10^4 fissions ($\times 10^8$)	Maximum energy of β particles, Mev
Kr^{85}	9,4 years	1,7	3,15	0,54	0,65	0,01	0,01	0,7
Pm^{147}	2,6 .	15,6	2,9	no γ-radiation	—	—	—	0,2
Cs^{137}	33 .	18	33	no γ-radiation	—	—	—	0,6
Ba^{137}	2,6 min	18	33,5	0,661	100	22,1	22,1	—
Sr^{90}	19,9 years	22	40,9	no γ-radiation	—	—	—	0,5
Y^{90}	61 hrs	22	40,9	no γ-radiation	—	—	—	2,2

Table A13

γ Radiation of Fragments 20 Years after Fission

u(20 years) = 1.80 x 10^{-7} Mev/sec x 10^4 fissions

Contribution of radiation of individual isotopes to u(20 years), %

Cs^{137} & Ba^{137} 100

Isotopes	Half life	Fraction of decays of the isotope in the total number of decays of all the fragments, percent	Absolute number of decays per second per 10^4 fissions (x 10^8)	Energy of γ quanta from fragments, Mev	Yield of γ quanta with energy Eγ percent of number of decays	Intensity of radiation of the energy of the corresponding γ quantum, Mev/sec per 10^4 fissions x 10^8	Overall intensity of radiation of energy by the given isotope Mev/sec per 10^4 fissions (x 10^8)	Maximum energy of β particles, Mev
Kr^{85}	9,4 years	1,25	1,54	0,54	0,65	0,005	0,005	0,7
Pm^{147}	2,6 .	3,4	4,2	no γ - radiation	-	—	—	0,2
Cs^{137}	33 .	22	27,2	no γ - radiation	-	—	—	0,6
Ba^{137}	2,6 min	22	27,2	0,661	100	18,0	18,0	—
Sr^{90}	19,9 years	24	29,7	no γ - radiation	-	—	—	0,5
Y^{90}	61 hrs	24	29,7	no γ - radiation	-	—	—	2,2

Table A14

γ Radiation of Fragments 100 Years after Fission

u(100 years) = 3.60 x 10^{-8} Mev/sec x 10^{4} fissions

Contribution of radiation of individual isotopes to u(100 years), %

Cs^{137} & Ba^{137} 100

Isotopes	Half life	Fraction of decays of the isotope in the total number of decays of all the fragments, percent	Absolute number of decays per second per 10^4 fissions (x 10^8)	Energy of γ quanta from fragments, Mev	Yield of γ quanta with energy Eγ percent of number of decays	Intensity of radiation of the energy of the corresponding γ quantum, Mev/sec per 10^4 fissions x 10^8	Overall intensity of radiation of energy by the given isotope Mev/sec per 10^4 fissions (x 10^8)	Maximum energy of β particles, Mev
Sr^{90}	19,9yrs	17,5	2,98	no γ-radiation	—	—	—	0,5
Y^{90}	61hrs	17,5	2,98	no γ-radiation	—	—	—	2,2
Cs^{137}	33 years	32	5,43	no γ-radiation	—	—	—	0,6
Ba^{137}	2,6 min	32	5,43	0,661	100	3,6	3,6	—

APPENDIX II

ADDITIONAL INFORMATION ON THE PASSAGE OF γ RAYS THROUGH MATTER

Table A15*

Cross section of photoeffect σ_{ph} and of Compton scattering $a\sigma_C$ in units of 10^{-24} cm/atom at different values of γ quantum energy ε

ε, Mev	Nitrogen		Aluminum		Iron		Lead	
	$a\sigma_C$	σ_{ph}	$a\sigma_C$	σ_{ph}	$a\sigma_C$	σ_{ph}	$a\sigma_C$	
0,102	3,430	0,0540	6,370	0,991	12,74	20,5	40,18	1782
0,127	3,245	0,0262	6,026	0,492	12,05	10,8	38,01	985
0,170	2,991	0,0104	5,555	0,196	11,11	4,43	35,04	465
0,255	2,621	0,00313	4,868	0,0554	9,735	1,27	30,70	161
0,340	2,358	0,00111	4,380	0,0214	8,760	0,546	27,63	75,7
0,408	2,198	0,000651	4,082	0,0128	8,163	0,325	25,74	47,8
0,510	2,005	0,000350	3,725	0,00691	7,451	0,190	23,50	27,7
0,681	1,770	0,000165	3,287	0,00324	6,574	0,0844	20,73	14,5
1,022	1,463	0,0000661	2,717	0,00129	5,434	0,0342	17,14	6,31
1,362	1,264	0,0000394	2,347	0,000774	4,695	0,0206	14,81	3,86
1,533	1,187	—	2,205	—	4,410	0,0170	13,91	—
2,043	1,012	0,0000209	1,880	0,000415	3,759	0,011	11,86	2,08
5,108	0,5718	0,0000064	1,062	0,000127	2,124	—	6,698	0,675

*Compiled on the basis of reference [7].

Table A16*

Cross section of Compton scattering σ_C of the transfer of energy to a quantum σ_γ and to an electron σ_e in units of 10^{-25} cm^2/electron at different values of γ-quantum energy in units mc^2 = 511 kev

$\alpha = \varepsilon mc^2$	σ_C	σ_γ	σ_e
0,025	6,31	6,31	0,00
0,05	6,07	5,79	0,28
0,1	5,599	5,138	0,461
0,2	4,900	4,217	0,683
0,4	4,032	3,152	0,880
0,8	3,140	2,158	0,982
1,0	2,866	1,879	0,987
2,0	2,090	1,164	0,926
3,0	1,696	0,852	0,844
4,0	1,446	0,674	0,772
6,0	1,136	0,477	0,659
8,0	0,946	0,370	0,576
10,0	0,817	0,302	0,515

*Compiled on the basis of reference [25].

Table A17*

Coefficients of absorption μ and ranges of γ quantum in air (density $\rho = 0.00129$ g/cm^3) at different values of energy ε

ε, Mev	$\frac{\mu}{\rho}$, cm^2/g	$\frac{\mu_e}{\rho}$, cm^2/g	μ, см$^{-1}$	μ_e, см$^{-1}$	λ, м	λ_e, м
0,1	0,153	0,0227	$0,197 \cdot 10^{-3}$	$0,0293 \cdot 10^{-3}$	50,8	341
0,15	0,133	0,0240	$0,172 \cdot 10^{-3}$	$0,0310 \cdot 10^{-3}$	58,2	323
0,2	0,123	0,0262	$0,159 \cdot 10^{-3}$	$0,0338 \cdot 10^{-3}$	62,9	296
0,3	0,107	0,0282	$0,138 \cdot 10^{-3}$	$0,0364 \cdot 10^{-3}$	72,5	275
0,4	0,096	0,0292	$0,124 \cdot 10^{-3}$	$0,0376 \cdot 10^{-3}$	80,6	266
0,5	0,087	0,0295	$0,112 \cdot 10^{-3}$	$0,0380 \cdot 10^{-3}$	89,3	263
0,6	0,081	0,0293	$0,104 \cdot 10^{-3}$	$0,0378 \cdot 10^{-3}$	96,2	265
0,8	0,071	0,0285	$0,0915 \cdot 10^{-3}$	$0,0368 \cdot 10^{-3}$	109	272
1,0	0,0635	0,0275	$0,0818 \cdot 10^{-3}$	$0,0354 \cdot 10^{-3}$	122	282
1,5	0,0515	0,0247	$0,0664 \cdot 10^{-3}$	$0,0319 \cdot 10^{-3}$	151	314
2,0	0,0435	0,0230	$0,0561 \cdot 10^{-3}$	$0,0296 \cdot 10^{-3}$	178	338
3,0	0,0350	0,0205	$0,0452 \cdot 10^{-3}$	$0,0264 \cdot 10^{-3}$	221	379
4,0	0,0305	0,0193	$0,0393 \cdot 10^{-3}$	$0,0249 \cdot 10^{-3}$	254	402
5,0	0,0270	0,0180	$0,0348 \cdot 10^{-3}$	$0,0232 \cdot 10^{-3}$	287	432
6,0	0,0245	0,0170	$0,0316 \cdot 10^{-3}$	$0,0219 \cdot 10^{-3}$	316	457
8,0	0,0220	0,0157	$0,0284 \cdot 10^{-3}$	$0,0203 \cdot 10^{-3}$	352	492
10,0	0,0200	0,0150	$0,0258 \cdot 10^{-3}$	$0,0193 \cdot 10^{-3}$	388	518

*Compiled on the basis of reference [24].

Table A18*

Coefficients of absorption μ and ranges of γ-quantum in water (ρ = 1 g/cm^3) at different values of the energy ε

ε, Mev	$\frac{\mu}{\rho}$, cm^2/g	$\frac{\mu_e}{\rho}$, cm^2/g	μ, см$^{-1}$	μ_e, см$^{-1}$	λ, см	λ_e, см
0,1	0,171	0,0253	0,171	0,0253	5,85	39,5
0,15	0,151	0,0278	0,151	0,0278	6,63	36,0
0,2	0,137	0,0299	0,137	0,0299	7,30	33,5
0,3	0,119	0,0320	0,119	0,0320	8,40	31,2
0,4	0,106	0,0328	0,106	0,0328	9,44	30,5
0,5	0,0967	0,0330	0,0967	0,0330	10,3	30,3
0,6	0,0894	0,0329	0,0894	0,0329	11,2	30,4
0,8	0,0786	0,0321	0,0786	0,0321	12,7	31,1
1,0	0,0706	0,0310	0,0706	0,0310	14,2	32,2
1,5	0,0576	0,0283	0,0576	0,0283	17,4	35,3
2,0	0,0493	0,0260	0,0493	0,0260	20,3	38,4
3,0	0,0396	0,0227	0,0396	0,0227	25,2	44,0
4,0	0,0339	0,0204	0,0339	0,0204	29,5	49,0
5,0	0,0302	0,0189	0,0302	0,0189	33,1	52,9
6,0	0,0277	0,0178	0,0277	0,0178	36,1	56,2
8,0	0,0242	0,0163	0,0242	0,0163	41,3	61,3
10,0	0,0221	0,0154	0,0221	0,0154	45,2	65,0

*Compiled on the basis of reference [8].

Table A19*

Coefficients of absorption μ and ranges of γ quanta in aluminum (ρ = 2.7 g/cm^3) at different values of the energy

ε, Mev	$\frac{\mu}{\rho}$, cm^2/g	$\frac{\mu_e}{\rho}$ cm^2/g	μ, см$^{-1}$	μ_e, см$^{-1}$	λ, см	λ_e, см
0,1	0,169	0,0371	0,457	0,100	2,19	10,0
0,15	0,138	0,0282	0,372	0,0762	2,69	13,1
0,2	0,122	0,0275	0,329	0,0743	3,04	13,4
0,3	0,104	0,0283	0,281	0,0764	3,56	13,1
0,4	0,0927	0,0287	0,250	0,0775	4,00	12,9
0,5	0,0844	0,0287	0,228	0,0775	4,38	12,9
0,6	0,0779	0,0286	0,210	0,0772	4,77	13,0
0,8	0,0683	0,0278	0,184	0,0750	5,44	13,3
1,0	0,0614	0,0269	0,166	0,0726	6,02	13,7
1,5	0,0500	0,0246	0,135	0,0664	7,42	15,0
2,0	0,0431	0,0227	0,116	0,0613	8,63	16,3
3,0	0,0353	0,0201	0,0953	0,0543	10,5	18,4
4,0	0,0310	0,0188	0,0837	0,0507	11,9	19,7
5,0	0,0284	0,0180	0,0767	0,0486	13,0	20,6
6,0	0,0266	0,0174	0,0718	0,0470	13,9	21,3
8,0	0,0243	0,0169	0,0656	0,0456	15,2	21,9
10,0	0,0232	0,0167	0,0627	0,0451	15,9	22,2

*Compiled on the basis of reference [8].

Table 20*

Coefficients of absorption μ and ranges of γ quanta in iron ($\rho = 7.8$ g/cm^3) at different values of the energy ε

ε, Mev	$\frac{\mu}{\rho}$, cm^2/g	$\frac{\mu_e}{\rho}$, cm^2/g	μ, см$^{-1}$	μ_e, см$^{-1}$	λ, см	λ_e, см
0,1	0,370	0,219	2,88	1,71	0,34.	0,585
0,15	0,196	0,0801	1,53	0,625	0,654	1,60
0,2	0,146	0,0485	1,14	0,378	0,877	2,64
0,3	0,110	0,0340	0,857	0,265	1,17	3,77
0,4	0,0939	0,0306	0,733	0,238	1,36	4,20
0,5	0,0840	0,0293	0,655	0,228	1,53	4,38
0,6	0,0769	0,0286	0,600	0,223	1,67	4,48
0,8	0,0668	0,0272	0,521	0,212	1,92	4,71
1,0	0,0593	0,0261	0,467	0,204	2,14	4,90
1,5	0,0484	0,0237	0,378	0,185	2,64	5,40
2,0	0,0422	0,0219	0,329	0,171	3,04	5,85
3,0	0,0359	0,0203	0,280	0,158	3,57	6,33
4,0	0,0330	0,0198	0,258	0,154	3,87	6,50
5,0	0,0314	0,0198	0,245	0,154	4,08	6,50
6,0	0,0305	0,0200	0,238	0,156	4,20	6,41
8,0	0,0298	0,0206	0,232	0,161	4,31	6,20
10,0	0,0300	0,0213	0,234	0,166	4,27	6,02

*Compiled on the basis of reference [8].

Table 21*

Coefficients of absorption μ and ranges of γ quanta in lead (ρ = 11.3 g/cm^3) at different values of the energy ϵ

ϵ, Mev	$\frac{\mu}{\rho}$, cm^2/g	$\frac{\mu_e}{\rho}$, cm^2/g	μ, $см^{-1}$	μ_e, $см^{-1}$	λ, $см$	λ $см$
0,1	5,46	2,16	61,7	24,4	0,0162	0,0410
0,15	1,92	1,08	21,7	12,2	0,0461	0,0820
0,2	0,942	0,586	10,6	6,63	0,0943	0,151
0,3	0,378	0,241	4,27	2,72	0,234	0,368
0,4	0,220	0,136	2,48	1,54	0,403	0,650
0,5	0,152	0,0901	1,72	1,02	0,581	0,980
0,6	0,119	0,0684	1,34	0,773	0,746	1,29
0,8	0,0866	0,0477	0,978	0,539	1,03	1,85
1,0	0,0703	0,0384	0,795	0,434	1,26	2,30
1,5	0,0523	0,0280	0,591	0,316	1,69	3,16
2,0	0,0456	0,0248	0,515	0,280	1,94	3,57
3,0	0,0413	0,0238	0,467	0,269	2,14	3,72
4,0	0,0416	0,0253	0,470	0,286	2,13	3,50
5,0	0,0430	0,0272	0,486	0,307	2,06	3,26
6,0	0,0445	0,0287	0,503	0,324	1,99	3,08
8,0	0,0471	0,0309	0,532	0,349	1,88	2,87
10,0	0,0503	0,0328	0,568	0,371	1,76	2,70

*Compiled on the basis of reference [8].

Table A22*

Dependence of the dose build-up factor B_r (μR) on the energy ϵ of a point source of quanta in the passage of γ radiation through an infinite medium for water, aluminum, iron, and lead

Substance	Quantum energy ϵ, Mev	Dose build-up factors B_r (μR) at distances μR						
		1	2	4	7	10	15	20
Water....	0,255	3,09	7,14	23,0	72,9	166	456	982
.	0,5	2,52	5,14	14,3	38,8	77,6	178	334
.	1,0	2,13	3,71	7,68	16,2	27,1	50,4	82,2
.	2,0	1,83	2,77	4,88	8,46	12,4	19,5	27,7
.	3,0	1,69	2,42	3,91	6,23	8,63	12,8	17,0
.	4,0	1,58	2,17	3,34	5,13	6,94	9,97	12,9
.	6,0	1,46	1 91	2,76	3,99	5,18	7,09	8,85
.	8,0	1,38	1,74	2,40	3,34	4,25	5,66	6,95
.	10,0	1,38	1,63	2,19	2,97	3,72	4,90	5,98
Aluminum.	0,5	2,37	4,24	9,47	21,5	38,9	80,8	141
.	1,0	2,0	3,31	6,57	13,1	21,2	37,9	58,5
.	2,0	1,75	2,61	4,62	8,05	11,9	18,7	26,3
.	3,0	1,64	2,32	3,78	6,14	8,65	13,0	17,7
.	4,0	1,53	2,08	3,22	5,01	6,88	10,1	13,4
.	6,0	1,42	1,85	2,70	4,06	5,49	7,97	10,4
.	8,0	1,34	1,68	2,37	3,45	4,58	6,56	8,52
.	10,0	1,28	1,55	2,12	3,01	3,96	5,63	7,32
Iron.....	0,5	1,98	3,09	5,98	11,7	19,2	35,4	55,6
.	1,0	1,87	2,89	5,39	10,2	16,2	28,3	42,7
.	2,0	1,76	2,43	4,13	7,25	10,9	17,6	25,1
.	3,0	1,55	2,15	3,51	5,85	8,51	13,5	19,1
.	4,0	1,45	1,94	3,03	4,91	7,11	11,2	16,0
.	6,0	1,34	1,72	2,58	4,14	6,02	9,89	14,7
.	8,0	1,27	1,56	2,23	3,49	5,07	8,50	13,0
.	10,0	1,20	1,42	1,95	2,99	4,35	7,54	12,4
Lead.....	0,5	1,24	1,42	1,69	20,0	2,27	2,65	(2,73)
.	1,0	1,37	1,69	2,26	3,02	3,74	4,81	5,85
.	2,0	1,39	1,76	2,51	3,66	4,84	6,87	9,00
.	3,0	1,34	1,68	2,43	3,75	5,30	8,44	12,3
.	6,0	1,18	1,10	1,97	3,31	5,59	13,8	32,7
.	8,0	1,14	1,30	1,74	2,89	5,07	14,1	44,6
.	10,0	1,11	1, 3	1,78	2,52	4,34	12,5	38,2

*Data from reference [10].